**UNIVERSITÀ DEGLI STUDI DI PADOVA**

DIPARTIMENTO DI INGEGNERIA INDUSTRIALE

CORSO DI LAUREA MAGISTRALE IN INGEGNERIA CHIMICA E DEI PROCESSI INDUSTRIALI

**Tesi di Laurea Magistrale in**
**Ingegneria Chimica e dei Processi Industriali**

# THE EFFECT OF DIFFERENT SOLVENTS ON ELECTROSPINNING OF HIGH PERFORMANCE FIBERS FOR ELECTRODES IN PEM FUEL CELL APPLICATION

***Relatore: Prof. Michele Modesti***
***Correlatore: Prof. Peter N. Pintauro***
***Correlatrice: Dott.ssa Martina Roso***

***Laureando: ENRICO CINQUETTI***

ANNO ACCADEMICO 2016 - 2017

*Dedicated to my Family.*

**Abstract**

Durante i sei mesi passati alla Vanderbilt University in Tennessee (USA) nel laboratorio di ingegneria elettrochimica, è stato portato avanti lo studio sulla fabbricazione di elettrodi per PEM Fuel Cells tramite la tecnica di electrospinning la quale permette di ottenere fibre polimeriche che fungono inoltre da supporto al catalizzatore per la reazione di ossido-riduzione.

L'obiettivo del progetto è stato quello di avanzare un'analisi dettagliata sull'influenza dei singoli o insieme di solventi sulle prestazioni degli elettrodi.

Lo studio ha condotto all'identificazione di parametri chiave per la produzione di fibre ad alte rese, quali viscosità e punto di ebollizione della soluzione da elettrofilare. Sono stati valutati diversi solventi della famiglia degli alcoli quali: metanolo, etanolo, n-propanolo, iso-propanolo e etilene glicole.

La miscela composta da parti uguali di acqua distillata e iso-propanolo ha dato le migliori rese all'inizio della vita, e una più lenta degradazione dopo processi di corrosione del carbonio, mantenendo prestazioni elevate. Le fibre ottenute hanno dimostrato di avere prestazioni a 0.65 $V$ fino al 35% migliori rispetto a quelle ottenute negli studi precedenti, con una perdita di resa di solo il 24% dopo 1000 cicli di carbo-corrosione. Inoltre un grande miglioramento è stato osservato in ambiente a bassa umidità, dove la scarsa presenza di acqua non riesce a mantenere la membrana umidificata, diminuendone drasticamente le prestazioni.

**Abstract**

During the six months spent in Vanderbilt University in Tennessee (USA) in the electrochemical engineering laboratory, a study on the manufacture of electrodes for PEM Fuel Cells has been carried out. To do that the electrospinning technique has been adopted, which allows to obtain polymer fibers which also act as support to the catalyst for the reaction of oxidation-reduction.

The goal of the project was to advance a detailed analysis on the influence of the individual or set of solvents on electrode performance.

The study led to the identification of key parameters for the production of high-yield fibers, such as viscosity and boiling point of the electrospinning ink. Several Alcohol solvents have been evaluated, such as methanol, ethanol, n-propanol, iso-propanol and ethylene glycol.

The mixture composed of equal parts of distilled water and iso-propanol gave the best yields at the beginning of life, and a slower degradation after carbon corrosion processes, while maintaining high performance. The obtained fibers have been shown to have performance at 0.65 $V$ up to 35 % better than those obtained in previous studies, with a loss of yield of only 24% after 1000 carbon corrosion cycles. In addition, a great improvement was observed in a low humidity environment, where the lack of the presence of water is unable to maintain the membrane humidified, thus decreasing the performance dramatically.

# Contents

# Chapter 1

# Introduction

Fuel cells and more specifically the hydrogen/air proton exchange membrane (PEM) fuel cell is a promising candidate for automotive power plants due to its high power output, moderate operating temperature, and quick start-up. The successful integration of a sizable fleet of Electric Vehicles into the transportation sector would greatly diminish localized air pollution and alleviate our dependence on depleting oil reserves. Presently, mass commercialization of fuel cell vehicles is challenging due in large part to issues related to the cost and durability of membrane-electrode-assemblies (MEAs)[1].

A principal strategy to reduce the cost of MEAs is to minimize the amount of the platinum catalyst in the electrodes without sacrificing power generation. In this regard, recent R&D efforts have been directed at the investigation of platinum metal alloys[2], coreshell nanostructures[3], and the use of platinum-free metal-nitrogen-carbon catalysts[4,5]. Although these studies have shown some promise in terms of catalytic activity and potential cost savings, they do not currently meet automotive power density and durability targets. Carbon support corrosion in Pt/C catalysts during fuel cell start-up/shut-down is another ongoing issue that has drawn considerable research attention. In particular, when a hydrogen-air mixture is present in the anode during start-up, the cathode potential spikes as high as 1.5 V vs. SHE, resulting in severe carbon corrosion of the cathode catalyst layer[6].

Researchers have worked to mitigate carbon corrosion at the materials level by investigating catalyst that can better withstand the harsh automotive operating environment. Current efforts are focused on metal oxides and thermally treated carbon supported catalysts[7–10].

Another potential strategy to improve the power density and durability of fuel cell electrodes is to alter the catalyst electrode morphology. Electrospinning is a potentially useful technique for creating nanostructured fuel cell electrodes with superior catalyst utilization and long-term durability. The method is well documented for creating various fibrous polymeric materials for lithium battery separators[11], filtration media medical and pharmacological products[12,13], textiles[14], and sensors[15,16]. Pintauro and co-workers have

used ionomer electrospinning to fabricate a series of proton-exchange and anion-exchange membranes for fuel cell applications with excellent ionic conductivity, moderate water swelling, and good mechanical properties.[17,18]

In the present thesis, new results are presented on nanofiber electrode MEAs for hydrogen/air fuel cells. The work is an extension of the very promising results published by Zhang and Pintauro[19], who showed:

1. one can electrospin cathode nanofiber mats composed of Pt/C powder with an ionomer binder;

2. electrospun nanofiber cathodes with a Pt loading of $0.1 - 0.4\ mg_{Pt}/cm^2$ performed very well ;

3. the nanofiber cathode exhibited superior long-term durability, as compared to a traditional decal cathode;

The excellent performance of nanofiber fuel cell electrodes is attributed to facile oxygen and proton transport to catalytic sites and efficient product water removal, which is a direct consequence of the unique nanofiber electrode morphology, with significant inter-fiber and intra-fiber porosity and a well-mixed dispersion of catalyst powder and ionomer binder.

In the present study, both cathodes and anodes have been fabricated by electrospinning an alcohol/water suspension of Pt/C catalyst powder with a binder composed of Nafion® polymer and poly(acrylic acid) (PAA). Fuel cell power output was correlated with:

- the overall Pt loading of a fibrous electrospun cathode;

- various operating conditions including different temperatures and backpressures.

The aim of the project was to investigate the influence of different solvents on fibers preparation. The electrospinning ink is composed by:

- Water/alcohol solvents;

- Platinum catalyst on Carbon support;

- Ionomer and carrier Polymers;

The goal of this research has been to find out the best solvents composition for high performance fibers fabrication, while maintaining the other ink's components fixed. In order to do that, the focus of this study was to prepare several inks with different solvents, bringing to the attention on the physical properties of each solvent.

It is very important to underline that solvents physical properties are not the only factor that can provide the final shape and quality of fibers. For example solubility

relationship between solvents and Polymers is not investigated, since the topic is delicate. In fact the chemical structure of the Nafion consists of a hydrophobic perfluorocarbon backbone and hydrophilic vinylether side chains terminated with sulfonic acid groups. The two structures are incompatible and have dual solubility parameters.

In this thesis qualitative and quantitative tests have been done, giving particularly attention to fibers shape and maximum power reached at the beginning and at the end of life. Besides the maximum power, also the MEA behaviour at 0.65 $Volts$ it was extracted from data, which is a compromise between efficiency and power generation. The efficiency of a fuel cell is directly proportional to the operating voltage (the higher the voltage, the higher the efficiency). However, at high voltages, current density is low and therefore power is low. Maximum power occurs at lower voltages (usually around 0.5 $V$ and or 0.45 $V$). It's an industry standard to consider 0.65 $V$. Though recently some companies are considering even higher voltages for operation.

At the end of the project, the data collected has been compared with previous Vanderbilt studies, and more specifically with "Brodt, M., T. Han, N. Dale, E. Niangar, R. Wycisk, and P. Pintauro (2015) *Fabrication, in-situ performance and durability of nanofibers fuel cell electrodes* Journal of the Electrochemical Society, 162, F84-F91" paper. On this paper, a thorough study on fibers vs. others type of electrodes has been done. The outcome was that fibers have better performance and better durability than a slurry or sprayied GDE.

Starting from this premise, the goal of the six months research experience in Vanderbilt has been to improve electrodes performance by focusing on some parameters (solvents) in order to better understand the very complex electrospinning mechanism.

# Chapter 2

# PEM Fuel Cell Theory

In the XXI Century more than 80% of world energy demand is supplied with fossil fuels[20]. Two main problems have to be faced:

1. In the very next period there will be a gap between demand and production of fluid fuels;

2. The environment is seriously compromised because of the use of fossil fuels, leading to global warming, climate changes, melting of ice caps, rising sea levels, acid rains, ozone layer deplation and so on;

To avoid the environmental problems over mentioned, new energy sources have to be investigated. Early in the 1970s Hydrogen Energy System had been proposed as a solution of these two interconnected global problems. Hydrogen is as excellent energy carrier with many unique properties. It is the lightest, most efficient and cleanest fuel. One of its unique properties is that through electrochemical processes, it can be converted to electricity in fuel cells with higher efficiencies than conversion of fossil fuels to mechanical energy in internal combustion engines or to electrical energy in thermal power plants. For this reason, Hydrogen Fuel Cells have been selected as one of the best choice for the future in the automotive power plant. That's because Hydrogen Fuel Cells are electrochemical engines, not heat engines, and as such they are not subject to Carnot Cycle limitations. Several types of fuel cells have been researched in over 40 years, such as alkaline fuel cells, solide oxide fuel cells, molten carbonate fuel cells, phosphoric acid fuel cells, proton exchange fuel cells etc. The automotive industry requires fuel cells that are small in volume, light in weight, low temperature functioning, and small thermal losses. To match all those requests the Proton Exchange Membrane fuel cells (PEM) has been selected. For this reason, all the buses and cars, using this new clean technology, are powered with PEM fuel cells.

## 2.1 What is a Fuel Cell?

The conversion of fossil fuels to electrical energy in thermal power plants involves several energy conversion steps:

- Combustion of fuel converts chemical energy of fuel into heat;
- The heat is then used to boil water and generate steam;
- Steam is used to run a turbine in a process that converts thermal energy into mechanical energy;
- In the last step, mechanical energy is used to run a generator that produces energy;

A fuel cell is an electrochemical energy converter that converts chemical energy of fuel into DC electricity in a single step, circumventing all these processes and without any moving parts.

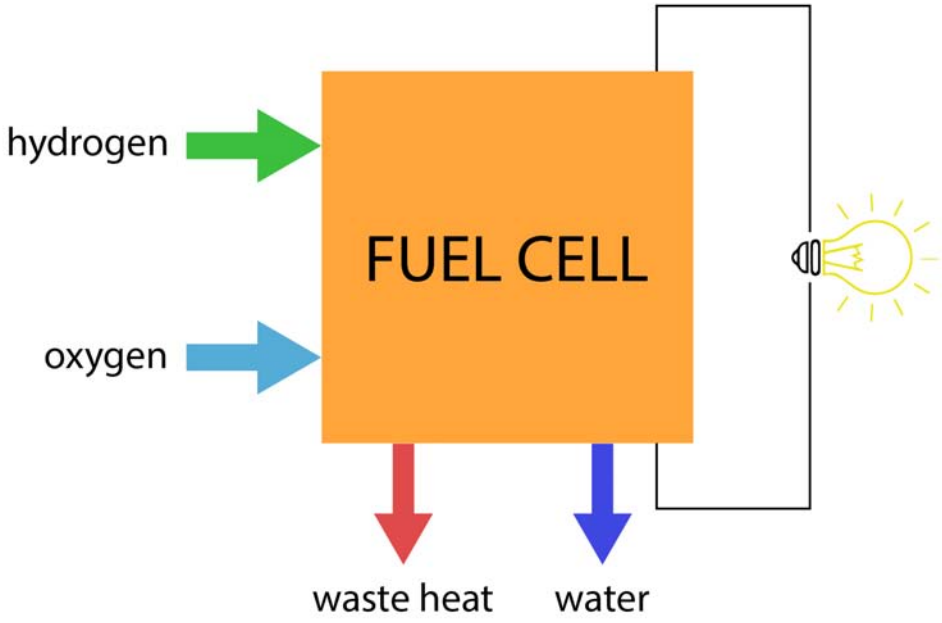


Figure 2.1: Fuel cell generates DC electricity from fuel in one step

Unfortunately fuel cells don't have only benefits, some drawbacks are listed below:

- Hydrogen fuel cells are extremely expensive to manufacture. However, just like other new technologies, their costs would come down to price levels that are affordable by normal consumers with mass production. Now, we are in a transition period, where many fuel cell manufacturers are investing literally hundreds of millions of dollars in gearing up for mass manufacturing and, at the same time, trying to develop a variety of markets for such products. Though these cells' price is seen as a great disadvantage, things are changing now;

- Hydrogen fuel cells are incredibly sensitive to high temperatures and contamination from outside elements, which means that they would easily overheat, break down and malfunction than other battery technologies;

- They cannot be stored conveniently; vehicles powered by hydrogen are safe for the environment, but certain parameters, such as storage, costs incurred in vehicle infrastructure, vehicle weight and safety measures, might still be in the works. Also, their supply needs to be replenished continuously for them to work;

- They use complex infrastructure. The major issue with hydrogen fuel cells is the infrastructure involved in their creation. They run on hydrogen, and the fueling stations, pipelines, truck transport and hydrogen generation plants are way too complex and costly

So why do we need fuel cells?

1. Promise of high efficiency, because the fuel cell efficiency is much higher than the efficiency of internal combustion engines, fuel cells are attractive for automobile application;

2. Promise of low or zero emissions, the only exhaust is unused air and water (in the case of PEMFC). This may be attractive not only for transportation but also for many indoor applications;

3. Fuel cells may be made in a variety of sizes, from microwatts to megawatts, which makes them useful in a variety of applications, from powering electronic devices to powering entire buildings;

4. No moving parts and promise of long life. Fuel cell durability must be improved to reach a minumum life time at stationary power of no less than 60.000-80.000 hours;

5. Fuel cells are by their nature modular, more power may be generated simply by adding more cells;

6. Fuel cells are inherently quiet, which may make them attractive for a variety of applications;

7. National security: fuel cells use hydrogen as fuel. Although hydrogen is not a readily available fuel it may be produced from indigenous sources, either by electrolysis of water or by reforming hydrocarbon fuels. Use of indigenous sources to generate hydrogen may significantly reduce dependence on foreign oil, which would have a positive impact on national security;

## 2.2 Fuel Cell basic Chemistry and Thermodynamics

A fuel cell is an elctrochemical energy converter. It converts chemical energy of fuel, typically hydrogen, directly into electrical energy. As such, it must obey the laws of thermodynamics.

**Basic reactions**

The electrochemical reactions in fuel cells happen simultaneously on both sides of membrane (the anode and the cathode). The basic fuel cell reactions are:

At the anode:

$$H_2 \longrightarrow 2H^+ + 2e^- \tag{2.1}$$

At the cathode:

$$\frac{1}{2}O_2 + 2H^+ + 2e^- \longrightarrow H_2O \tag{2.2}$$

Overall:

$$H_2 + \frac{1}{2}O_2 \longrightarrow H_2O \tag{2.3}$$

These reactions may have several intermediate steps, and there may be some (unwanted) side reactions.

**Heat of Reaction**

The overall reaction is the same as the reaction of hydrogen combustion. Combustion is an exothermic process, which means that there is energy releaed in the process:

$$H_2 + \frac{1}{2}O_2 \longrightarrow H_2O + heat \tag{2.4}$$

The heat (or entalphy) of a chemical reaction is the difference between the heats of formation of products and reactants. For the previous Equation this means:

$$\Delta H = (h_f)_{H2O} - (h_f)_{H2} - \frac{1}{2}(h_f)_{O2} \tag{2.5}$$

Heat of formation of liquid water is $-286 kJ mol^{-1}$ (at 25 °C) and heat of formation of elements is by definition equal to zero. Therefore:

$$\Delta H = (h_f)_{H2O} - (h_f)_{H2} - \frac{1}{2}(h_f)_{O2} = -286 kJ/g - 0 - 0 = -286 kJ mol^{-1} \tag{2.6}$$

The negative sign for enthalpy of a chemical reaction means that heat is being released in the reaction, that is, this is an exothermic reaction. Equation may now be rewritten as:

$$H_2 + \frac{1}{2}O_2 \longrightarrow H_2O(l) + 286 kJ/mol \tag{2.7}$$

This equation is valid at 25 °C only.

**Theoretical Fuel Cell Potential**

In general, electrical work is a product of charge and potential:

$$W_{el} = q \cdot E \tag{2.8}$$

where:

$W_{el} = electrical\ work$
$q = charge\ (Coulombs\ mol^{-1})$
$E = potential\ (Volts)$

The total charge transferred in a fuel reaction per mol of $H_2$ consumed is equal to:

$$q = n \cdot N_{Avg} \cdot q_{el} \tag{2.9}$$

where :

$n = number\ of\ electrons\ per\ molecule\ of\ H_2 = 2 electrons\ per\ molecule$
$N_{Avg} = number\ of\ molecules\ per\ mole\ (Avogadro's\ number) = 6{\times}10^{23}\ molecules/mole$
$q_{el} = charge\ of\ 1\ electron = 1.602 \times 10^{-19}\ Coulombs/electron$

The product of Avogadro's number and charge of 1 electron is known as Faraday's constant:

$$F = 96,465\ Coulombs/(electron \cdot mol) \tag{2.10}$$

Electrical work is therefore:

$$W_{el} = n \cdot F \cdot E \tag{2.11}$$

The maximum amount of electrical energy generated in a fuel cell corresponds to Gibbs free energy, $\Delta G$:

$$W_{el} = -\Delta G \tag{2.12}$$

The theoretical potential of fuel cell is then:

$$E = \frac{-\Delta G}{n \cdot F} \tag{2.13}$$

Because $\Delta G$, $n$, $F$ are all known, the theoretical fuel cell potential of hydrogen/oxygen can also be calculated:

$$E = \frac{-\Delta G}{n \cdot F} = \frac{237,340}{2 \cdot 96,485} \frac{Jmol^{-1}}{Asmol^{-1}} = 1.23\ Volts \tag{2.14}$$

At 25 °C , the theoretical hydrogen/oxygen fuel cell potential is 1.23 Volts.

### Effect of Temperature

The theoretical cell potential changes with temperature:

$$E = -\left(\frac{\Delta H}{n \cdot F} - \frac{T\Delta S}{n \cdot F}\right) \tag{2.15}$$

An increase in the cell temperature results in a lower theoretical cell potential. Note that both $\Delta H$ and $\Delta S$ are functions of temperature:

$$h_t = h_{298.15} + \int_{298.15}^{T} c_p dT \tag{2.16}$$

$$s_t = s_{298.15} + \int_{298.15}^{T} \frac{1}{T} c_p dT \tag{2.17}$$

Specific heat of any gas is aslo a function of temperature. An empirical relationship may be used:

$$c_p = a + bT + cT^2 \tag{2.18}$$

where $a$, $b$ and $c$ are the empirical coefficients, different for each gas.

At temperature below 100 °C, changes in $C_p$, $\Delta H$ and $\Delta S$ are very small, but at higher temperatures, such as those experienced in solid oxide fuel cells, they must not be neglected.

However, in operating fuel cells, in general, a higher cell temperature results in a higher cell potential. This is because the voltage losses in operating fuel cells decrease with temperature, and this more than compensates for the loss of theoretical cell potential.

### Theoretical Fuel Cell Efficiency

The efficiency of any energy conversion device is defined as the ratio between useful energy output and energy input.

in the case of a fuel cell, the usefull energy output is the electrical energy produced, and energy input is the enthalpy of hydrogen, that is, hydrogen's higher heating value. Assumed that all of the Gibbs free energy can be converted into electrical energy, the maximum possible (theoretical) efficiency of a fuel cell is:

$$\eta = \frac{\Delta G}{\Delta H} = \frac{237.34}{286.02} = 83\% \tag{2.19}$$

If both $\Delta G$ and $\Delta H$ in Equation 2.19 are divided by $nF$, the fuel cell efficiency may be expressed as a ratio between two potentials:

$$\eta = \frac{-\Delta G}{-\Delta H} = \frac{\frac{-\Delta G}{nF}}{\frac{-\Delta H}{nF}} = \frac{1.23}{1.482} = 0.83 \tag{2.20}$$

where:

$\frac{-\Delta G}{nF} = 1.23\ V$ is the theoretical cell potential

$\frac{-\Delta H}{nF} = 1.482\ V$ is the potential corresponding to hydrogen's higher heating value, or the thermoneutral potential.

**Effect of Pressure**

A fuel cell may operate at any pressure, typically from atmospheric all the way up to 6-7 bar. For an isothermal process, the change in Gibbs free energy may be shown to be:

$$dG = V_m dP \tag{2.21}$$

where:

$V_m$ = molar volume, $m^3 mol^{-1}$ $P$ = pressure, $Pa$

For an ideal gas:

$$PV_m = RT \tag{2.22}$$

Therefore:

$$dG = RT\frac{dP}{P} \tag{2.23}$$

After integration:

$$G = G_0 + RT \ln\left(\frac{P}{P_0}\right) \tag{2.24}$$

Where $G_0$ is Gibbs free energy at standard temperature abd pressure (25 °C and 1 atm), and $P_0$ is the reference or standard pressure (1 atm).

For any chemical reaction:

$$jA + kB \longrightarrow mC + nD \tag{2.25}$$

The change in Gibbs free energy is the change between products and reactants:

$$\Delta G = mG_C + nG_D - jG_A - kG_B \tag{2.26}$$

After substituting into Equation (2.24):

$$\Delta G = \Delta G_0 + RT \ln\left[\frac{\left(\frac{P_C}{P_0}\right)^m \cdot \left(\frac{P_D}{P_0}\right)^n}{\left(\frac{P_A}{P_0}\right)^j \cdot \left(\frac{P_B}{P_0}\right)^k}\right] \tag{2.27}$$

This is known as the Nerst equation, where $P$ is the partial pressure of the reactant or product species and $P_0$ is the reference pressure.

for the hydrogen/oxygen fuel cell reaction, the Nerst equation becomes:

$$\Delta G = \Delta G_0 + RT \ln\left(\frac{P_{H2O}}{P_{H_2} P_{O2}^{0.5}}\right) \tag{2.28}$$

By introducing Equation 2.15 into Equation 2.29:

$$E = E_0 + \frac{RT}{nF} \ln\left(\frac{P_{H_2} P_{O2}^{0.5}}{P_{H2O}}\right) \tag{2.29}$$

Note that the previous equations are only valid for gaseous products and reactants. When liquid water is produced in a fuel cell, $P_{H2O} = 1$. From Equation 2.37 it follows that at higher reactant pressures the cell potential is higher. Also, if the reactants are diluted,

for example, if air is used instead of pure oxygen, their potential is lower. In case of air vs. Oxygen, the theoretical voltage loss/gain is:

$$\Delta E = E_{O2} - E_{Air} = \frac{RT}{nF} \ln \left( \frac{P_{O2}}{P_{Air}} \right)^{0.5} = \frac{RT}{nF} \ln \left( \frac{1}{0.21} \right)^{0.5} \tag{2.30}$$

At 80 °C this voltage gain/loss becomes 0.012 V.

**Summary**

The ideal cell potential, if all Gibbs free energy is utilized, is:

$$\Delta E_{25\,^\circ\mathrm{C},1atm} = \frac{-\Delta G}{nF} = \frac{237,340}{2 \cdot 96,485} \frac{Jmol^{-1}}{Asmol^{-1}} = 1.23\ Volts \tag{2.31}$$

Cell potential is a function of temperature and pressure:

$$E_{T,P} = -\left( \frac{\Delta H}{nF} - \frac{T\Delta S}{nF} \right) + \frac{RT}{nF} \ln \left[ \frac{P_{H2} P_{O2}^{0.5}}{P_{H2O}} \right] \tag{2.32}$$

Ignoring the changes of $dH$ and $dS$ with temperature (which has a very small error for temperatures below 100 °C), this equation becomes:

$$E_{T,P} = 1.482 - 0.000845T + 0.0000431T \ln(P_{H2} P_{O2}^{0.5}) \tag{2.33}$$

For example, a hydrogen/air fuel cell, operating ar 60 °C with reactant gases at atmospheric pressure and with liquid water as a product, is expected to have a potential of:

$$E_{T,P} = 1.482 - 0.000845 \times 333.15 + 0.0000431 \times 333.15 \ln(1 \times 0.21^{0.5}) = 1.189\ V \tag{2.34}$$

The ideal fuel cell efficiency is:

$$\eta = \frac{\Delta G}{\Delta H} = \frac{237.34}{286.02} = 83\% \tag{2.35}$$

The ideal efficiency decreases with temperature. In the case we are operating at 60 °C, the ideal efficiency of a hydrogen/air fuel cell is:

$$\eta = \frac{E_0}{1.482\ V} = \frac{1.189}{1.482} = 80\% \tag{2.36}$$

## 2.3 How does a PEM Fuel Cell works?

A proton exchange membrane fuel cell (PEMFC) is an electrochemical device that directly converts chemical energy into electricity, as opposed to a spark ignition internal combustion engine, which burns a fuel to create heat that is converted into mechanical energy. With hydrogen as the energy carrier, a PEMFC can operate at thermodynamic efficiencies over 55%, compared to internal combustion engines that have efficiencies around 20%[21]. This is one of the primary advantages of fuel cells.

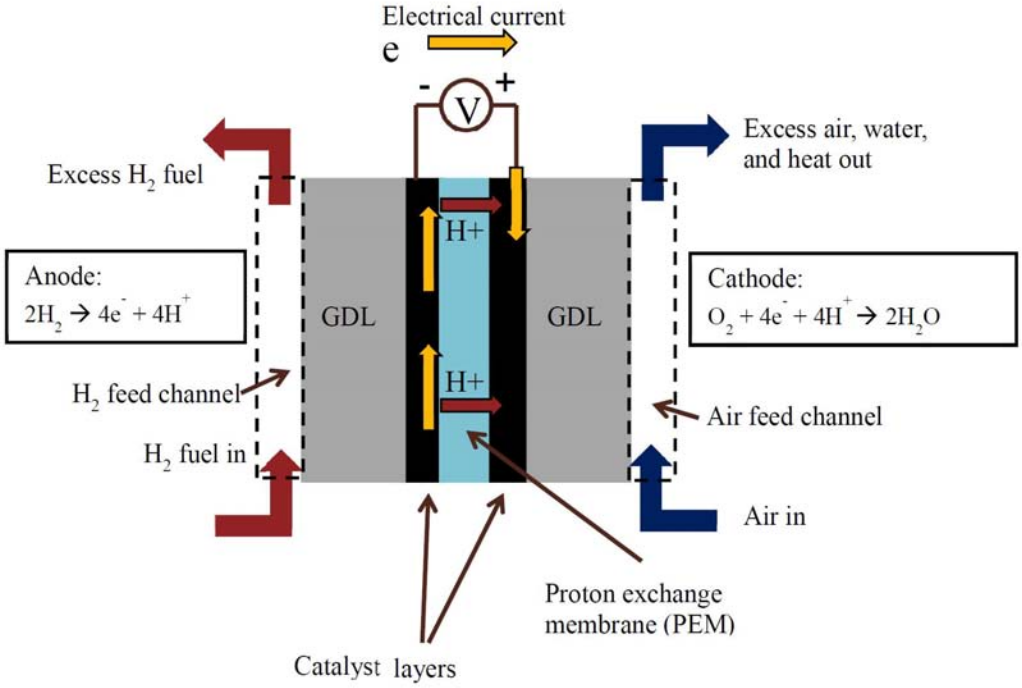


Figure 2.2: Schematic of a typical PEMFC

A hydrogen/air PEMFC cell schematic is shown in Figure 2.2. At the anode, hydrogen gas is electrochemically oxidized to protons and electrons. The protons travel through the proton exchange membrane (PEM), while electrons travel through an external circuit where a portion of their energy is extracted to generate power. At the cathode, oxygen reacts with electrons and protons from the anode in a reduction reaction to form water. Porous carbon, electrically conductive layers with specific/controlled hydropho-

bic/hydrophilic properties, known as the gas diffusion layers (GDLs) are attached to the electrodes. The structure consisting of the membrane, electrodes, and GDLs is known as a membrane-electrode-assembly (MEA). The GDLs allow passage of gases, aid in water management at the electrode surface, and electrically connect the electrodes to the bipolar plates (graphitic or metallic plates that separate but electronically connect cells) in a fuel cell stack (an assembly of cells that produce a higher voltage and power than a single cell). The standard material for the PEM is Nafion, a perfluorosulfonic acid ion exchange polymer with excellent thermal and chemical stability that was developed by DuPont in the 1960's[22]. In a hydrogen/air PEMFC, the kinetics of the oxygen reduction reaction (ORR) are much slower than hydrogen oxidation, thus the cathode is the problematic electrode and is the focus of most research studies.

Presently, the most common catalyst for the anode and cathode of a hydrogen/air PEMFC is platinum supported on carbon powder. A proton-conductive ionomer is dispersed with the Pt/C powder to bind the particles to one another and to the membrane. A schematic picture of a catalyst layer, located between the membrane and GDL (the GDL is shown as electronically conductive fibers) in an MEA is shown in Figure 2.3. To efficiently utilize Pt during fuel cell operation, the "triple phase" contact area must be maximized, where catalyst (for reaction sites), ionomer (for delivery of protons) and void space (for gas delivery and removal of product water) meet[23].

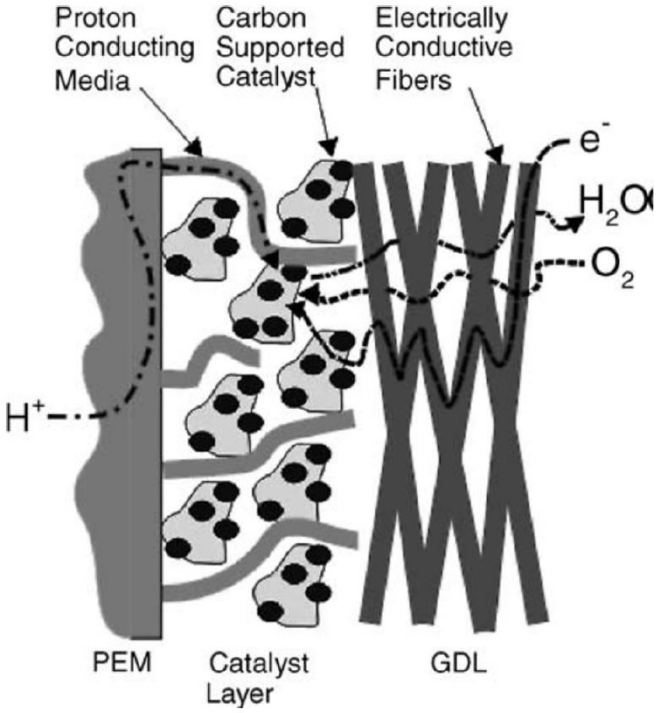


Figure 2.3: Schematic half of an MEA, depicting membrane, electrode as well as gas diffusion layer.

**Cathode Characterization**

The most common method to assess the performance of the cathode in an MEA is to collect current-voltage polarization data, where the results are plotted as cell potential verse current density. These are steady-state measurements under constant load, where either a voltage is recorded at a set current (galvanostatic operation) or a current is recorded at a set voltage (potentiostatic operation) for each data point. The voltage is the potential difference between the two half cells (hydrogen oxidation at the anode and oxygen reduction at the cathode). As hydrogen is oxidized and oxygen is reduced, electrons travel from the anode to the cathode, producing current. In pure oxygen, the theoretical (thermodynamic) voltage of the four-electron oxygen reduction reaction is 1.23 V vs. a standard hydrogen reference electrode (SHE) when operating at 25 °C and 1 atm oxygen. In a hydrogen/air fuel cell, this potential cannot be achieved at open circuit (zero current) because of finite feed gas crossover through the electrolyte membrane (most notably, H2 from the anode to the cathode) and because the reversible open circuit voltage is a function of oxygen partial pressure and air is only 21% oxygen. The crossover of hydrogen fuel causes a mixed reaction at the cathode (hydrogen oxidation and oxygen reduction) that reduces the voltage from the thermodynamic ideal value. During steady-state current flow (i.e., during power generation) the voltage decreases further due to various overpotentials, which are explained below.

A fuel cell steady-state polarization curve generally has three distinct regions which are characterized by the primary source of voltage loss (due to overpotentials). A typical curve is depicted in Figure 2.4. At high potentials (and low current densities) activation (kinetic) losses of the ORR dominate. This region follows a non-linear Tafel behavior (an exponential drop in voltage with current density). The kinetics of the hydrogen oxidation reaction at the anode are much faster than the ORR, so the polarization curve kinetic voltage losses originate solely from the cathode reaction[24]. The second region of a fuel cell polarization curve at higher current densities (and lower voltages) is dominated by ohmic losses (resistances) in the membrane and electrode, losses are associated with finite transport rates for protons from the catalyst sites in the anode to sites within the cathode, through the membrane and electrode layer. Voltage losses associated with finite conductivity follow Ohm's law, thus they scale linearly with current density, as can be seen from the straight line region in the V-i polarization plot in the ohmic region. In the third region of the polarization curve (at very high current densities), mass transfer effects dominate. Here, the cathode reaction is oxygen diffusion-limited as the reactant (O2) concentration at the electrode surface becomes significantly lower than that of bulk air. Oxygen mass transfer limitations can be caused by any one of a number of effects, such as insufficient air flow rates, low catalyst layer porosity, and water accumulation in the cathode [25]. In order to minimize oxygen diffusion limitations, high stoichiometric air flow rates are often used, in which much more oxygen is fed to the cathode than is

consumed in the ORR. High air flow rates maintain higher concentrations of oxygen near the Pt surface and also help to remove water generated in the cathode. There are no mass transfer limitations at the anode in a PEMFC because the feed is pure hydrogen gas.

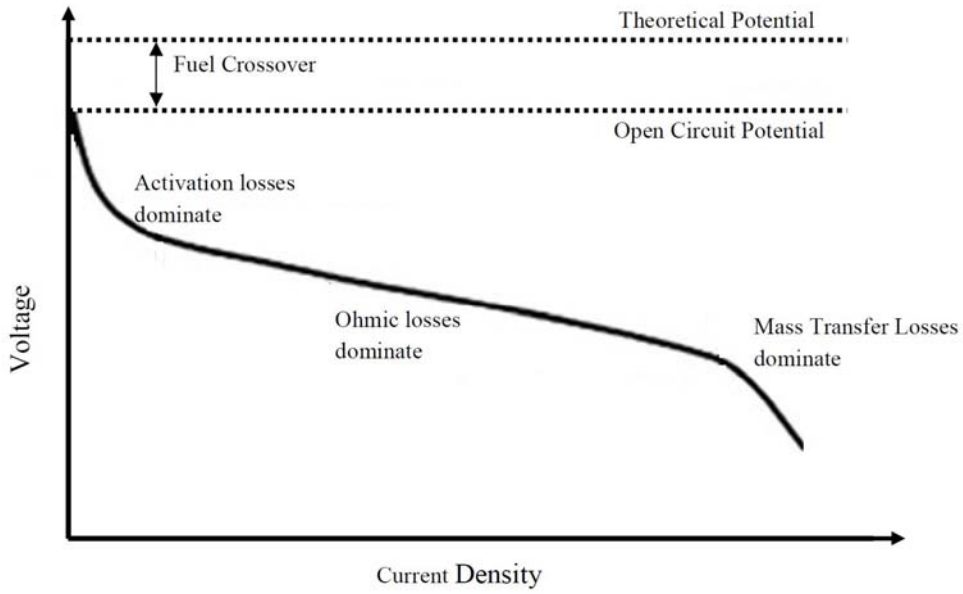


Figure 2.4: Typical polarization curve of a PEMFC with a hydrogen/air feed.

The accessible Pt surface area of an MEA cathode is often less than the actual surface area of the Pt on Pt/C powder due to imperfect triple-phase boundaries. Only metal surfaces in close contact with oxygen, electrons and protons contribute to catalysis and power generation [26]. The electrochemical surface area (ECA) of the Pt in a PEMFC cathode can be measured by in-situ cyclic voltammetry (CV), where the charge (integrated current) associated with hydrogen gas oxidation and reduction on catalyst sites is measured. The Pt surface area is calculated by assuming the charge required to reduce one monolayer of hydrogen atoms on Pt is $210\mu C/cm^2$. It is always assumed that the ECA measured via equation 2.37 is the same area available for oxygen reduction (i.e. $O_2 + 4H^+ + 4e^- \longrightarrow 2H2O$).

$$Pt - H_{ads} \longrightarrow Pt + H^+ + e^- \tag{2.37}$$

In a traditional/conventional Pt/C fuel cell cathode (made by painting a catalyst-binder-solvent ink on a GDL), the Pt ECA varies between 13 and $72m^2/g$, depending on the type/source of Pt/C catalyst powder as well as the binder loading and type of binder[27]. Even though the high potential region in a polarization curve is dominated by activation (kinetic) losses at the cathode, mass transfer losses can effect power output for cell voltages as high 0.8 $V$ when the cathode feed gas is air[28]. Thus, the kinetics of the oxygen reduction reaction in a fuel cell MEA are studied/measured using pure oxygen as the cathode feed and at a low current densities to minimize oxygen mass transfer effects. Nor-

mally, the oxygen reduction reaction rate is quantified in terms of a mass activity which is reported as current per mass of Pt at a given fuel cell potential, temperature, and oxygen partial pressure. The Tafel slope for the oxygen reduction reaction at an MEA cathode is obtained from the slope of a voltage vs. log(current) curve after the measured voltage is corrected for membrane ohmic resistance and the measured current is corrected from the current loss associated with hydrogen gas crossover from the anode to the cathode. A typical Tafel slope for the four-electron oxygen reduction reaction in PEMFC at 80 °C is $70 mV/decade$. This value can increase if there is a significant contribution of the undesired two-electron transfer pathway in which oxygen is reduced to hydrogen peroxide, or if the Pt surface has oxide layers[29]. The Tafel slope can also be used to calculate the exchange current density, which is the current density at zero overpotential and a quantification of catalyst activity.

**PEMFC Electrode Development**

*PTFE-bound Catalyst Layer*

In the 1960's, first-generation catalyst layers for PEMFC MEAs used Pt black (unsupported Pt) bound with polytetrafluoroethylene (PTFE, e.g. DuPont's Teflon ®)[30]. These were designed for H2/O2 fuel cells and used as auxiliary power on space missions. Pt black was mixed with a PTFE emulsion and spread on a carbon paper GDL, which was subsequently hot-pressed to either a sulfonated polystyrene membrane or, later in the mid 1960's, a more stable Nafion membrane. The PTFE fixed the Pt to the GDL and its hydrophobicity aided in water management at the cathode by preventing excess water accumulation (flooding). During the Gemini space flights in the 1960's, 3 stacks of 32 MEAs produced 620 W. The platinum loading was $28 mg/cm^2$ [31]. Thus, these early electrodes produced high power, but with very high amounts of Pt catalyst. MEAs showed good durability over a timeframe of days, and only minimal power losses were reported. However, these electrodes were not subjected to the harsh voltage cycling durability testing methods that are performed today.

*Catalyst Layers with Nafion*

The performance of PTFE-bound electrodes was improved when they were brushed with a Nafion dispersion, which dripped into and partially filled the porous catalyst layer (such a step is referred to as "impregnation"). The Nafion added hydrophilicity and proton conduction to the electrodes. An MEA with a Nafion-impregnated cathode and anode ($5 mgPt/cm^2$) and a Nafion membrane produced $900 mW/cm^2$ at 0.6 $V$ with humidified H2/O2 at 30 psig and 95 °C[32]. The Pt loading was reduced much further when the un-

supported Pt was replaced with a Pt/C catalyst, which increased Pt utilization[33]. With a much lower Pt loading of $0.35 mg/cm^2$, $180 mW/cm^2$ at 0.6 $V$ was produced in an H2/O2 fuel cell operating at 50 °C and 1 atmg, and $110 mW/cm^2$ were produced at 0.6 $V$ with H2/air gas feeds at the same pressure and temperature. The most common method of fabricating electrodes today for PEMFC is the thin film method, in which a carbon-supported Pt catalyst powder is dispersed with ionomer in an electrode ink (as opposed to only impregnation or the coating of an already dried catalyst layer with ionomer) in an alcohol/water solvent, and then applied directly to either the membrane (to create what is referred to as a catalyst coated membrane or CCM) or to the carbon paper gas diffusion layer (to transform the GDL into a so-called gas diffusion electrode or GDE[34]). For the CCM method, the ink may be painted or sprayed directly onto the proton conducting membrane that separates the two electrodes in a MEA or it can first be coated on an inert polymer film such as Kapton and then transferred (during a hot-pressing step) onto the membrane using the so-called "decal method"[35]. These thin film layers, which have typical Pt loadings between 0.10 and $0.5 mg/cm^2$, have been shown to produce much higher power than the Nafion-impregnated layers, and have become the present day convention. For example, a conventional thin film electrode MEA with $0.50 mgPt/cm^2$ at the cathode and anode produced $360 mW/cm^2$ at 0.6 $V$ at 70 °C with H2/air feed gases at ambient pressure[36]. However, these thin film catalyst layers have durability issues in an automotive environment, as will be described in the next section.

**Durability Issues of Pt/C Catalyst in an Automotive Environment**

Carbon has many properties than make it an excellent support for Pt-based catalysts. Carbon blacks have a high electronic conductivity and high surface area, and they are also relatively inexpensive. Small platinum particles ($\sim 3\ nm$) can be grown on carbon with a much higher active surface area than Pt black powder[37]. However, the oxidation of carbon to gaseous carbon dioxide at a potential of 0.207 V vs. SHE makes carbon thermodynamically susceptible to corrosion (oxidation) reactions throughout most of the operational voltage range of a hydrogen/air fuel cell[38].

$$C + H_2 = O \longrightarrow C - O_{ads} + 2H^+ + 2e^-, E_0 = 0.207\ V \tag{2.38}$$

$$C - O_{ads} + H_2O \longrightarrow CO_2 + 2H^+ + 2e^- \tag{2.39}$$

The presence of platinum also increases the rate of carbon corrosion because platinum

catalyzes the carbon oxidation reaction and significantly reduces the overvoltage for the reaction shown in Equation 2.39[39]. Fortunately, carbon oxidation kinetics are only fast above $\sim 1.0\ V$ vs SHE. While hydrogen/air fuel cells typically do not experience such high voltages under normal operating conditions (the open circuit voltage in a hydrogen/air fuel cell, which represents the maximum potential of the system before current flow is typically $\sim 0.95\ V$), the cathode potential can spike as high as $1.5\ V$ during the start-up of a fuel cell stack. This spike in cathode voltage is explained next. Air is typically present on both fuel cell electrodes after a long shutdown, because air enters the anode compartment by permeating across the membrane from the cathode and the remaining hydrogen in the anode is consumed by hydrogen oxidation. During start-up, when hydrogen fuel is fed to the anode, a hydrogen-air front passes through the anode. Due to this maldistribution of hydrogen, fuel-rich regions drive a "reverse current" in the fuel-starved regions[40]. During normal operation, hydrogen is consumed at the negative electrode (anode) via hydrogen oxidation and air is reduced at the positive electrode (cathode). These spontaneous reactions establish a potential difference across the cell ($\sim 0.95\ V$ at open circuit) which is normally harnessed to drive an external load. This potential difference, however, can also drive reactions that would not otherwise occur spontaneously. During start-up with an external load, localized regions of the fuel cell where the anode does not have hydrogen, but are in parallel with regions where the anode does have hydrogen, have a potential of $\sim 1.5\ V$ vs. SHE. In the fuel-starved regions, in order to simultaneously maintain current and potential difference, the respective domains reverse, and the cathode catalyst layer is utilized as fuel while oxygen on the anode side is reduced[41]. A schematic of this reverse current process is depicted in Figure 2.5, which shows a H2/air front moving through the anode on start-up (from left to right). Hydrogen is introduced in region A, which is in parallel to region B with air at the anode. Normal fuel cell operating conditions (Figure 2.6) are restored shortly after start-up when normal H2 distribution is restored[39].

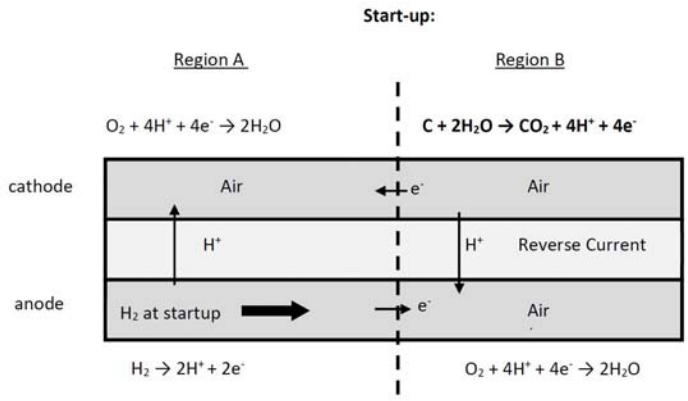


Figure 2.5: Schematic of reverse current mechanism that causes cathode carbon corrosion during fuel cell stack start-up. Localized regions with hydrogen (Region A) polarize localize regions without hydrogen (Region B)

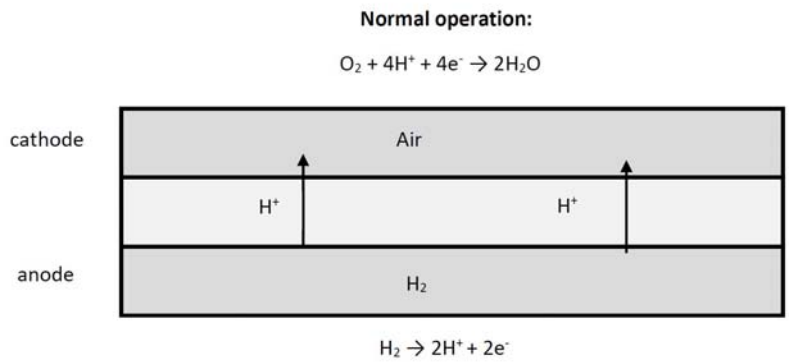


Figure 2.6: Schematic of a Normal fuel cell operation.

After many shut-down/start-ups cycles, there will be severe degradation of the cathode catalyst layer, including loss of carbon, electrode layer thinning and disintegration, and platinum nanoparticles agglomeration into larger particle sizes. These phenomena decrease the electrochemically active platinum surface area and lower the fuel cell power output. For example, a conventional thin film electrode MEA with a cathode loading of $0.50 mgPt/cm^2$ and an initial power density of $360 mW/cm^2$ at 0.6 $V$ only produced $120 mW/cm^2$ at 0.6 $V$ after 750 stop-start cycles[42]. The formation of surface oxide species on the carbon support (e.g., C=O and C-OH), as intermediate/precursor species during $CO2$ production, is also an issue. Such species make the cathode layer more hydrophilic and more prone to water flooding (excessive water build up in the cathode layer), which reduces oxygen access to active catalytic sites[43]. Engineering strategies have been sought to minimize these voltage spikes, such as using high velocity hydrogen at start-up, drying out the MEA at shut-down (carbon corrodes slower at low humidity), or using a shorting resistor to limit the cathode voltage spike, but no practical/simple solutions have emerged to eliminate the problem of carbon corrosion.

Platinum nanoparticles are also subject to electrochemical degradation during typical automotive acceleration/deceleration events but no test has been made during this research on this topic.

## 2.4 PEM Fuel Cell Components

The design of electrodes for polymer electrolyte membrane fuel cells (PEMFC) is a delicate balancing of transport media. Conductance of gas, electrons, and protons must be optimized to provide efficient transport to and from the electrochemical reactions. This is accomplished through careful consideration of the volume of conducting media required by each phase and the distribution of the respective conducting network. In addition, the issue of electrode flooding cannot be neglected in the electrode design process.

A PEM fuel cell is an electrochemical cell that is fed hydrogen, which is oxidized at the anode, and oxygen that is reduced at the cathode. The protons released during the oxidation of hydrogen are conducted through the proton exchange membrane to the cathode. Since the membrane is not electrically conductive, the electrons released from the hydrogen travel along the electrical detour provided and an electrical current is generated. These reactions and pathways are shown schematically in Figure 2.7

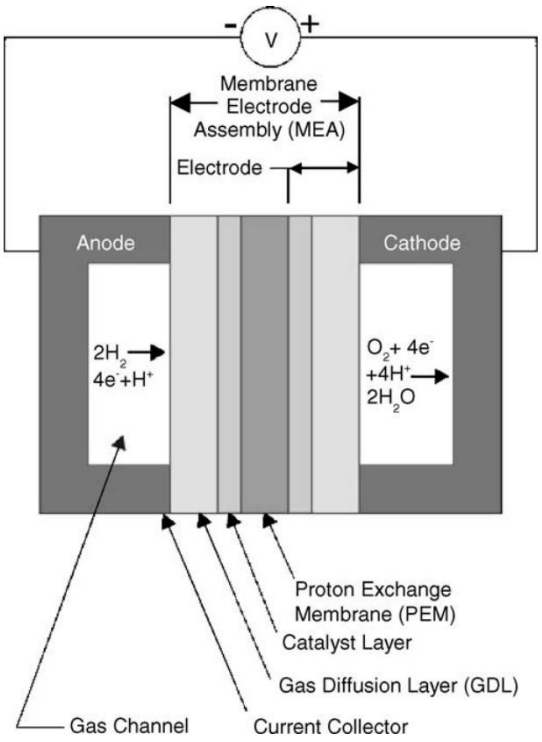


Figure 2.7: Schematic of a single typical proton exchange membrane fuel cell

At the heart of the PEM fuel cell is the membrane electrode assembly (MEA). The MEA is pictured in the schematic of a single PEM fuel cell shown in Figure 2.7. The MEA is typically sandwiched by two flow field plates that are often mirrored to make a bipolar plate when cells are stacked in series for greater voltages. The MEA consists of a proton exchange membrane, catalyst layers, and gas diffusion layers (GDL). Typically,

these components are fabricated individually and then pressed to together at high temperatures and pressures. As shown in Figure 2.7, the electrode is considered herein as the components that span from the surface of the membrane to gas channel and current collector. A schematic of an electrode is illustrated in *Figure* 2.3.

### 2.4.1 Membrane

In order for a PEM fuel cell to operate, a Proton Exchange Membrane is needed that will carry the hydrogen ions, proton, from the anode to the cathode without passing the electrons that were removed from the hydrogen atoms. These polymer membranes that conduct proton through the membrane but are reasonably impermeable to the gases, serve as solid electrolytes (vs. liquid electrolyte) for variety of electrochemical applications, and are commonly known as Proton Exchange Membrane and/or Polymer Electrolyte Membranes (PEM). These membranes have been identified as one of the key components for various consumer related applications for fuel cells, e.g. automobiles, back-up power, portable power etc. Due to its application for many consumer markets, the technology keeps on evolving to make these membranes suitable for longer duration, and even high temperature operations. For PEM fuel cell and electrolyzer applications, a polymer electrolyte membrane is sandwiched between an anode electrode and a cathode electrode. During electrochemical reaction, oxidation reaction at the anode generates protons and electrons; reduction reaction at the cathode combines protons and electrons with oxidants to generate water. To complete the electrochemical reaction, the proton exchange membrane plays a critical role that conducts protons from anode to cathode through the membrane. The proton exchange membrane also performs as a separator for separating anode and cathode reactants in fuel cells and electrolyzers[44].

There are several types of membrane to use in PEMFC. One of the most used is the Nafion®. Nafion is a sulfonated tetrafluorethylene copolymer that was discovered in the late 1960s by Dr.Walther Gustav Grot of DuPont de Nemours. The first of a class of perfluorinated ionomers—a fully fluorinated polymer material terminated at points with ionic groups—it was originally developed as a membrane material for the chlor-alkali process. The material is generated by the copolymerization of a perfluorinated vinyl ether comonomer with tetrafluoroethylene. The chemical structure of Nafion is shown Figure 2.8. The fluorinated backbone of the polymer is essentially polytetrafluoroethylene (PTFE) or Teflon® and gives Nafion exceptional resistance to harsh chemical environments, good mechanical strength, and a fairly high maximum operating temperature. Fluorinated ether linkages terminate in sulfonate groups.

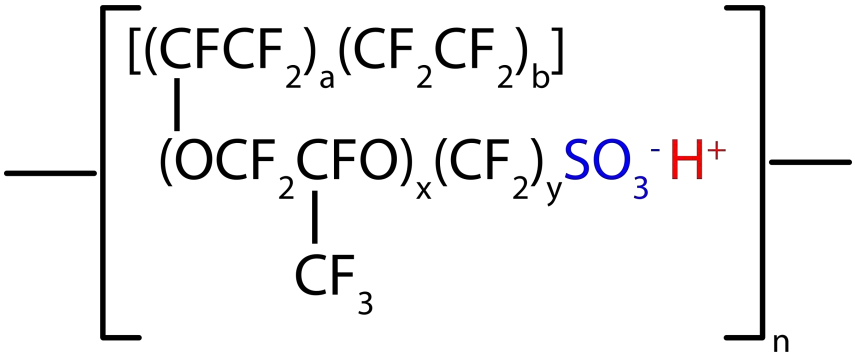

Figure 2.8: Molecular structure of Nafion

The ratio of the number of grams of polymer per mole of sulfonic acid groups of the material in the acid form and completely dry is referred to as equivalent weight (EW). Equivalent weight can be varied and strongly affects mechanical and transport properties. Increasing EW (decreasing sulfonic acid group concentration) improves mechanical properties, but decreases proton conductivity. 1,100 EW Nafion is typically used in PEM fuel cell applications since it has a reasonable balance of proton conductivity and mechanical integrity.

**Morphology**

Nafion's morphology has been investigated extensively since the early 1970s and is, to this day, a topic of debate as well as current research. However, the following general statements about Nafion's morphology can be made with reasonable confidence:

1. Nafion phase separates into distinct hydrophobic and hydrophilic regions;
2. The hydrophobic region is a continuous semi-crystalline region which is Teflon®-like, being made up of main chain TFE segments;
3. The hydrophilic regions consist of sulfonate groups, swell and change size/shape with water uptake, eventually forming a continuous network, and allow water and proton/ion transport;

**Importance of water in PEM fuel cells**

PEM fuel cells incorporating present day membrane materials require water for operation. This is because water is essential for proton conductivity in the membrane, increasing by nearly 6 orders of magnitude from dry to fully hydrated. Water is usually introduced at the anode and cathode with humidifying the gas feeds. Water is also produced at the cathode as part of the overall reaction.

If liquid water forms at the catalyst surface, so-called "flooding" occurs. This is the result of liquid water at the catalyst surface blocking the transport of fuel/oxidant to

the catalyst surface. It is for this reason that electrodes are typically wet-proofed with PTFE. Water management in PEM fuel cells is one of the major engineering hurdles in their commercialization.

Water moves by convection and diffusion to the membrane surface where it enters the membrane and travels by diffusion through the membrane. Water can reach the membrane surface in the vapor or liquid phase. Diffusion of water through the membrane is driven by chemical potential gradients, or differences in water activity. Diffusion is the main process by which differences in water activity in the membrane are equalized. Water uptake by and transport though Nafion are critically important for determining the steady state and dynamic response of fuel cells. To properly understand and model fuel cell behavior in order to optimize operation and design fuel cell systems, water transport must be properly understood.

#### Mechanical properties of membrane

The mechanical properties of membranes in PEM fuel cells are important to their performance, both in the long and short term. In the short term, uptake of water is partially controlled by polymer relaxation. In the long term, membrane creep caused by clamping pressure and swelling due to water uptake can cause delamination of electrodes from the membrane as well as pin hole formation due to membrane thinning. The mechanical properties of Nafion are strongly dependant on temperature and hydration[45].

During the research in Vanderbilt University only Nafion® 211 has been used.

### 2.4.2 Gas Diffusion Layer

The Gas Diffusion Layer (GDL) is a very important supporting material in a Membrane Electrode Assembly (MEA). Gas diffusion layers are a porous material composed of a dense array of carbon fibers, which also provides an electrically conductive pathway for current collection. GDL plays an important role of electronic connection between the bipolar plate with channel-land structure and the electrode. In addition, the GDL also performs the following essential functions: passage for reactant transport and heat/water removal, mechanical support to the membrane electrode assembly (MEA), and protection of the catalyst layer from corrosion or erosion caused by flows or other factors. Physical processes in GDLs, in addition to diffusive transport, include bypass flow induced by in-plane pressure difference between neighboring channels, through-plane flow induced by mass source/sink due to electrochemical reactions, heat transfer like the heat pipe effect, two-phase flow, and electron transport[46].

The two types of gas diffusion layers most commonly used are carbon paper and carbon cloth. Both are carbon fiber based porous materials: carbon paper is non-woven,

while carbon cloth is woven fabric, thus no binder is needed.

The main funtions of a Gas Diffusion Layer are:

- A gas diffused pathway from flow channels to the catalyst layer;
- Help to remove by-produced water outside of the catalyst layer and prevent flooding;
- Keep some water on surface for conductivity through the membrane;
- Heat transfer during cell operation;
- Provide enough mechanical strength to hold membrane electrode assembly from extension caused by water absorbance (membrane swelling);

### 2.4.3 Bipolar Plates

Bipolar plates (BPs) are a key component of proton exchange membrane (PEM) fuel cells with multifunctional character.They uniformly distribute fuel gas and air, conduct electrical current from cell to cell, remove heat from the active area, andprevent leakage of gases and coolant. BPs also significantly contribute to the volume, weight and cost of PEM fuel cell stacks.Hence, there are vigorous efforts worldwide to find suitable materials for BPs. The materials include non-porous graphite,coated metallic sheets, polymer composites, etc.

A significant part of the PEMFC fuel cell stack is the bipolar plates (BPs), which account for about 80% of total weight and 45% of stack cost[46].

### 2.4.4 Gaskets

Gaskets provide correct compression and act as a 'barrier' for potential fuel leaks, maximizing the highest possible efficiency. Gaskets are an important component for a fuel cell. It also works as a sealing agent for the fuel cell assembly. The proper selection of a gasket is dependent on various parameters such as the operating temperature of the cell, the thickness of the MEA[47].

As written above one of the important parameters in a fuel cell build is the thickness of the gaskets. The gasket thickness determines how much the flow fields are allowed to pinch into the electrode. For a good contact (i.e. low contact resistance), it is essential that the values are 0.002" to 0.003" for a carbon paper backing and 0.010" to 0.015" for a carbon cloth backing. Since electrode thickness for anode and cathode may vary, gasket

thickness for each side is determined separately using the formula[48]:

$$Gasket\ thickness = (individual\ electrode\ thickness) - (desired\ pinch) \tag{2.40}$$

### 2.4.5 Electrodes

The importance of electrodes have been explained very briefly in the first chapter. Since the electrode is the main topic of this research, a more accurate enlightment on what is an electrode and how to prepare it is dealt with in the next Section.

## 2.5 Electrodes fabrication

The goal of the new century is to develope fuel cell components with the highest ratio performance/cost possible.

As stated previously in the *Introduction*, the amount of Platinum per gram of Carbon used early in the 1960s for the space missions was up 28 $mg/cm^2$. In order to switch the use of fuel cells from space vehicles to automotive production, the Platinum loading must be significantly reduced, but a decrease in Pt loading needs a huge increase of specific area so as to be able to reach the maximum active catalyst surface. For this reason, in the last decades, scientists have been investing new way to produce electrodes with high surface area.

The aim of my research was to produce high performance electrodes with a very low Platinum loading ($\simeq 0.10 mg/cm^2$), which is more or less 300 times less than the amount used 50 years ago.

In Pintauro's Laboratory at Vanderbilt University this was not the only topic to work on. Other colleagues were researching on non-PGM electrodes (non-Platinum Group Metal), high hydrophobic electrodes (with PVDF polymer), electrodes with Pt-alloys (Pt-Co, Pt-Ru, Pt-Ni) for high performance vehicles, and also on anion and cation exchange membranes production.

In order to make the electrode, an "ink" must be prepared. The "ink" is a dispersion of Platinum on Vulcan Carbon, ionomer polymer, carrier polymers and solvents solution. Once the dispersion is ready there are different ways to produce electrodes, which are listed below:

- Painted electrodes;
- Sprayed electrodes;
- Electrospraying;

- Electrospinning;

The latter, is the most studied procedure to produce high performance electrodes. The product can be either be placed directly on the membrane (CCM: Catalyst Coated Membrane) or painted/placed on the Gas Diffusion Layer first and then pressed with the membrane.

### 2.5.1 Painted electrodes

In Vanderbilt laboratories the painting technique was mostly used to study the effects of different components on Fuel Cell performance, more than for high performance electrodes preparation.

Brushing is a combination of brushing and dripping ink. The electrode is weighed and laid horizontal on a flat surface, which can be either the GDL or the membrane. The surface is wetted with a small amount of ink on a paint brush. Ink spreads evenly and, upon drying, results in a uniform catalyst layer provided appropriate ink viscosity and the electrode surface is adequately wetted, flat and level.

Viscosity and surface tension are important properties especially for particle modified catalyst inks. Particulates may settle to form a resistive barrier to either fuel, oxydants, ions, or electrons if the viscosity is too lowInks are difficult to mix and apply evenly if the viscosity is too high. Inks leak through the porous electrode structure and results in a poor (low) distribution of catalyst near the separator if the surface tension is too low. A high surface tension implies a low vapor pressure and result in a excessive drying time.

In the case of paintig directly on the membrane (CCM), a more uniform catalyst layer might be difficult to achieve through this method as there could be a significant distortion on the membrane during painting and drying. This can be overcome by drying the membrane in a special vacuum table heating fixture. Also the bulk of the solvent is removed at a lower temperature to alleviate cracking, and later the final traces of solvent are rapidly removed at higher temperature (it depends on the boiling temperature of solvents). In the last step, the catalyzed membranes are rehydrated and ion-exchanged to $H^+$ form by immersing them in slightly boiling sulphuric acid followed by rinsing in deionized water[49,50].

In Brush Painting, it is necessary to iterate the procedure of painting, drying and massing a number of times before the final GDE is obtained for the MEA manufacturing process (as shown in Figure 2.9). This increases cost and cannot be scaled to high volumes. Also, there are inherent problems in the process itself. The uniformity with which the catalyst is distributed is not easily controlled. It will also depend person to person whoever is responsible for application of the catalyst. Hence it is not a process in which the components are easily reproducible[51]

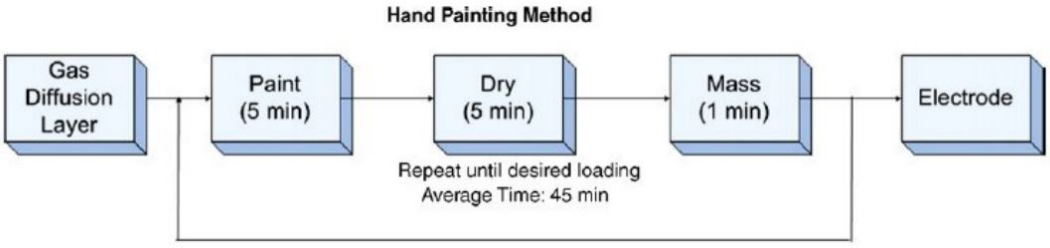


Figure 2.9: Time duration for bruch painting method

### 2.5.2 Sprayed electrodes

Spray painting is an evolution of the brush painting procedure. It is an automated assembly and can easily produce similar components in high volumes. But it hasn't been very successful in reducing the loading of the catalysts. Also, periodic clogging due to the catalyst particles takes place thus requiring frequent maintenance.

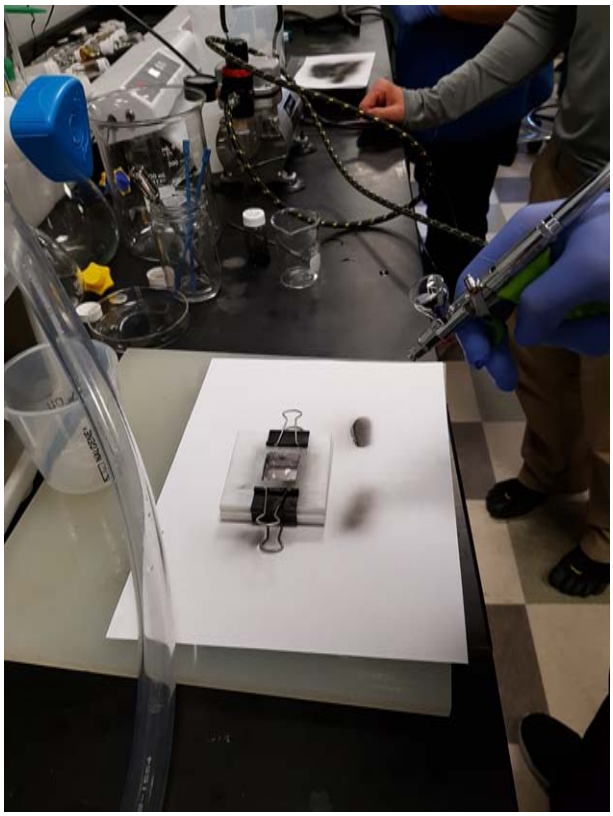

Figure 2.10: Example of ink sprayed directly on the Nafion membrane

Also in the procedure the ink deposition is very difficult to control because of ink viscosity and the jet speed. The best way to achieve a good deposition control is to use elctrospray and electrospinning technique.

### 2.5.3 Electrospraying

Electrospray has been widely used for aerosolizing liquids. It relies on electrostatic forces to expel micrometer sized droplets from a charged liquid. The liquid is pumped through a capillary, and, under ideal conditions, the applied electric field causes the liquid to emerge in the shape of a cone, called the Taylor cone. The high electric field concentrated at the tip of the cone induces the emission of a fine spray of charged droplets. If the liquid is a solution of solvent and solute and sufficient evaporation occurs as the droplets are accelerated towards the grounded substrate, the resulting charge concentration induces break-up of the droplet and the ultimate deposition of sub-micron to nanoscale particles on the substrate. A wide range of chemical and physical parameters can be varied to tune the characteristics of the resultant structure, which can span from dense thin films to porous electrodes. These parameters include solvent concentration, solution composition (affecting solution conductivity, surface tension, viscosity), spraying temperature, gas flow rate, and spray geometry[52].

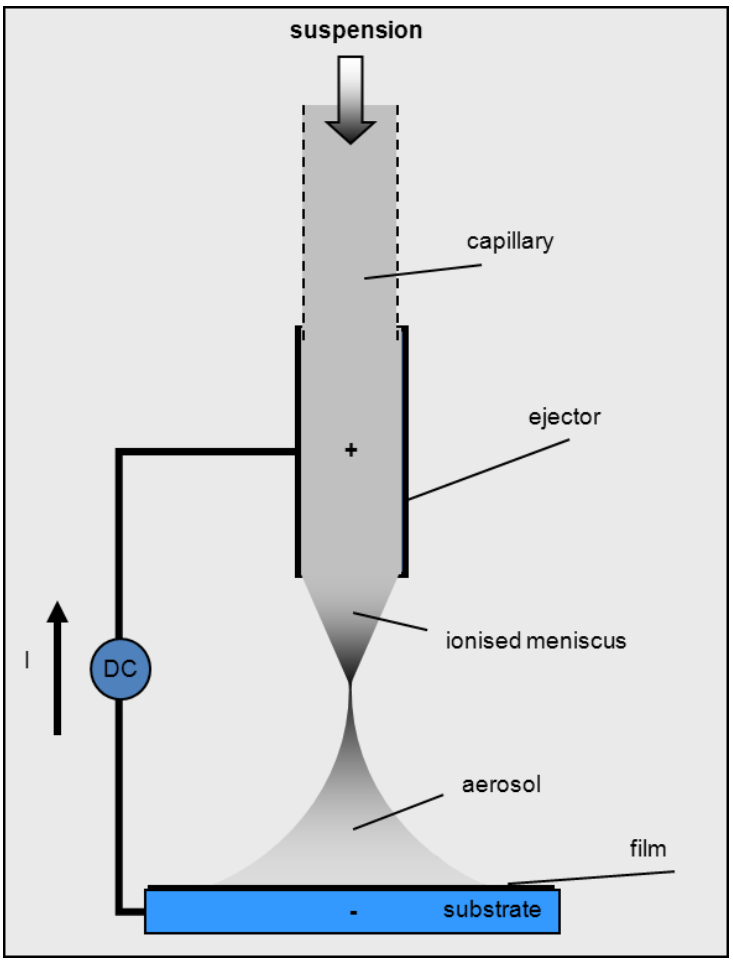


Figure 2.11: Schematic of electrospraying process [53]

### 2.5.4 Electrospinning

Besides spraying small particle clusters ("electrospraying"), a voltage field can also be used to create nanofiber structures from polymer and polymer/particle solutions and melts when appropriate requirements are met. Over the past 20 years, a variety of polymers have been electrospun into nanofibrous materials. Electrospinning (derived from "electrostatic spinning") is a versatile and low-cost method of creating continuous fiber materials with a diameter ranging from several microns to several nanometers. The technique is welldocumented for creating various polymeric fibrous structures for lithium battery separators, filtration media, medical and pharmacological products, textiles, and sensors, both in the laboratory and at the commercial scale.

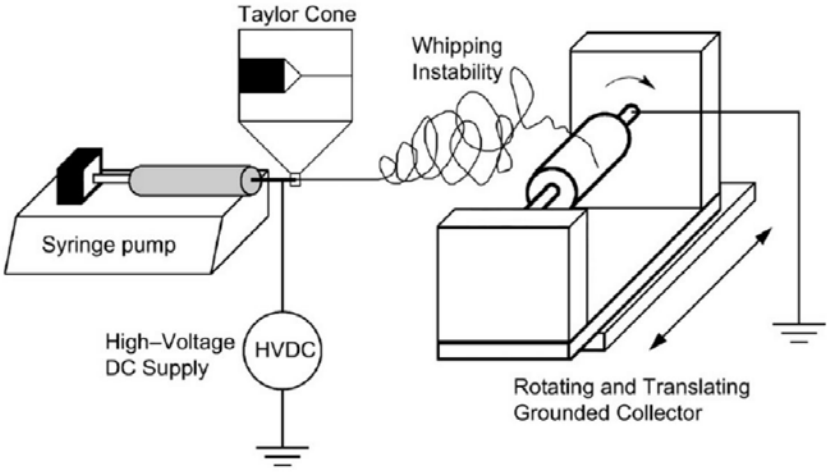


Figure 2.12: Schematic of an electrospinning procedure

A typical laboratory electrospinning setup is shown in Figure 2.12. A high electric field, typically 0.5-5 kV/cm, is applied between the spinneret tip and an electrically grounded collector. The applied voltage induces surface charges on the emerging electrospinning solution/melt. When the applied electric field reaches a critical value, the repulsive electrical forces overcome the surface tension forces and deform the emerging polymer filament into what is known as a Taylor cone. On the way to the grounded counter electrode, the solvent evaporates and solid fibers are precipitated. The fiber jet is thought to accelerate in a whipping motion that coils and elongates the fibers. In order to be electrospun, a polymer solution/melt needs to have proper chain entanglements and viscosity, and appropriate electrospinning conditions must be found (voltage, spinneret to collector distance, relative humidity, and solution flow rate). Nafion® forms a micellar dispersion in alcohol/water and organic solvents and it cannot be electrospun into fibers without the use of a carrier polymer. Nafion® has been successfully electrospun with poly(acrylic acid), poly(ethylene oxide), and poly(vinyl alcohol).

A more detailed understanding on the process will be scrutinized in *Chapter 4*

Pintauro and co-workers have used ionomer electrospinning to fabricate a series of proton-exchange and anion-exchange membranes for fuel cell applications with excellent ionic conductivity, moderate water swelling, and good mechanical properties.[17,18]

After that, several researchers in Vanderbilt laboratories have taken over Pintauro's work, among which Brodt M., which wrote *Fabrication, in-situ performance and durability of nanofibers fuel cell electrodes* with whom all this thesis data are compared.

# Chapter 3

# Materials and Characterization Methods

As written before, in the present study the goal was to find out a relatioship between solvents and performance of electrospun fibers. To do that some ink components are variables and others are fixed. As second step, after the fibers fabrication, qualitative and quantitative studies have been done.

## 3.1 Materials

The electrospinning ink is composed by:

- Catalyst on Carbon support;
- Ionomer polymer;
- Carrier polymer;
- Solvents;

In this research *Vulcan Hispec 4000* was used as Platinum catalyst on High surface Carbon. The Ionomer was *Nafion D2021 1100 EW*. The carrier was Poly Acrylic Acid with an average $Mv \simeq 450.000$. For what concern the solvents, water is always used with the addition of one or more alcohols which are: methanol, ethanol, iso-propanol, n-propanol and ethylen glycol.

The equipments available in the laboratory are (See Figure 3.1):

- 3 Fuel Cell Test Systems, which allow to test three different MEAs at the same time; two potentiostats which are used for some tests which will be written in the next section;
- 1 Oxygen bottle;

- 1 Hydrogen bottle;
- 1 air bottle;
- 2 Nitrogen bottles, one is used to feed the fuel cell with inert gas and the other is used as gas to pressurize a tank containg deionized water, which keeps the feed gases humidified;
- 2 Desktop Pc with softwares to control the Fuel Cell Stations

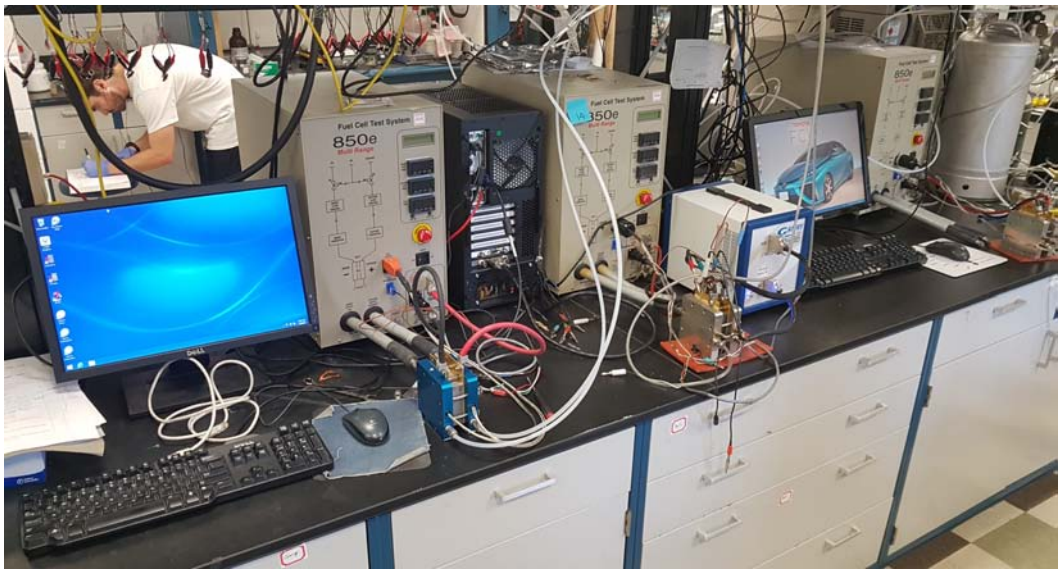


Figure 3.1: Fuel Cell test workstation

## 3.2 Characterization Methods

In order to make a qualitative and quantitative analysis of the electrodes performance, there are two types of characterization[55]:

1. Electrochemical Characterization Techniques (In Situ);
2. Ex Situ Characterization Techniques;

All those analysis have been made in the Vanderbilt Laboratory.

### 3.2.1 In situ techniques

Fuel cell tests were performed on 5 $cm^2$ MEAs, using a Scribner Series 850e test station with mass flow, temperature, and manual backpressure control. The fuel cell test fixture

accommodated a single MEA and contained single anode and cathode serpentine flow channels.

In addition to the Fuel Cell Station a Gamry Reference 3000 Potentiostat has been used.

The tests carried out with the Scribner and the Gamry are:

- Linear Sweep Voltammetry (LSV);
- I-V polarization curve;
- Cyclic Voltammetry (CV);
- Electrochemical Surface Area (ECSA);
- Electrochemical Impedance Spectroscopy (EIS);
- Carbon Corrosion (CC);
- Mass Activity;

**Linear Sweep Voltammetry - LSV**

Permeation of reactant from one electrode to the other through the PEM is referred to as crossover. Although crossover of both fuel (hydrogen) and oxidant (oxygen) occurs, the latter generally occurs at a lower rate and thus most often fuel crossover is the property of interest. Reactant crossover is important because it degrades fuel cell performance, efficiency and durability. Direct reaction of hydrogen with oxygen at the fuel cell cathode decreases the cell's open circuit voltage through generation of a mixed potential. Fuel efficiency is also lowered because although the reactant is consumed, the electrical work is not captured. In addition, severe crossover autocatalytically accelerates membrane degradation and pinhole formation via locally generated heat leading to proximate membrane thinning, which further accelerates the crossover process.

Permeability is the product of diffusivity and solubility and therefore factors impacting these properties influence crossover rate. For example, the crossover rate increases at elevated temperature in part because diffusivity increases with temperature. All else being equal, a fuel cell with a thin membrane will exhibit higher crossover than one with a thick membrane because the concentration gradient of the reactant across the membrane that is the driving force for diffusion is larger. Similarly, direct conduction of electrons between the electrodes through the electrolyte is also a source of loss within a fuel cell. Although the electrolyte is designed to be an ionic but not electronic conductor, finite electrical shorts between the electrodes may occur as a result of electrolyte thinning (cell electrical resistance typically decreases with age) or as a result of pinhole formation. As with

crossover, excessive electronic conduction through the electrolyte results in degradation of cell performance.

To experimentally determine the fuel crossover, a suitable inert gas such as nitrogen is used to purge the fuel cell cathode while hydrogen is passed through the fuel cell anode. The potential of the fuel cell cathode is swept by means of a linear potential scan to potentials at which any hydrogen gas present at the fuel cell cathode is instantaneously oxidized under mass transfer limited conditions. Such experiments are referred to as *Linear Sweep Voltammetry (LSV)*[56].
In Figure 3.2a it is possible to see that the curve reaches an asymptote around a value of current that is slightly greater than 0 $mA$. For the Fuel Cell standards, a LSV that is in the surrounding of 10 $mA$ is still fine, this means that the fuel crossover is present but it is small and confined. In practice an MEA with null fuel crossover is quite impossible. The goal of the scientist is to build an MEA with the lowest fuel crossover possible. Moreover, several cases presented a fuel crossover close to the 0 $mA$ value, but then the performance were not as good as expected.

Low fuel crossover is a necessary condition but it is not sufficient to ensure good performance.

On the other hand, in Figure 3.2b the LSV curve presents a run away behaviour. This is maybe either a symptom of a bad assembled MEA, or MEA with holes in the membrane or on the other components like GDEs, or in the worst case scenario is the sum of the two effects. It is possible to fix the problem only in the first case, by opening the MEA and re-assembling it with more precautions.

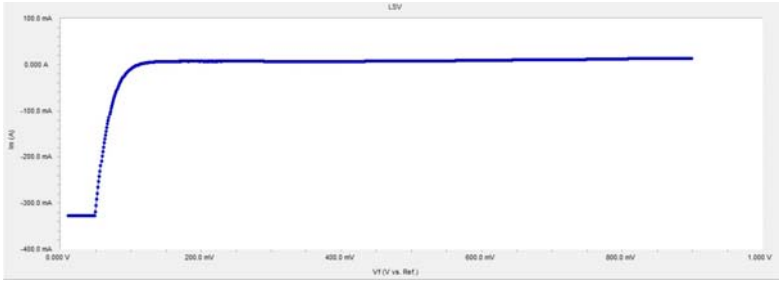

(a) LSV with normal Fuel Crossover

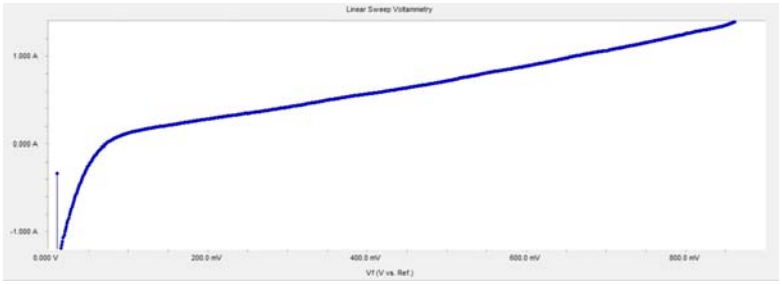

(b) LSV with high Fuel Crossover

Figure 3.2: LSV test on two different MEAs

### I-V Polarization Curve

Fuel cells convert chemical energy into electrical energy. They produce an electric current through a load when connected in an electric circuit. In the hydrogen–oxygen fuel cell, hydrogen oxidation occurs at the anode producing protons and electrons. The protons move through an electrolyte to the cathode while electrons move through an external circuit. At the cathode the electrons combine with the protons and oxygen to produce water. The current and voltage depend on both the electro-chemical reaction in the fuel cell and the external load impedance. Fuel cell performance has traditionally been characterized by the voltage drop across the external load expressed as a function of the current through that load. By sweeping out a range of external loads, an IV curve (often referred to as a polarization curve) is obtained as shown in Figure 3.3 in the next page. The polarization curve is helpful in explaining the chemistry and physics associated with fuel cell operation. The current is the rate of chemical reaction in the fuel cell. The voltage is the driving force for the reaction. Different operating regimes of the fuel cell are identified with the help of the polarization curve. At open circuit (infinite external load resistance), no current flows; chemical reaction equilibrium prevails at the electrodes and the voltage is a direct measure of the difference in chemical activity of hydrogen at the anode and cathode. With a finite load resistance, current flows between the anode and the cathode; an electron current goes through the external circuit, which is balanced by an ion current going through the electrolyte. At large load resistances the voltage drops rapidly with increasing current; the steep initial decrease is attributed to the barrier for the electron transfer reactions occurring at the electrodes. This is referred to as the activation polarization region. As the load resistance is decreased further, there is a range of load resistances where the voltage decreases almost linearly with the current. This is referred to as the "ohmic polarization region", where the current is limited by the internal resistance of the electrolyte to ion flow. The ohmic region is the desirable operating regime for a fuel cell. As the external resistance is decreased further, the current reaches a limiting value where the mass transfer of reactants to the electrode/electrolyte interface limits the reaction. This is known as the concentration, or mass transfer, polarization region[57].

To have a better understanding on where the different regions are collocated, see Figure 2.4 on *Chapter 1.*

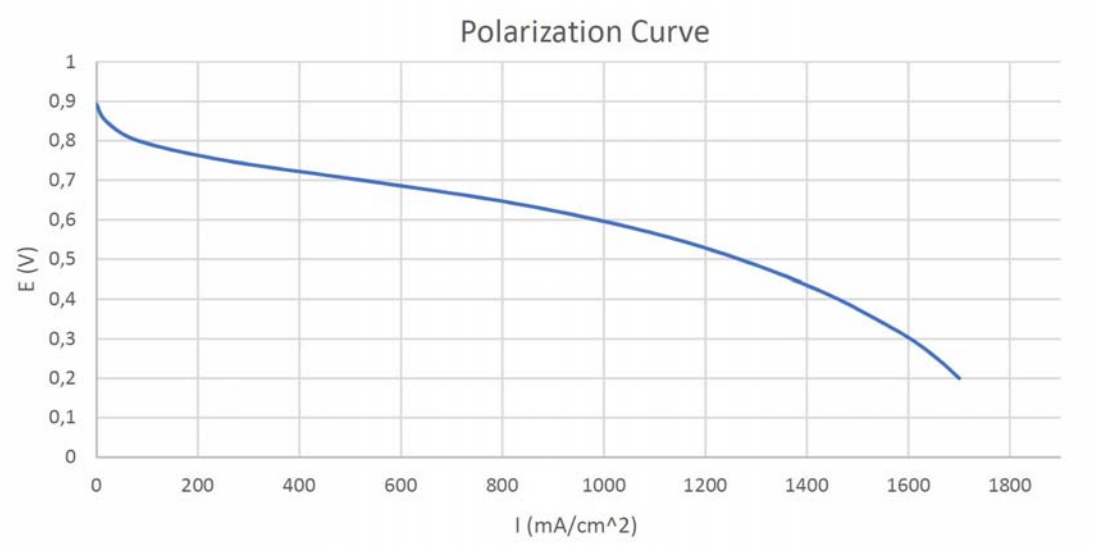


Figure 3.3: Real example of an I-V curve taken with Scribner Fuel Cell Station 850e

### Ciclic Voltammetry - CV

Cyclic voltammetry is a well-known electroanalytical method, which is based on linear voltage sweep between two fixed values.

The potential is scanned linearly from an initial value to a predetermined potential limit, $E_{Max}$, where the direction of the scan is reversed. The potential is then scanned to the lower potential limit, $E_{Min}$, where the scan is again reversed. The current response as a result of this polarization is then plotted as a function of the applied potential. This current-voltage curve is referred to as the cyclic voltammogram and it gives information about reactions occurring on the surface. These can for instance be compounds added to the electrolyte being oxidized or reduced at the surface. Other information possible to obtain is knowledge of the surface structure sensitive processes occurring with the surface atoms of the electrodes and electrolyte, for instance creation of a surface oxide or reduction of this oxide, or in the case of catalytically active metals also the adsorption of a hydrogen layer and removal (desorption) of this layer[58].

In this research Ciclic Voltammetry test has been used only to be sure that the Fuel Cell was working well (since the shape of the curve is well known) and to clean the fuel cell in between a test and the other.

**Electrochemical Surface Area - ECSA**

A typical proton exchange membrane fuel cell (PEMFC) catalyst layer is a porous, three dimensional structure consisting of carbon support, platinum (Pt) catalyst and ionomer such as Nafion®, all in intimate contact. The carbon support enhances the bulk electronic conductivity of the electrode and dispersion of the catalyst nanoparticles. The ionomer serves to bind the electrode layer and facilitate proton conduction to the reaction site. Voids allow for mass transport of gas or liquid phase reactants and products to and from the carbon-supported electrocatalyst. The electrochemical activity (current/nominal area) of the catalyst layer is a function of the extent and quality of the three phase boundaries where reactants, ionically and electrically conducting material and active catalyst sites are in intimate contact.

Electrochemical surface area and catalyst utilization are critical performance metrics for catalyst and membrane electrode assembly (MEA) developers and manufacturers. The technique for determining the electrochemical surface area (ECSA) of fuel cell electrodes by CV analysis has been used for several decades. The procedure involves cycling the electrode of interest over a voltage range where charge transfer reactions are adsorption-limited at the activation sites. That is, the electrode potential is such that the number of reactive surface sites can be obtained by recording the total charge required for monolayer adsorption/desorption[59].

Common reactions used when characterizing PEMFC electrodes are the hydrogen adsorption/desorption:

$$Pt - H_{ads} \leftrightarrow Pt + H^+ + e^- \tag{3.1}$$

Or the oxidative stripping of adsorbed carbon monoxide:

$$Pt - CO_{ads} + H_2O \rightarrow Pt + CO_2 + 2H^+ + 2e^- \tag{3.2}$$

Figure 1 shows a typical CV voltammogram of the HAD (Hydrogen Adsorption Desorption) reaction. The process of interest is the electroreduction of protons and adsorption of hydrogen on the catalyst surface, that is, reaction 3.1 in the reverse direction. The hydrogen adsorption charge density ($q_{Pt}$ *in* $Coulombs/cm^2$) due to this reaction determined from the CV experiment is used to calculate the $ECSA$ of the fuel cell electrode. The electrochemical surface area ($ECSA$) of the Pt catalyst is calculated from the charge density $q_{Pt}(C/cm^2_{electrode}$ ) obtained from the CV experiment; the charge required to reduce a monolayer of protons on Pt, $\Gamma = 210\ \mu C/cm^2_{Pt}$ ; and the Pt content or loading in the electrode, $L$ in $g_{Pt}/cm^2_{electrode}$.

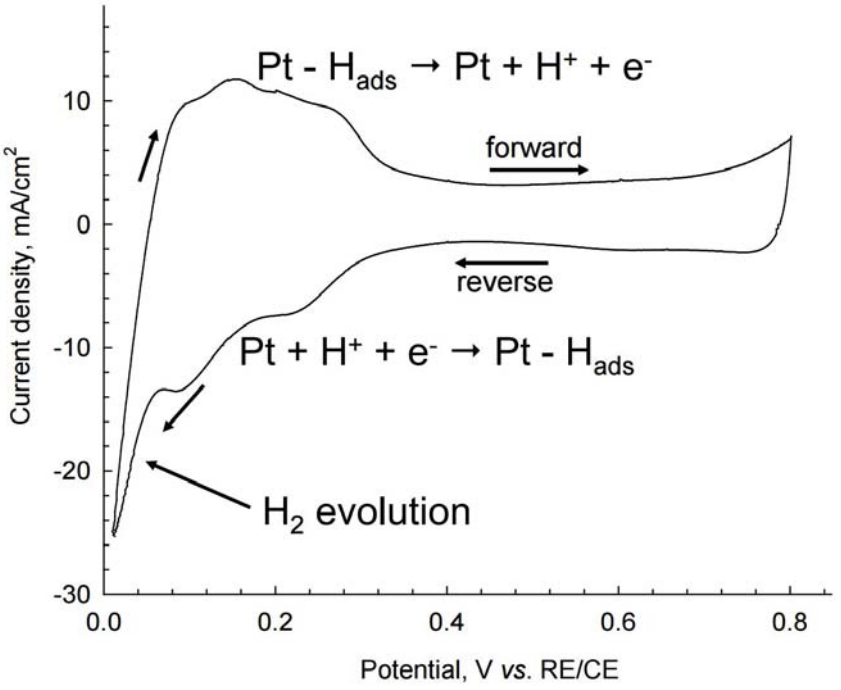


Figure 3.4: Typical CV voltammogram of the HAD reaction

$$ECSA(cm^{2_{Pt}}/g_{Pt}) = \frac{q_{Pt}}{\Gamma \cdot L} \tag{3.3}$$

This ratio is referred to as *utilization*. Higher catalyst utilization is better. Utilization is an idealized condition because the very low reaction rate used during the ECSA measurement results in negligible transport limitations. In a fuel cell operating at a practical current density, oxygen and/or proton transport resistances could decrease the amount of catalyst that participates in the cathode reaction, effectively decreasing utilization.

In situ experiments use a two-electrode configuration in which one of the electrodes of the fuel cell serves as both a Counter Electrode and a pseudo-Reference Electrode (CE/RE). Typically, the electrochemical activity of the fuel cell cathode is of most interest because of the sluggish kinetics of the oxygen reduction reaction. Therefore, the cathode is often chosen to be the working electrode (WE). The fuel cell anode is used as the CE/RE with the inherent assumption that polarization of this electrode is small relative to the polarization imposed on the fuel cell cathode, the working electrode. The current densities obtained in the ECSA tests are relatively small and justify this assumption. The fuel cell electrode of interest (the WE) is filled with a non-reactive gas such as nitrogen, while hydrogen is fed to the other electrode (the CE/RE).

In order to find the $ECSA$ we need to calculate $q_{Pt}$, and to do that, by using the Scribner Software the area in between 0.1 V and 0.4 V of the reverse reaction must be calculated (as shown in Figure 3.5). Once the charge density ($q_{Pt}$) is found out and $\Gamma$ and $L$ (which is $0.001 g_{Pt}/cm^2$ for most of my research) are known, it is possible to calculate

the electrochemical surface area by using the Equation 3.3.
(The test conditions for in situ ECSA evaluation by CV are similar to those used for fuel cell crossover evaluation presented in the *2008 Fuel Cell Seminar*.)

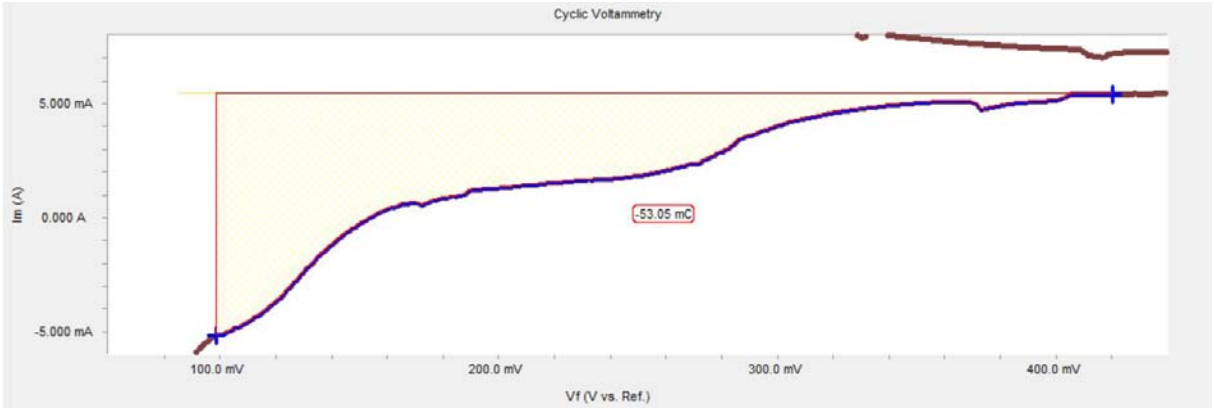


Figure 3.5: Charge density data extraction by integrating the curve of the reverse reaction in between 0.1 V and 0.4 V

### Electrochemical Impedance Spectroscopy - EIS

The electrochemical impedance spectroscopy (EIS) measurement involves producing a constant current from the fuel cell (direct current) and superimposing a much smaller alternating current with an external potentiostat (Gamry Reference 3000). The frequency of the alternating current varies from $0.1Hz$ to $10000Hz$. From this experiment, a Nyquist plot is generated.

Once found out that the system has electrochemical impedance capability, it is possible

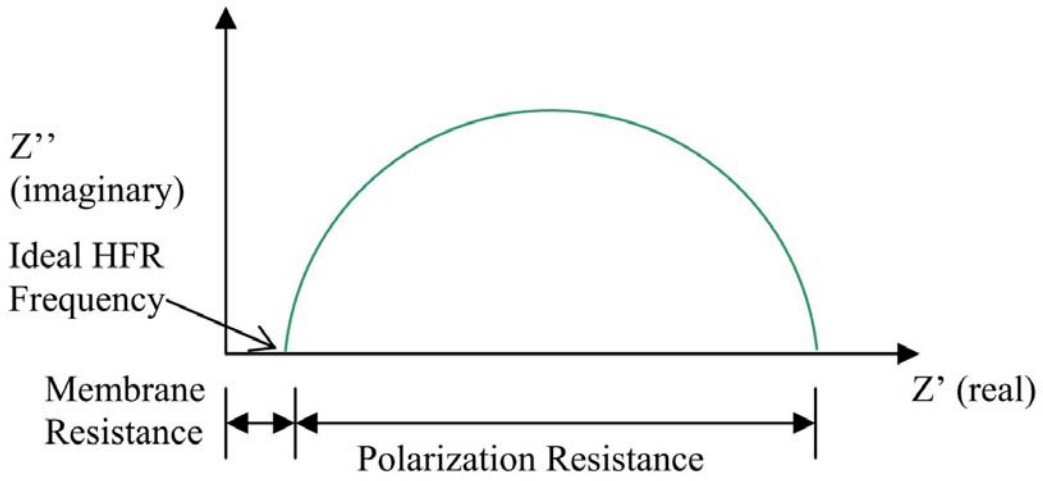


Figure 3.6: Nyquist Plot of Fuel Cell Impedance

to extract the value of the High Frequency Resistance (HFR)[60]. The HFR is the standard

measurement determining resistance in a fuel cell. To find it the imaginary impedance is plotted against the real impedance and the intersection with the real impedance at the high frequency region (as shown in Figure 3.7) yields the high frequency resistance value.

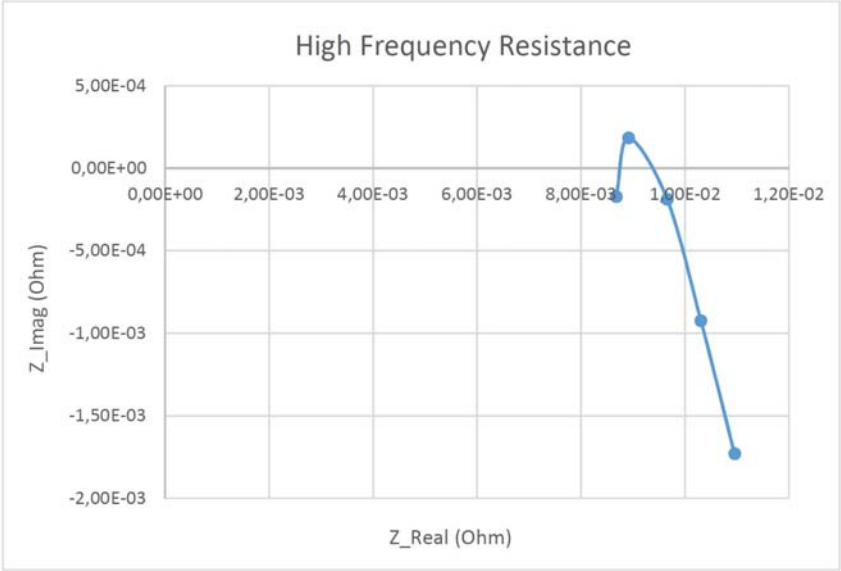


Figure 3.7: Determination of High Frequency Resistance from real data

The High Frequency Resistance is an important value to determine the membrane resistance of fuel cell. It can also be an indicator of membrane water content and therefore of the effectiveness of gas purging as consequence[61].

**Carbon Corrosion - CC**

This accelerated durability test simulates start-up and shut-down of a stack without the application of any operational controls that may mitigate fuel cell performance losses. During start-up, if the stack has been shut down for some time, the anode and cathode are filled with ambient air and are pinned to the air-air potential. Introducing hydrogen gas causes a hydrogen-air front to move through the anode chamber, with a large shift in the cell potential (to a value as high as 1.5 $V$). The start-stop durability protocol simulates this event many times by cycling from 1.0 $V$ to 1.5 $V$ at a scan rate of 500 $mV/s$ (see Figure 3.8). In the present study, 1,000 voltage cycles were performed on a single MEA, where the fuel cell was supplied with H2 at the anode and N2 at the cathode (both at 0.5 $L/min$ and 80 °C, with fully humidified feed gases), and the cell potential was cycled using a potentiostat.

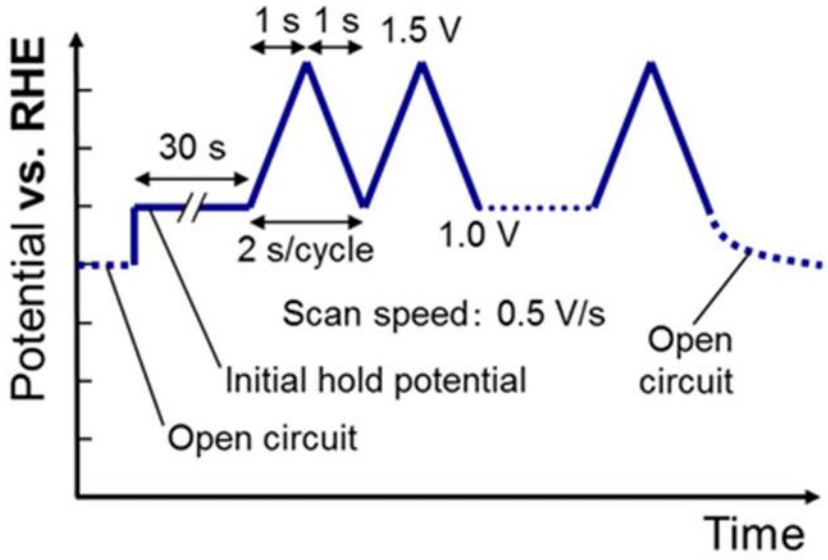


Figure 3.8: Start-stop cycling protocol for accelerated carbon corrosion durability testing

**Mass Activity**

The mass activity is defined as the current generated per miligram of platinum at 0.9V excluding ohmic contributions. In this experiment, the cathode feed gas is oxygen and 7psig backpressure is applied to minimize concentration overpotential. The current is scanned from 1 $A$ to 0.01 $A$ (two decades) and the voltage is measured at 4 points per decade. From this experiment, the current at 0.9 $V$ is determined and divided by the cathode loading to arrive at a current per mass of catalyst – often in units of $A/mg_{Pt}$. This value is defined as the mass activity and this procedure was first established by Gasteiger and colleagues (Applied catalysis B-environmental, 2005, Vol. 56. 9-35.)

### 3.2.2 Ex Situ Techniques

In this section it is explained how to make qualitative studies on the electrodes produced. There are several techniques to study the product like porosity determination, gas permeability to understand the mass transport in fuel cell electrodes, chemical determination and structure determination with optical microscope and Scanning Electrons Microscope.

In this study, only structure determination was performed.

#### Optical Microscope

The Optical Microscope has been used only during the electrospinning process. As written in the $3^{rd}$ Chapter, the goal of the electrospinning method is to produce very thin fibers by the application of an electric field. Since the fibers' diameter is very small it becomes really difficult to see if they are growing on the collection drum. To avoid this problem the scientist has to collect the electrospinning product on a microscope glass slide and observe it with the optical microscope. The Vanderbilt Laboratory was equipped with a *Fisher Scientific*$^{TM}$*compound Microscope* showed in Figure 3.9

Figure 3.9: Fisher Scientific Optical Microscope

The microscope is not used only to observe if fibers are growing or not. As a matter of fact if fibers are present on the collector, it doesn't mean that fibers quality and shape are good as a consequence. The electrospinning method depends on several different parameters (process parameters and Ink physical and chemical properties) and the observation with microscope is the best way to change those parameters and get close enough to the optimal conditions.

Moreover sometimes the optical observation shows some drops on the glass slide but a more precise evaluation with the Scanning Electrons Microscope could be in contrast with the previous observation with no beads presence on the surface. This kind of analysis has, as rule of thumb, to take into account that fibers must be present on the glass sample and that the less drops are present the higher will be the probability to have a good product. In the image below it is possible to see some fibers collected ot the microscope slide. In this case no drops were present on the sample and the quality of fibers were really high.

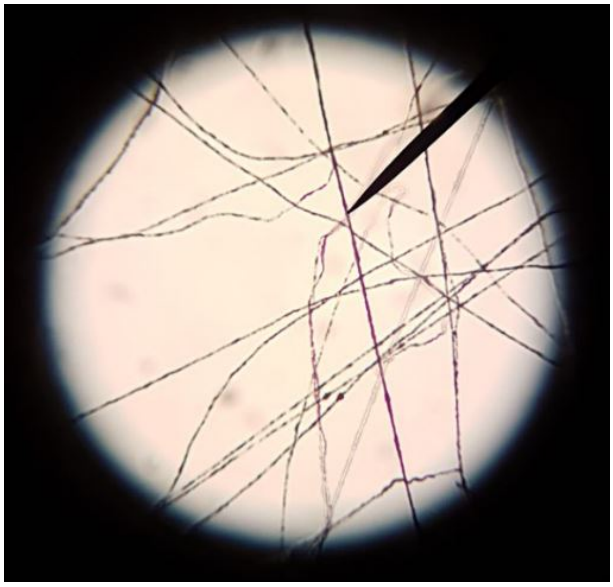

Figure 3.10: Example of fibers collected on a glass slide and observed with the optical microscope

**Scanning Electrons Microscope - SEM**

A Scanning Electron Microscope provides very detailed surface information by tracing a sample in a raster pattern with an electron beam.

The process begins with an electron gun generating a beam of energetic electrons down the column and onto a series of electromagnetic lenses. These lenses are tubes, wrapped in coil and referred to as solenoids. The coils are adjusted to focus the incident electron beam onto the sample; these adjustments cause fluctuations in the voltage, increasing/decreasing the speed in which the electrons come in contact with the specimen surface.

Controlled via computer, the SEM operator can adjust the beam to control magnification as well as determine the surface area to be scanned. The beam is focused onto the stage, where a solid sample is placed. The interaction between the incident electrons and the surface of the sample is determined by the acceleration rate of incident electrons, which carry significant amounts of kinetic energy before focused onto the sample. When the incident electrons come in contact with the sample, energetic electrons are released

from the surface of the sample. The scatter patterns made by the interaction yields information on size, shape, texture and composition of the sample.

The SEMs available for morphological characterization are the following::

1. Oxford Instrument$^{TM}$ SEM
2. Zeiss Merlin$^{TM}$ SEM

Below it is possibile to see an image of the Oxford Instruments SEM and a fiber's picture captured with it.

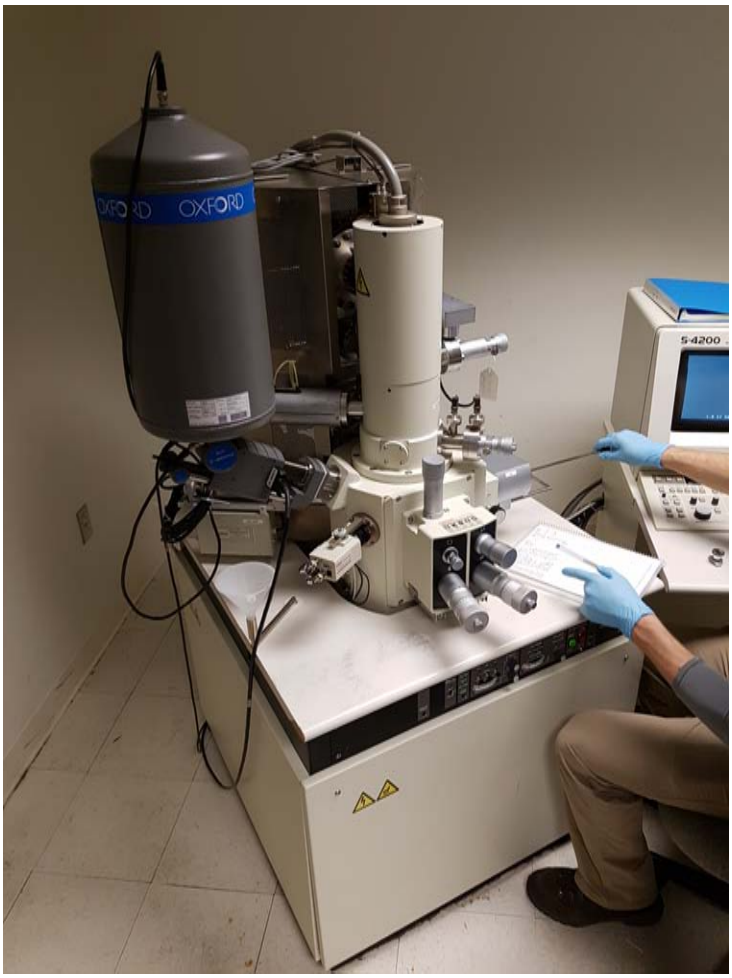


Figure 3.11: Oxford Instruments SEM

Thanks to this technology it has been possible to better understand how the different electrospinning and ink parameters influence the quality and shape of fibers. For what concern the aspect, the optimal product is characterized by a very uniform diameter, with the polymer that is completely covered by catalyst on carbon particles and in absence of "beads", which are considered as poor quality fibers.

For example from Figure 3.12 it is possible to state that fibers' shapes are almost all within the norms, the diamater is not very uniform, infact some parts are very thin and others are covered by too much catalyst.

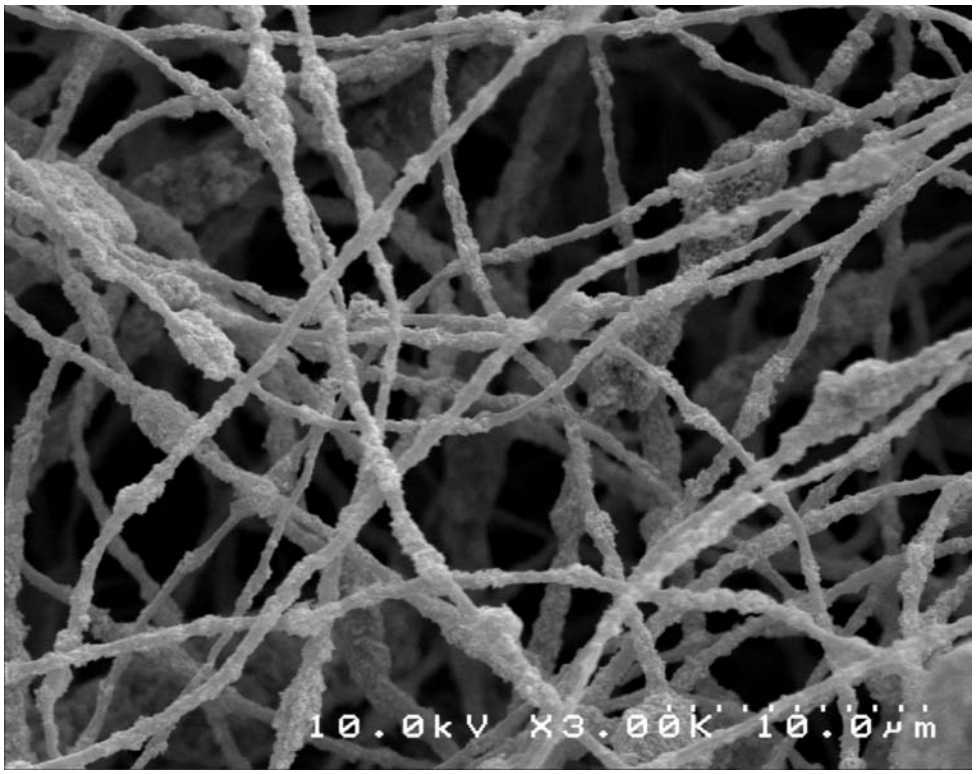


Figure 3.12: SEM image of fibers produced with Pt/C on Polymers

# Chapter 4

# Procedure and Results

There has been considerable research over the past 20 years on new catalysts for proton exchange membrane (PEM) fuel cells. The motivation has been to increase catalytic activity, particularly for the cathode in a hydrogen/air fuel cell. Most fuel cell electrodes are fabricated by a decal method or by air-brushing catalyst-ink onto a carbon paper gas diffusion layer. The Pt catalyst utilization efficiency in such structures, however, is low ($\sim 30\%$). Surprisingly, there has been little research done on new electrode structures and new methods of fabricating fuel cell membrane-electrode-assembly (MEA) with improved catalyst utilization.

One of the main challange in the scientific community is the reduction of the cost of Fuel Cells' components fabrication by maintaing high performace or even increasing them. To achieve this objective the electrospinning method became the most investigated process.

Until today research has been capable to face the problem with very good results. In the automotive field million dollars are invested every year to improve the technology.

The aim of this research was to explore the possibility to get electrodes by using methanol as one of the solvents, because in the literature it is possible to find that a solvent with a high dielectric constant, low surface tension,and low viscosity could increase the electrospinnability of the solution[67]. Moreover, methanol is easy to handle and it is a very common and cheap solvent. On the other hand methanol is well known for his toxicity (Companies are not looking only for high performance fuel cells but also on the environment and how to deal with the society feedback).

The procedure requires to prepare inks for the GDL painting method as first step (it allows to verify if the ink could be a good candidate for the electrospinning in terms of performance). There is a sensible difference between this kind of ink and the ink used to prepare fibers with the electrospinning method. Painting inks were prepared by mixing different ratio of an water/methanol mix:

- 50/50 water/methanol
- 80/20 water/methanol
- 70/30 water/methanol

The catalyst used was *Vulcan Hispec 4000* which is $40\%_{w/w}$ of Platinum on Carbon. The ionomer was $20\%_{w/w}$ Nafion dispersed is a 2:1 solution of water/isopropanol.

*Nafion D2021 Alcohol based 1100 EW at 20% weight* is initially bought from *Ion Power*, a limited quantity of the product is poured in a flat Teflon jar and covered with a paper filter which allows the solvent mixture to evaporate. After 48 hours the remainder, containg Nafion and trace of solvent is crumbled in very small pieces. In the last step the crumbled Nafion is dried in a vacuum oven at room temperature for at least 6 hours (The oven is a *Yamato ADP 21 Vacuum Drying Oven* showed in Figure 4.1).

The product is pure Nafion, with whom it is possible to prepare the dispersion desired.


Figure 4.1: Yamato ADP 21 Vacuum Drying Oven

In order to make a uniform painted Gas Diffusion Layer, the ink must be less viscous

possible. The ink is then prepared with a 5% solid weight composition. The solid part includes the dry ionomer and the catalyst. Another parameter has to be choosen, which is the the ionomer/catalyst ratio. In Pintauro's Lab this ratio usually ranges in between $0.4 - 0.65$ in weight terms. For this experiment $65\%_{w/w}$ of catalyst on total solid weight was chosen. In order to have a good mixing, a miminum quantity of ink in suggested, in this case was 1.5 $g$ of total mass.
The ink preparation is split in more than one step:

1. Obtain a vial and insert a magnetic bar, weigh out the required amount of Pt/C powder and put it into the vial, add the total amount of water and stir the product for 2 minutes (the balance is a *Denver Instrument scale* with a readability of 0.00001 *grams* see Figure 4.2) the magnetic stirrer is a *RO 10 IKA* with a speed range of $0 - 1200$ *rpm* in Figure 4.3a). This is necessary because of the high vapor pressure of methanol, which if poured directly on the Catalyst powder it would drag the Platinum particles in the air leading to a fast oxidation and generating a very exothermic reaction with sparks and fire.

2. Take the stirred water/powder dispersion and add half amount of methanol needed, stir it again for 2 minutes and sonicate it in a sonication bath (*Fisher Scientific FS20D* in Figure 4.3b) at room temperature for 30 minutes at 80 $W$ power. The sonication effect will improve the mixing between solvents and powder. In literature is suggested to work at room temperature because at higher temperature the sonication could lead to a separation of Platinum from the Carbon support.

3. Add the total amount of Nafion dispersion with a Pasteur pipette since the viscosity is very low. Stir the dispersion for 2 minutes and then sonicate it for 30 minutes. It is suggested to change the bath's water in order to work at room temperature. It has been observed that in 30 minutes the water temperature raise up to 6-7 degrees Celsius.

4. Add the left amount of methanol and repeat the stirring and sonication procedure.

5. To be sure that the ink is very homogeneous, let the ink stir overnight.

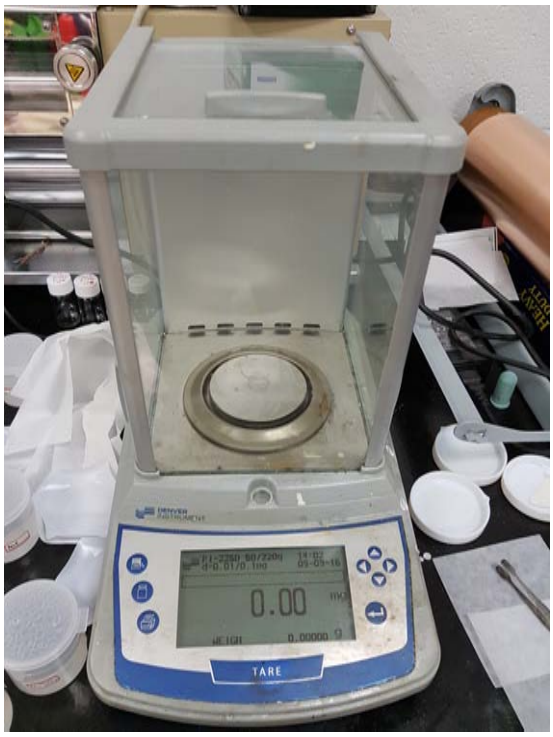


Figure 4.2: High precision Balance

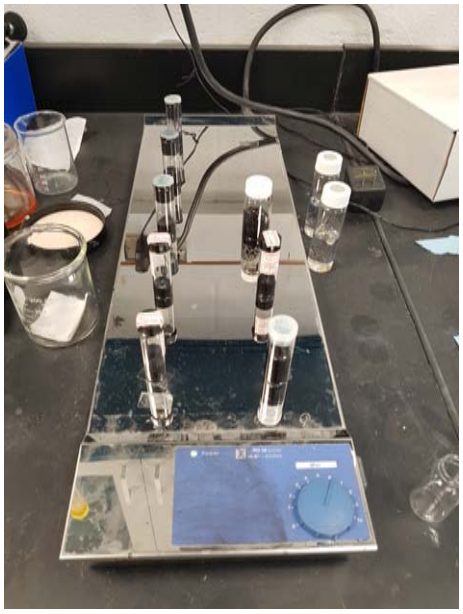

(a) Magnetic Stirrer

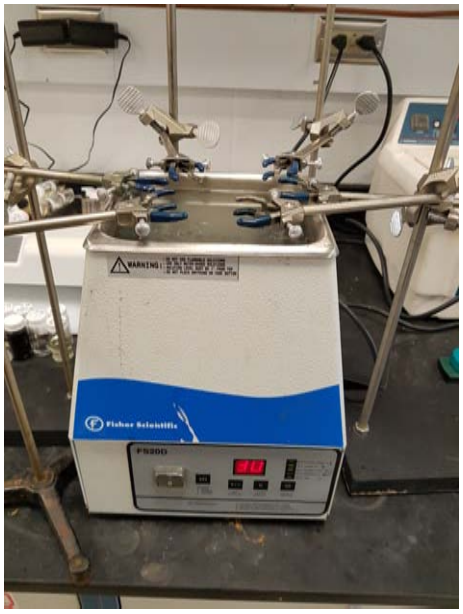

(b) Sonication Bath

Figure 4.3: Photos of Magnetic Stirrer (a) and Sonication bath (b) equipments

The day after the ink is ready and it looks like in Figure 4.4. The ink is totally black and is strongly suggested to keep it mixed until it is time to use it.

The next step was to paint the ink on the GDL. The gas diffusion layer used in my research was the *Sigracet 29 BC*. Sigracet 29 BC is a non-woven carbon paper with a Microporous Layer (MPL) that has been PTFE treated to 5 $wt\%$. The Teflon makes

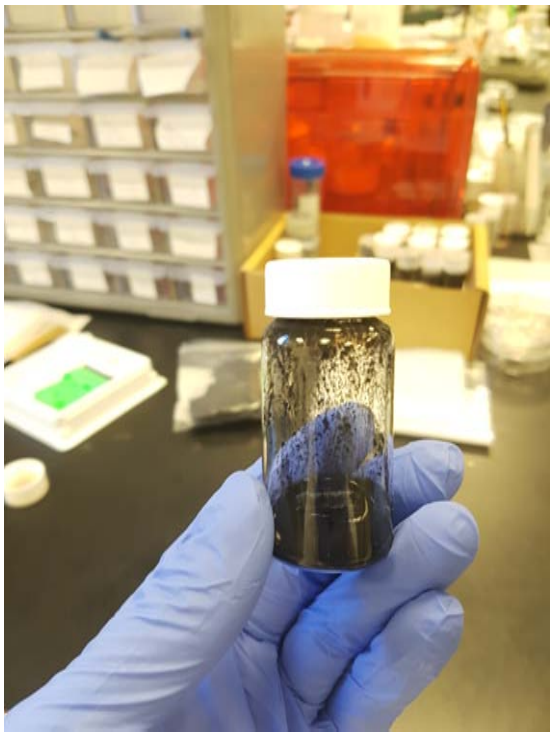

Figure 4.4: Mixed ink containing a dispersion of Catalyst, ionomer in solvent solution

the GDL surface hydrophobic and this is really important for the cathode, where water form and must be removed. In fact in the literature it is possibile to find that the PTFE impacts the microstructure of the compressed GDL[62]. The number of available wide transport paths is significantly increased as compared to the untreated material. These changes improve the transport capacity liquid water through the GDL and promote the discharge of liquid water droplets from the cell.

A photo about the hydrophobicity of the GDL has been taken and it is shown in Figure 4.5.

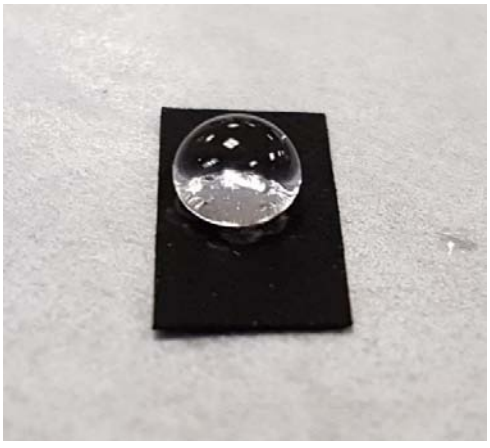

Figure 4.5: Photo of a water drop on a GDL treated with PTFE

The GDL's surface standard, for the laboratory equipment, is 5 $cm^2$ for both the anode and cathode. To paint a small size brush is used. It is strongly recommended to clean it carefully and dry it in the oven, or in the air for longer time, before use. The GDL must be weighed before the application of the ink, generally a 5 $cm^2$ of Sigracet 29BC weights $50mg$.

Three inks with different water/methanol ratio were painted on the Sigracet (example in Figure 4.6). It was more difficult to paint the first layer with the ink with higher water content of course. As written in the painting procedure in *Chapter 3*, after each painted layer, the GDL is put in the oven at a temperature above the mix boiling point for at least 5 minutes. The GDE is then weighed. The painting direction shall be rotated 90° each new layer. The procedure is repeated until a Platinum loading of $\approx 0.1 mg_{Pt}/cm^2$ is reached.

To calculate the Pt loading the equation is:

$$Pt_{loading} = \frac{[\%Catalist \cdot \%Pt\ onCarbon \cdot (Initial\ GDL\ weight\ - Final\ GDL\ weight)]}{5} \tag{4.1}$$

Where 5 is the GDL surface.
In this case, where the percent of Catalyst was 65%, the Pt amount on Carbon was 40%, the difference in weight must be $2mg$. The allowable error referred to the Pt loading is $\pm 0.05 mg_{Pt}/cm^2$.

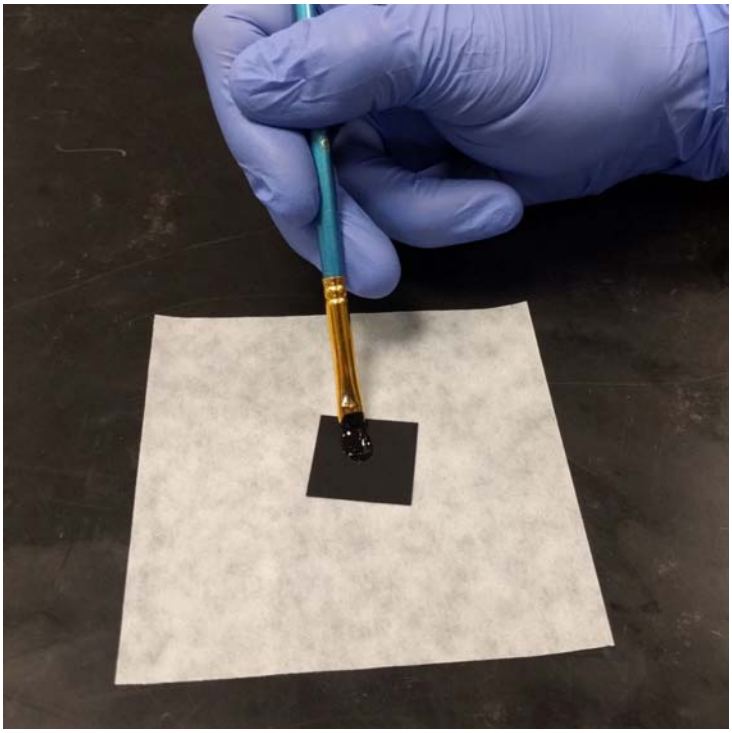

Figure 4.6: Application of the ink with hand painting method

The last step before the Fuel Cell test is the MEA fabrication. Even if it seems to be only a mechanical approach, in the reality it is a very important step with several parameters to control to achieve good performance. In fact the fabrication processing steps for PEM hydrogen/air fuel cell membrane-electrode-assembles (MEAs), have a strong impact on fuel cell performance and require optimization. The conditions for hot-pressing, the step that attaches the anode and cathode to the proton exchange membrane, in particular, has received considerable attention, including careful consideration of the hot-pressing temperature, time, and pressure. The hot-pressing step is important as it creates physical contact between the electrodes and the membrane and the hot-pressing conditions can change the porosity of the electrodes, which will affect the transport of gases and water during fuel cell operation. Hot-pressing with improper or too severe conditions can also damage the membrane and cause large parasitic hydrogen crossover currents. The hot-pressing step also serves to anneal the ionomer in the electrodes. Nafion's annealing crystallizes a portion of it and makes it insoluble in water. Fuel cell electrodes are typically not annealed in a separate step, but are annealed during the hot-pressing step. The hot-pressing temperature is set at or above the $\alpha$ -relaxation glass transition temperature of Nafion ($\sim 100\,^{\circ}\mathrm{C}$). At this temperature, the electrodes are softened, the binder is annealed, and the anode and cathode catalyst/binder layers are adhered to the proton-exchange membrane.

The MEA is composed by anode and cathode, 2 gaskets, and the Nafion membrane. To be sure that the membrane covers perfectly all the anode and cathode and covers enough gasket surface to stay cohesive, its dimension must be $4cmx4cm$. The type of membrane used during all my research period is the *Nafion 211 membrane*, which is $25\mu m$ thick, with total acid capacity around 1 $meq/g$ and a minimum conductivity of 0.1 $S/cm$.

A very important thing is to assign to the cathode, the GDE with the closest Pt loading to the standard one ($0.1mg_{Pt}/cm^2$). It has been demonstrated that the Anode Pt loading doesn't affect to much the Fuel Cell yield.

The first step requires to put gaskets, anode and cathode and membrane together. The anode and cathode must have the catalyst/polymer face laying directly on the membrane as shown in Figure 4.7.

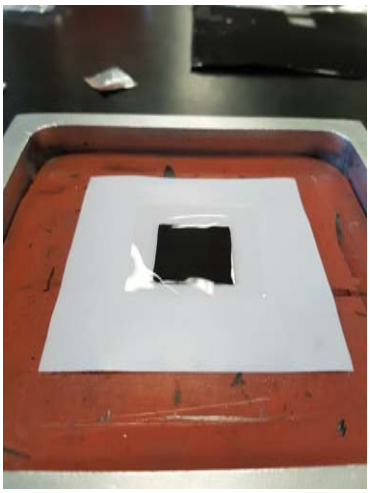

Figure 4.7: GDE placed on Nafion Membrane

To press the different componenents all together the MEA was sandwiched between two 6 x 6 cm polytetrafluoroethylene (PTFE) (Teflon) sheets ($\sim 300\ \mu m$ thickness each), and were placed between two silicone pads, housed in an aluminum fixture (4.7). The pads help to evenly distribute the pressure across the electrodes. The aluminum fixture, containing the MEA, is first preheated to the desired temperature. To heat and press a bench top laboratory manual press from *Carver, Inc, model number 3851-0* was used (see Figure 4.8a). When the sample reaches the desired temperature, a pressure is applied for a limited time.

The standard procedure requires to anneal the MEA at 140 °C and to press it at $4MPa$ for 10 minutes. After this amount of time the aluminum fixture is removed from the hot-pressing machine, and by using security gloves the MEA is pulled out, in order to stop the annealing and the membrane softening.

The MEA is now ready to be tested (see Figure 4.8b ).


(a) Carver Hot-pressing machine

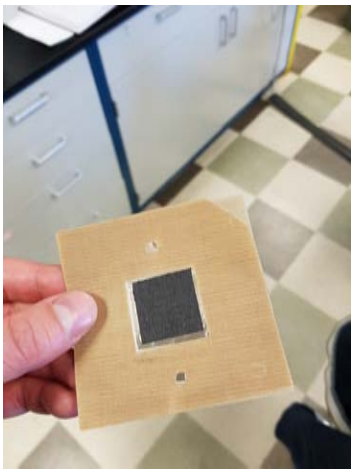

(b) Ready MEA

Figure 4.8: Photos of hot-pressing machine (a) and of the ready MEA (b)

To insert the MEA in the Fuel Cell station the hardware must be turned off, the feed pipes disconnected and the fuel cell open. The anode side of the MEA is placed on the side of the fuel cell fueled by Hydrogen (see Figure 4.9). Since the compression inside the fuel cell is fundamental, the fuel cell must be closed with a torque wrench at a torque of 75 $inch \cdot pounds$.

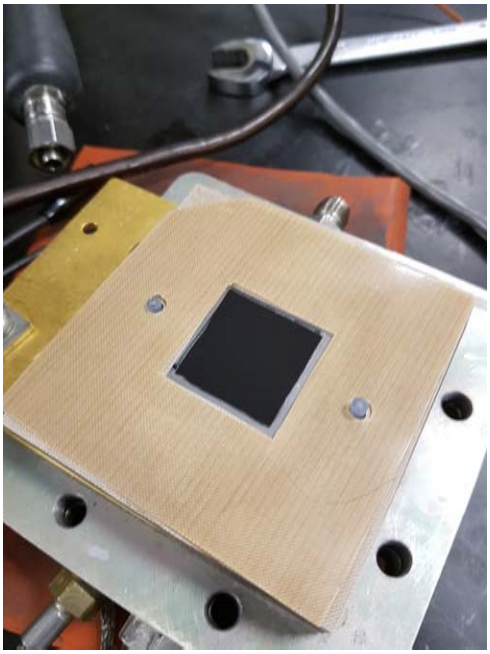

Figure 4.9: MEA with the anode side facing on the bottom of the fuel cell

Experiments with fully humidified $H_2$ and air at atmospheric (ambient) pressure were performed at 80 °C where the $H_2$ flow rate was 125 $sccm$ and the airflow rate was 500 $sccm$ (Standard Cubic Centimeters per Minute). The first test to run is the Linear Sweep Voltammetry in Nitrogen atmosphere instead of air or Oxygen. If the Fuel Crossover is around the standard value, the MEA can be tested. In this case all the three MEAs were working fine.

Prior to collecting polarization data, MEAs were pre-conditioned at 80 °C with fully humidified air and hydrogen by alternating every 2 minutes between operation at 0.2 $V$ and 0.6 $V$. This break-in process was continued until steady-state was achieved (typically less than 4 hours, but as long as 12 hours for cathodes with a neat PVDF binder).

Then polarization curves were taken and it has been observed that methanol was performing really good for all the MEAs, especially for the one with water/methanol 70/30 ratio. No more tests were conducted.

Since the goal of the research was to produce high performance fibers, inks with only ionomer and no carrier were not the aim of the project. As previously written the carrier is fundamental for Nafion fibers electrospinning but it lowers the performance. Nafion forms a micellar dispersion in alcohol/water mixtures and will not electrospin into wellformed fibers, unless a suitable carrier polymer is added to the electrospinning solution. So it is

important to prepare inks with carrier in either case of pianted GDL or fibers on GDL. I've selected the 70/30 water/MeOH composition, and I prepared a new ink with the addition of PAA carrier. The preparation procedure was quite the same of the ink without the carrier. After the second sonication, instead of adding only the solvent, also the carrier is added. The Nafion/PAA ratio was 2:1 in solid weight. In this case PAA was in a 20% solution of n-propanol. The solution is very viscous and to add the right amount in the ink a syringe is necessary. As in the first procedure, once the ink is ready, a third sonication step is required followed by an overnight stirring.

Also in this case the performance were well above the normal performance of a MEAs prepared with same Pt loading and polymers composition, reaching High Current density up to 1800 $mA/cm^2$ and High Power density up to 650 $mW/cm^2$.

The next step was to prepare fibers with the same composition and compare their performance with painted GDLs. Electrospinning with methanol is known to be really tough. This is due to the physical properties of the solvents like the high vapor pressure, the low viscosity and the high dieletric constant respect to others common alcohol solvents.

In this case, even if the ink preparation procedure remains the same, some parameters must be changed. The electrospinning ink requires a more viscous dispersion than the one used for painting, so the solid weight % content must be increased. Also, to be sure to have enough ink, a higher amount of ink will be prepared. Then instead of 5% solid weight the electrospinning ink will have a 15% solid weight and 2.5 *grams* of total mass.

When the ink is ready, a 3 *ml* plastic syringe is filled with the dispersion. It is very important to discharge all the air in the syringe by pushing out the ink with the syringe in vertical position (as shown in Figure 4.10a). When all the bubbles are purged a 22 *gauge* needle is installed on the syringe. The syringe is then equipped on the volumetric pump ( placed in the electrospinning set-up in Figure 4.10b ). To collect fibers a non-stick aluminum foil is used and wrapped on the collector drum.

We can control the air humidity, the ink flow rate, the electric field voltage, the needle-collector distance and the collector's rotational and translational velocity.

(a) Syringe containing the ink

(b) Working electrospinning machine

Figure 4.10: Photos of a syringe filled with ink (a) and a electrospinning machine (b)

After several attempts fibers were fabricated with the following parameters:

- Relative Humidity = 60%;
- Distance needle/collector = 11 $cm$;
- Flow rate = 1.5 $ml/h$;
- Electric field = 13.5 $kV$;

Even if fibers were present, their density on the foil was very low.

The following tests showed good performance but not as good as the painted GDE, lower Current density,up to 1550 $mA/cm^2$, lower Power density, up to 585 $mW/cm^2$. We were expecting at least 10-20% better performance. This was due maybe to the bad quality of fibers. A polarization curve comparison is showed in the next page (Figure 4.11).

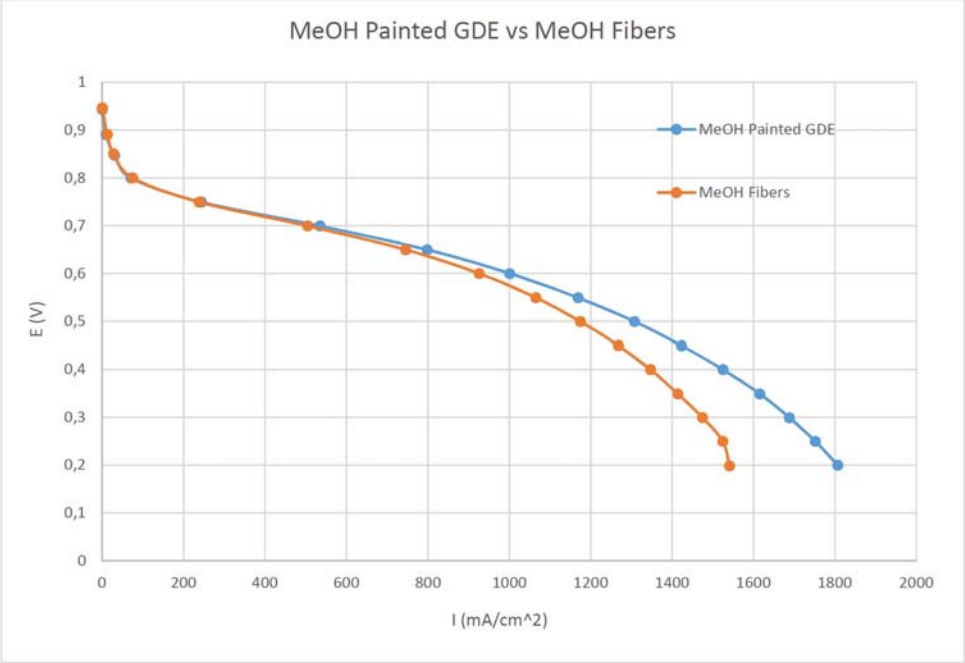


Figure 4.11: MeOH painted GDE-MeOH Fibers Polarization curve comparison

SEM images of the painted GDE (Figure 4.12a) and fibers were taken. The first one shows a very porous surface with some dense spots which are maybe due to polymers agglomeration. In the second one (Figure 4.12b) a fibers-beads coexistence is shown. Fibers are very thin but not uniform, some parts are more covered by Pt on carbon than others.

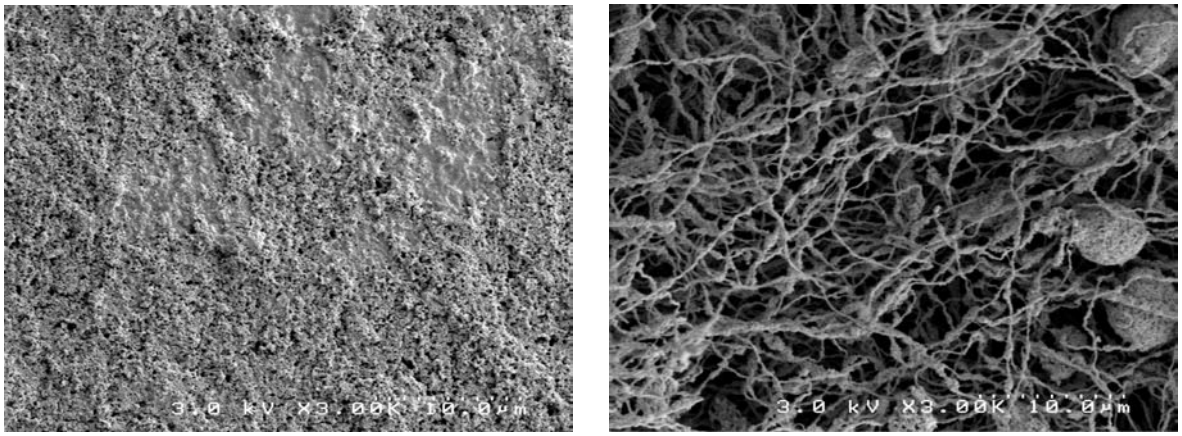

(a) Methanol Painted GDE SEM Image

(b) Methanol fibers SEM image

Figure 4.12: SEM images of methanol Painted GDE (a) and of methanol fibers (b)

At this point, it was thought that maybe a lot of solvents with different properties in a single ink was not recommended. In the literature it is possible to find different study on the effect of solvents on the final product. But no papers on solvents effect on Fuel cells with high performance fibers and Nafion membrane are published.

## 4.1 Solvent's influence on fibers fabrication and performance

Since the inks were composed by water and other three alcohol sovents (Nafion and PAA were pre dissolved), it has been decided to start a study on the effect of the single solvent on fuel cell performance, easiness of electrospinning and quality of fibers. To do that, Nafion and Carrier (PAA) must be used in the pure solid state.

As previous explained, Nafion for electrodes is purchased in a dispersion form from Ion Power™, so it needs to be dried very carefully (last drying step is done in Vacuum oven) to reach the Nafion pure form (Figure 4.13a). Poly(acrylic acid) with an average $Mv \sim 450.000$ is purchased from Sigma Aldrich and it is in powder (Figure 4.13b).

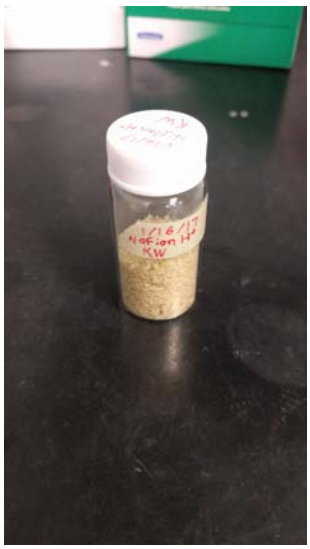

(a) Dried Nafion

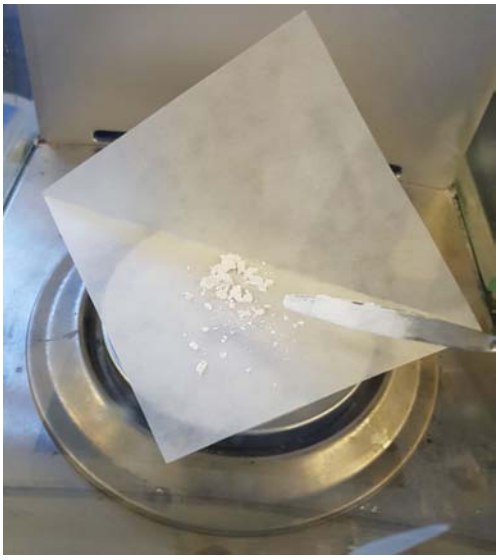

(b) Poly(acrylic acid) carrier

Figure 4.13: Photos of ionomer (a) and carrier (b)

Some studies will also be done on the way these polymers are mixed and treated.

To better understand which parameters deserve to be deepened,a research on the Literature has been done to find the effects of physical quantities on fibers electrospinning[65]. Putting aside for now process and ambient parameters, it has been decided to focuse on solution parameters which are:

- Boiling Temperature °C;
- Surface Tension $dynes/cm$;
- Density $g/cm^3$;
- Viscosity $cP$;
- Dieletric Constant;

Not all of these properties affect the fibers quality with the same weight. Solvents boiling point does not influence only the electrospinning quality, in fact beyond this process I've done several pre-study on painted GDE and to let the solvent evaporate as faster as possibile from the surface (in order also to maximize the porosity of the electrode) it is important to know at which minumum temperature the oven must be set.
Density is used only as an indicator of the total mass present in the syringe.

Solution viscosity is a critical key in determining the fiber morphology. It has been proven that continuous and smooth fibers cannot be obtained in very low viscosity[65], whereas very high viscosity results in the hard ejection of jets from solution, namely there is a requirement of suitable viscosity for electrospinning. For solution of low viscosity, surface tension is the dominant factor and just beads or beaded fiber formed. If the solution is of suitable viscosity, continuous fibers can be obtained.

Surface tension, as the function of solvent compositions of the solution, is quite important factor in electrospinning. Different solvents may contribute different surface tensions. With the concentration fixed, reducing the surface tension of the solution, beaded fibers can be converted into smooth fibers. Basically, surface tension determines the upper and lower boundaries of the electrospinning window if all other conditions are fixed[63].

The dielectric constant relates to the polymer solution's ability to conduct the electric charge in the electrospinning process. An insufficient dielectric constant will result in low solution conductivity and an inability to produce continuous electrospun fibers[64].

The mixture properties $\sigma_{mix}$ are calculated by a linear function of the properties of the pure solvent:

$$\sigma_{mix} = \varphi_1\sigma_1 + \varphi_2\sigma_2 \tag{4.2}$$

where $\sigma_1$ and $\sigma_2$ are the physical properties of the pure solvent and $\varphi_1$, $\varphi_2$ are the mass fraction of pure solvent in the mixture.

Other parameters which affect the fibers quality are:

- Polymers concentration;
- Polymers molecular weight;

There is a range of polymer concentration in the ink where it is possible to produce fibers, inside this range if the concentration is increased fibers diameter will increase. If the concentration is too low a lot of nanoparticles will be observed on the collecting drum. Of course the ink viscosity is directly correlated with polymers concentration.

Molecular weight of the polymer also has an important effect on morphologies of electrospun fiber. In principle, molecular weight reflects the entanglement of polymer chains in solutions, namely the solution viscosity. By keeping the concentration fixed, lowering the molecular weight of the polymer trends to form beads rather than smooth fiber. Increasing the molecular weight, smooth fiber will be obtained[65].

In this study deionized water is always present in the ink, the second solvent has been chosen from the following:

- methanol;
- ethanol;
- n-propanol;
- iso-propanol;
- ethylene glycol;

A table with the physical properties of the solvents at 20 °C is showed below:

| | **Physical Properties** | | | | |
|---|---|---|---|---|---|
| Solvent | $T_{eb}$ (°C) | $\rho$ $(g/cm^3)$ | $\mu$ $(cP)$ | $\gamma$ $(dynes/cm)$ | $\varepsilon$ |
| Water | 100 | 0.99 | 1 | 72.7 | 80 |
| Methanol | 64.6 | 0.791 | 0.545 | 22.1 | 32.7 |
| Ethanol | 78.4 | 0.789 | 1.1 | 22 | 24.3 |
| n-Propanol | 97 | 0.803 | 1.96 | 23.8 | 20.33 |
| iso-Propanol | 82.4 | 0.783 | 1.96 | 21.4 | 19.92 |
| Ethylene Glycol | 197 | 1.115 | 16.1 | 48.4 | 37.7 |

Table 4.1: Pysical Properties of solvents

Where $\rho$ is the density, $\mu$ is the viscosity, $\gamma$ is the surface tension and $\varepsilon$ is the dielectric constant.

In the first case study, the ink was prepared with 50-50 water/alcohol solution. The mixture properties are then calculated (see Table 4.2):

| | **Physical Properties** | | | | |
|---|---|---|---|---|---|
| Solvent | $T_{eb}$ (°C) | $\rho$ $(g/cm^3)$ | $\mu$ $(cP)$ | $\gamma$ $(dynes/cm)$ | $\varepsilon$ |
| Water/MeOH | 82.3 | 0.891 | 0.773 | 47.4 | 56.35 |
| Water/EtOH | 89.2 | 0.889 | 1.05 | 47.35 | 52.15 |
| Water/n-Prop | 98.5 | 0.897 | 1.48 | 48.3 | 50.17 |
| Water/iso-Prop | 91.2 | 0.887 | 1.48 | 47.1 | 49.96 |
| Water/EG | 148.5 | 1.05 | 8.55 | 60.55 | 58.85 |

Table 4.2: Pysical Properties of 50-50 Water-Alcohol solution

The procedure to prepare the inks is equal to the one used to prepare the electrospinning ink explained before.

**Water-Methanol 50-50**

The solution has the lowest boiling point and viscosity respect to the other mixtures, the dielectric constant is high and the suface tension is comparable with the others (except for the ethylene glycol). Since the viscosity has a very low value it was impossible to e-spin the ink, within a wide range of changed process parameters. By collecting the electrospun product on the glass slide and observing it with the optical microscope it was possible to see that in some parts of the glass, very short and non linear fibers were present (see Figure 4.14), but the final product was almost with electrosprayed beads.

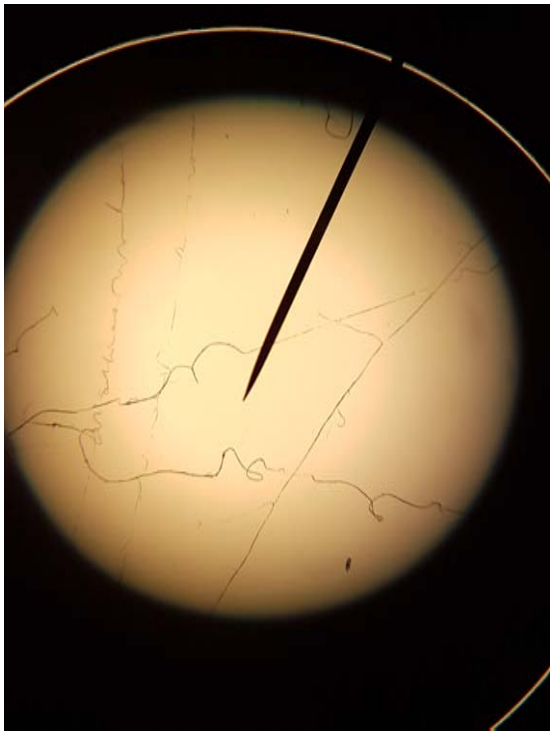

Figure 4.14: Water-methanol 50-50 fibers collected on the gas slide

Moreover, during the electrospinning process a lot of sparks were produced in between the syringe needle and the collecting drum. This phenomen must be avoided, not only because it may degrade fibers quality but also because of safety requirements (sparks can form also inside the syringe, melting down the plastic shell with possible fire starting, see Figure 4.15).

Figure 4.15: Example of sparks inside the syringe

Since fibers were not produced, no MEA was fabricated and tested. The first ink prepared to produce fibers with water and methanol was containing also other alcohols. This proves that solvents have a key role in the electrospinning process.

**Water-Ethanol 50-50**

In this case the solution's boiling point is 7 °C more than water/MeOH solution, the dielctric constant is decreased and the viscosity is close to that of the water.

By setting the process parameters to :

- Electric field = 4 $KV$;
- Flow reate = 0.8 $ml/h$;
- Relative Humidity = 40%;
- Distance needle-collector = 11 $cm$;

it is possible to produce fibers. The product quality is not high because also beads and agglomeration were present on the surface. A very interesting thing was the characteristic shape of the beads. In Figure 4.16it is possible to see that beads, instead of being with a spherical shape, their profile is similar to that of hemoglobin cells.

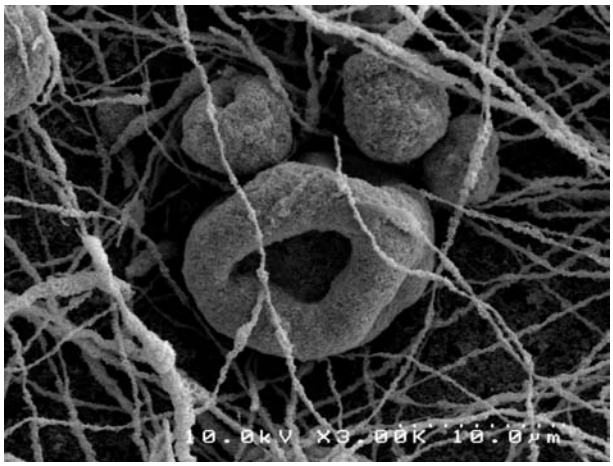


Figure 4.16: Beads formed on the surface by electrospinning water-EtOH 50-50 solution

An MEA was prepared and tested in the fuel cell station. Polarizatio test and ECSA have been taken at 100% Relative Humidity only. The MEA's maximum power output was 555 $mW/cm^2$ at ambient pressure and 797 $mW/cm^2$ at 1 atmosphere back pressure. Which means that the yield was still below the first MEA's performance. The electrochemical activity was 38 $m^2/g_{Pt}$.

**Water/n-Propanol 50-50**

The n-propanol was the solvent used as solution for the Nafion dispersion. Its mixing with water with 50/50 ratio leads to a solution with a boiling temperature close to 100 °C, and a higher viscosity respect to the other tested solutions, even if there was not a big difference in surface tension and dielectric constant values.

It has been difficult to electrospin good quality fibers, the ink was very sensitive to little step changes in the process parameters. Once the steady state was reached, it was necessary to keep the process under control in order to avoid the formation of beads on the aluminum foil.

The optimal parameters I've found were:

- Electric field = 3.5 $kV$;
- Flow rate = 0.7 $ml/h$:
- Relative Humidity = 30%;
- Distance needle-collector = 10.5 $cm$;

Through the SEM evaluation, it was possibile to see that fibers were present on the surface, and beads presence was almost zero, or close to zero. In Figure 4.17 it is possible

to see that fibers diameter is not uniform, in fact the diameter of fibers covered by the catalyst spaces from 600 $nm$ to more then 4000 $nm$.

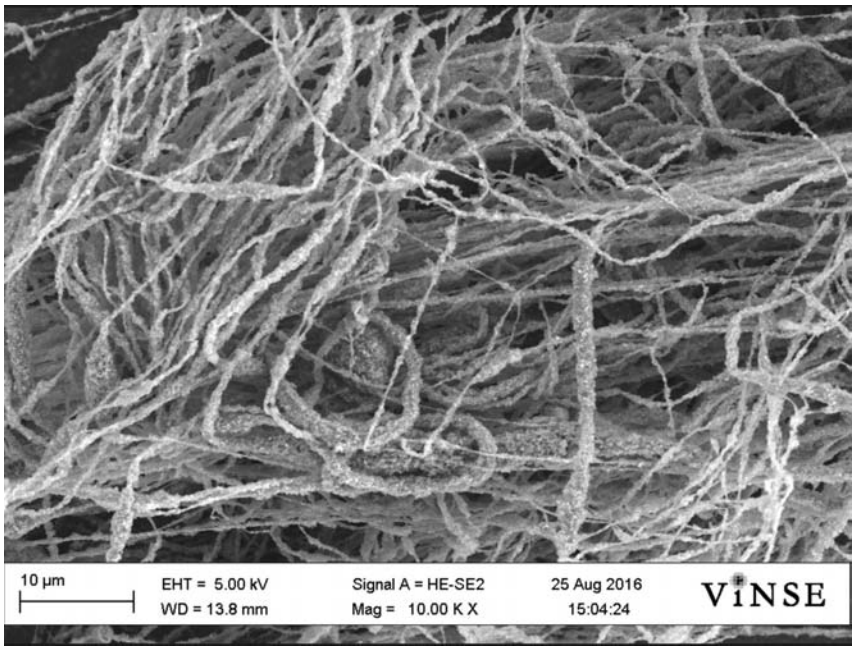


Figure 4.17: SEM image of fibers produced with water/n-propanol solvents at 10 K Magnification

Moreover a lot of fibers are naked (see Figure 4.18), it means that no Pt/C is present on the spinned polymer surface. One of the hypothesis is that the solvent solution doesn't work in the right way to keep all the elements well mixed.

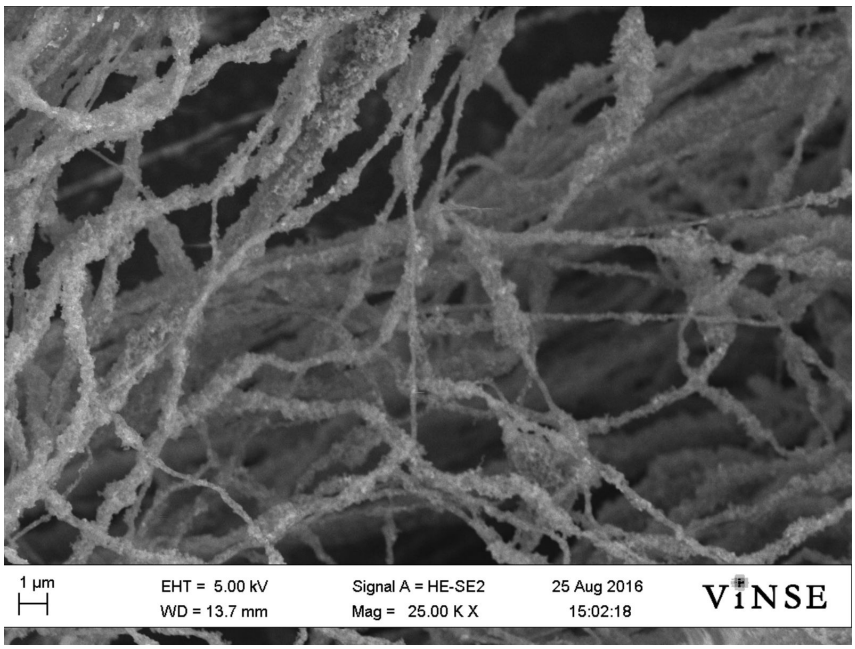


Figure 4.18: SEM image of uncovered fibers produced with water/n-propanol solvents at 25 K Magnification

For what concern the performance, at 100% $RH$ and ambient pressure the maximum power reached was 505 $mW/cm^2$. At one atmosphere backpressure the max power was 732 $mW/cm^2$. Meanwhile the $ECSA$ was 43 $m^2/g_{Pt}$. Also with this solvent mix I had a worse yield than that of water-methanol-npropanol-isopropanol solution.

### Water/iso-Propanol 50-50

Water/iso-propanol 50-50 solution has physical properties that are very close to water/n-propanol 50-50 properties, except for the boiling point, which is more than 7 °C lower.

Isopropyl Alcohol was used, before this study, as solvent for the carrier, which is PolyAcrylic Acid (PAA). Since iso-propanol and n-propanol properties are very similar, no one has considered the fact that there was the possibilty that one would have behaved differently from the other.

In my study, IPA (IsoPropyl Alcolhol) has become a good candidate to make high performance fibers. In fact, it has been easy to electrospin very good fibers. Fibers were present at different process parameters, which make the process more realizable in a scaled up process. Of course, even if it is possible to make fibers with different settings, I searched to find the optimal machine tuning, which was:

- Electric field = 3.8 $kV$;
- Flow rate = 0.6 $ml/h$:
- Relative Humidity = 38%;
- Distance needle-collector = 11 $cm$;

At this setting, no drops were present on the observed glass slide as shown in Figure 4.19. As first analysis with the optical microscope it is possible to see that fibers are linear and well covered.

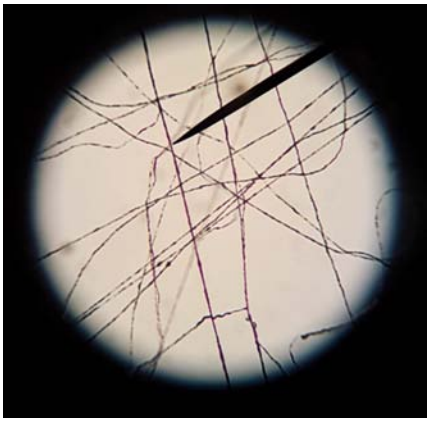

Figure 4.19: Optical microscope image of fibers prepared with water/iso-propanol 50-50 solution

A more precise evaluation of fibers shape has been done with the scanning electrons microscope. In Figure 4.20 at 3 K magnification the surface is completely covered by well shaped fibers. Platinum on Carbon is present on all the polymer surface.

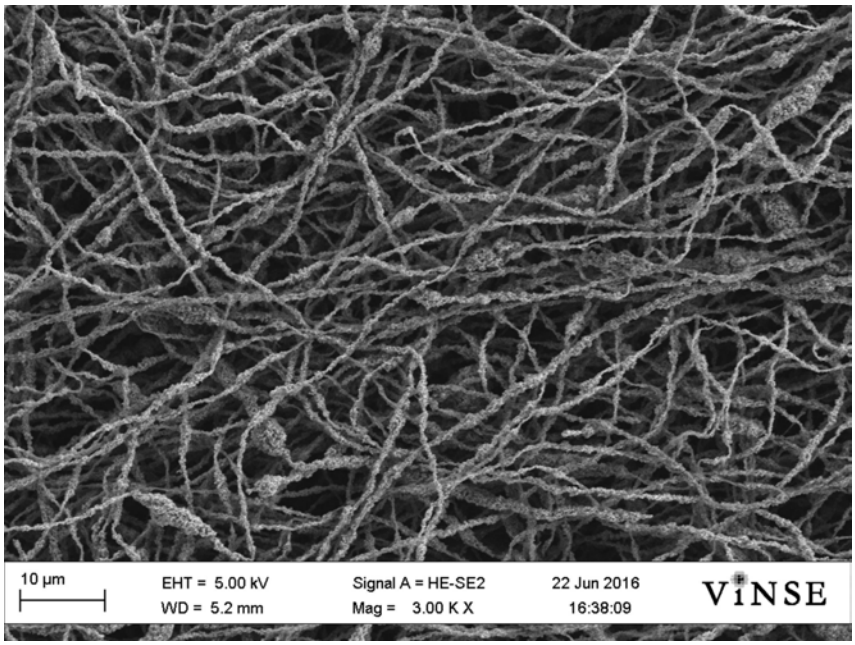


Figure 4.20: SEM image at 3 K Magnification of water/iso-propanol 50-50 fibers

At higher magnification (in Figure 4.21 ), it is also visible that the surface porosity is very high, so it was expected that performance and ECSA would have been better than the other fibers tested so far. Moreover the diameter of fibers is almost uniform, there are only few places where fibers are covered with more catalyst, and this is due maybe to some particle agglomeration in the ink. The average diameter ranges between $500 - 600\ nm$ which is good to have an high specic area.

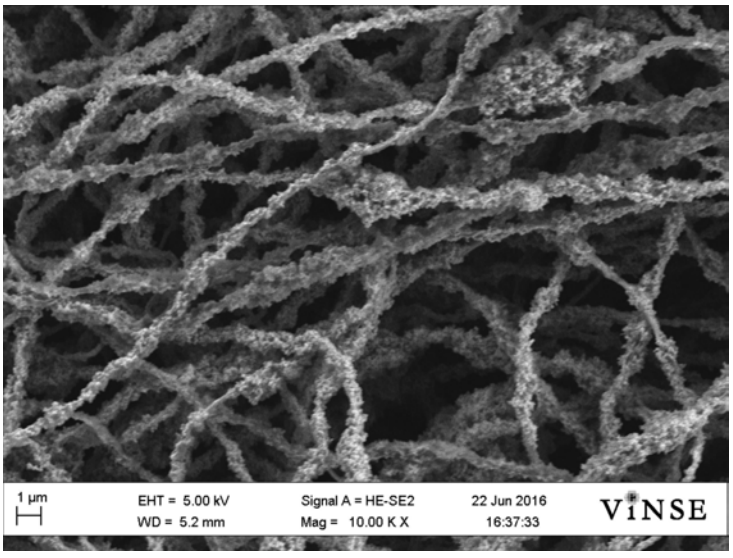


Figure 4.21: High magnification SEM image of water/iso-propanol 50-50 fibers

A previously assumed, these fibers turned out to have very high performance. The max power reached at 100% $RH$ and 0 backpressure was 701 $mW/cm^2$ and at 1 atmosphere backpressure was 971 $mW/cm^2$. The electrochemical surface area ($ECSA$) was up to 78 $m^2/g_{Pt}$.

Prior to investigate other properties of these fibers I wanted to study more solvents solution.

### Water-Ethylene Glycol 50-50

I chose to study a solution with ethylene glycol because of its high physical parameter values. In fact each property is greater than the other mixture properties. The biggest difference is given by the solution viscosity (8.55 $cP$).

As expected, the high viscosity has made it hard to do the electrospinning. The ink was too dense, with tendencies to clog the needle. After several attempts, the best product achieved was a foil covered by liquid drops (usually almost all the solvent evaporates on the path needle-foil).

Different water-solvent 50-50 solutions have been studied and what appeared till then was that all the solutions, except for the water/IPA, were less performant than the first one studied as shown in Figure.

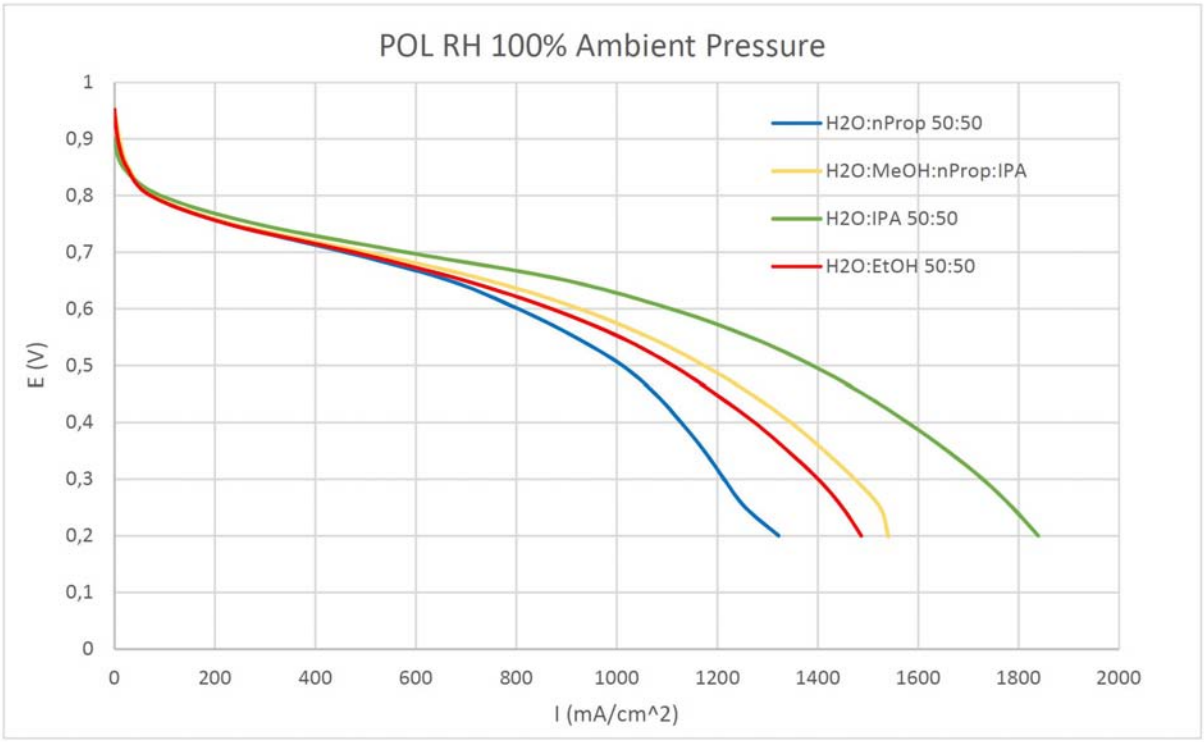


Figure 4.22: Comparison of different solvent mixtures performance

To better understand the results, some questions were asked:

1. Which solvent was increasing the performance?
2. In the case the Isopropanol was the key solvent to make high performance fibers, the addition of a third solvent will increase or decrease the MEA performance?

To answer the first question I have relied on the information obtained with my latest study. The n-propanol made fibers much less performant than IPA. Moreover only water/methanol solution was impossible to electrospin. To find an answer to the second question, one more study has been done. I decided to prepare solvents solution with water, isopropanol and a third solvent, chosen from the following:

- Methanol;
- Ethanol;
- Ethylene Glycol;

Also in this case physical properties of the three solvents mixture have been calculated with a linear function.

The weight ratio used for this study was: 50-30-20 water-IPA-third solvent.
A table with the mixtures' physical parameter is showed below in Table 4.3:

| | | **Physical Properties** | | | |
|---|---|---|---|---|---|
| Solvent | $T_{eb}$ (°C) | $\rho$ $(g/cm^3)$ | $\mu$ $(cP)$ | $\gamma$ $(dynes/cm)$ | $\varepsilon$ |
| Water/IPA/MeOH | 87.4 | 0.888 | 1.197 | 47.19 | 52.52 |
| Water/IPA/EtOH | 90.4 | 0.888 | 1.308 | 47.17 | 50.84 |
| Water/IPA/EG | 114.12 | 0.953 | 4.308 | 52.45 | 53.52 |

Table 4.3: Pysical Properties of 50-30-20 water-IPA-third solvent solution

**Water-IPA-MeOH 50-30-20**

Water/MeOH 50-50 was impossible to electrospin, and that was maybe due to the low viscosity of the solvent solution which was 0.773 $cP$. By adding IsoPropyl Alcohol the viscosity became 1.197 $cP$ and from the previous experience I have seen that around this viscosity value it was possible to fabricate fibers. As a matter of fact fibers were produced, but it was not easy to set the process parameters, because as happened with water/methanol 50/50 also in this case during the electrospinning fibers were always sparking, regardless of the parameters in the box.

Figure 4.23: Non dense fibers collected on the Aluminum foil

Even if fibers were present on the collecting drum, the final product (when all the ink in the syringe was electrospun) was a non dense deposition (Figure 4.23 ). For this reason several fiber layers were needed to reach the 0.1 $mg_{Pt}/cm^2$ standard Platinum loading.

At the polarization test the MEA showed very low performance, and this behaviour it was in contrast with the quality of the fibers observed with the SEM. In fact fibers shape was very thin and uniform. No beads were present in almost all the surface and the polymer filament was well covered by the catalyst (Figure 4.24). Since methanol showed good performace in my first experiments, the only reason of the poor performance could be that the more dense is the final product on the Aluminum foil the higher the MEA power will be (usually if fibers are dense, only one layer is enough to reach the standard Platinum loading).

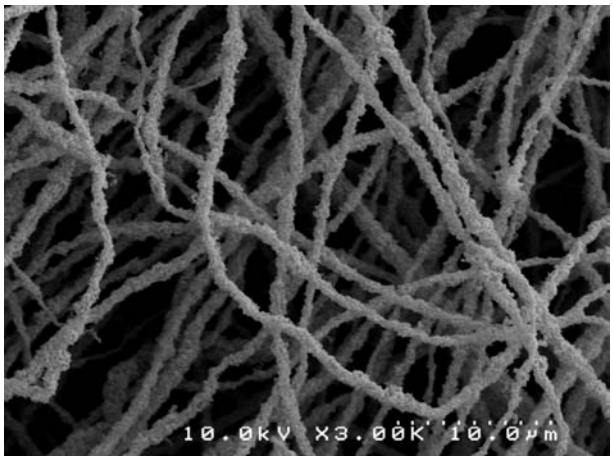


Figure 4.24: SEM image of water/IPA/MeOH fibers

**Water-IPA-EtOH 50-30-20**

This test was conducted to see if IPA had the ability to improve the water/EtOH 50/50 performance. It has been easy to electrospin good quality fibers with similar parameters used with water-IPA 50-50 solution:

- Electric field = 3.7 $kV$;
- Flow rate = 0.65 $ml/h$:
- Relative Humidity = 40%;
- Distance needle-collector = 11 $cm$;

The polarization test showed very good performance at 100% $RH$, at ambient backpressure the maximum power reached was 633 $mW/cm^2$ and at 1 atmosphere backpressure it was 874 $mW/cm^2$. The $ECSA$ test showed instead a normal value, which was 42 $m^2/g_{Pt}$.

This satisfactory outcome was still lower than that obtained with water-IPA 50-50, but higher than that of water-EtOH 50-50 (Figure 4.25), which means that IPA was the key solvent to produce high performance fibers.

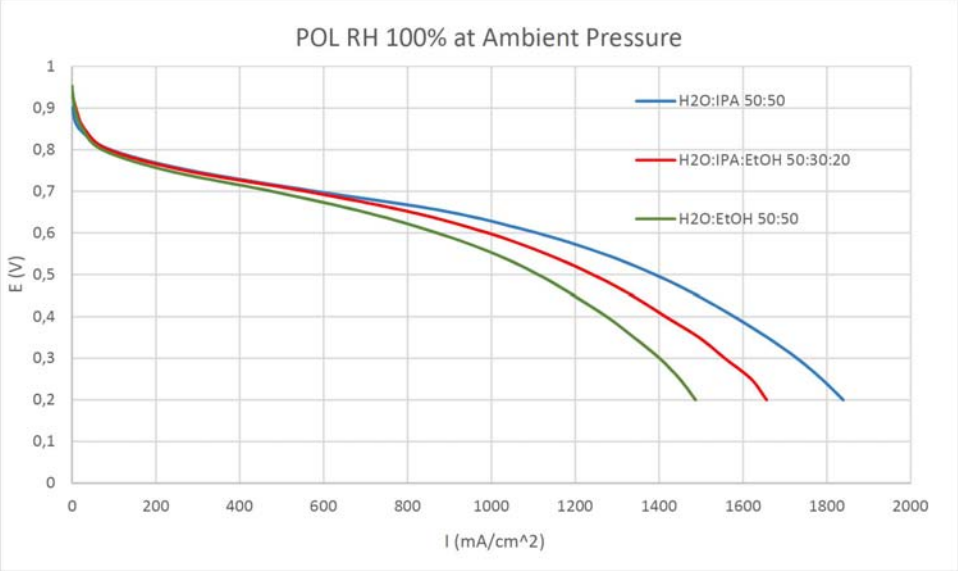


Figure 4.25: Polarization Curve comparison between H20:EtOH 50:50, H2O:IPA:EtOH 50:30:20 and H20:IPA 50:50

With SEM (Figure 4.26) it is possible to see that the "hemoglobin" shape beads are disappeared and that the fibers quality is good.

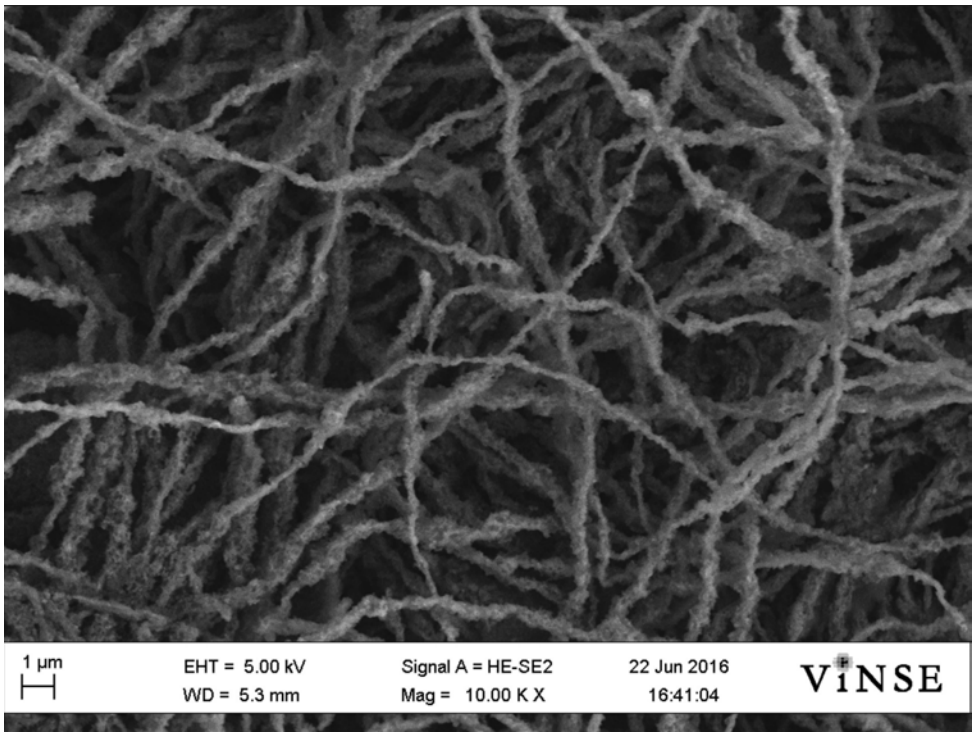


Figure 4.26: SEM image of H2O:IPA:EtOH 50:30:20 fibers

To better understand the difference between dense and non dense fibers collected on the Aluminum foil a comparison is showed below:

Figure 4.27: Comparison between dense and non dense fibers

**Water-IPA-Ethylene Glycol 50-30-20**

In order to evaluate if the viscosity is the key parametr to electrospin fibers, I tried to drastically decrease the viscosity by adding a big amount of IPA to the water-EG 50-50 mixture. The result has been curious. In fact on the glass slide it was possible to clearly see fibers. The latter, however, were covered by several drops (Figure 4.28 ). Not all the liquid was evaporating during the electrospinning, and some drops were dragged by the fiber filaments.

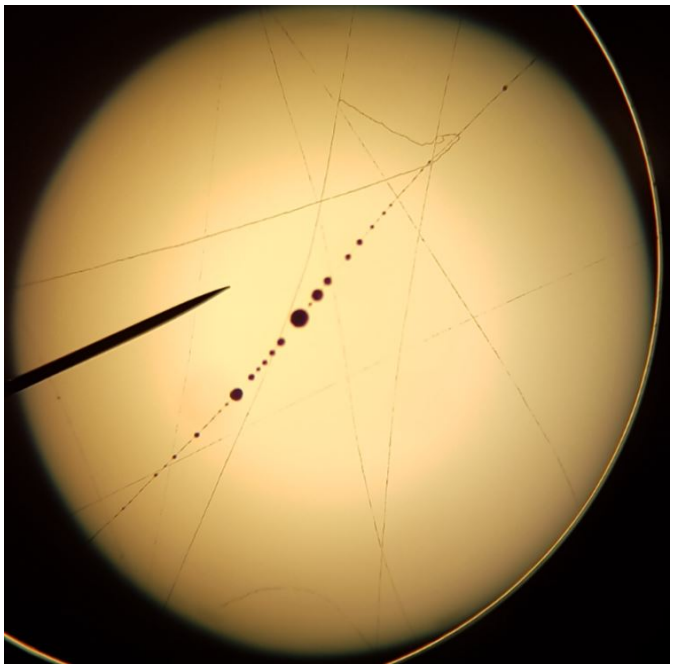

Figure 4.28: Image taken with Optical Microscope of fibers covered by liquid drops

Even more curious was the SEM observation. From Figure 4.29 it is possible to see that no "normal" fibers were present on the foil. Filaments with an undefined shape were covering all the surface. Their average diameter was above the 1000 $nm$. Some naked fibers are present in the background. It has been considered not necessary to test the MEA because it didn't meet the standards.

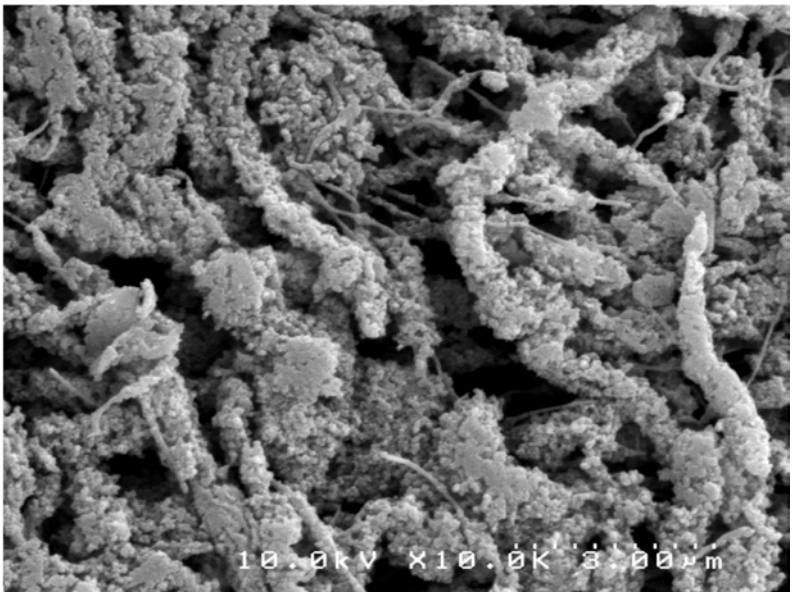


Figure 4.29: SEM image of H2O:IPA:EG 50:30:20 product

From these experiments it has been possible to investigate the effects of some solvent's parameters on the fibers quality. Isopropyl Alcohol seemed to be the key solvent to fabricate high performance fibers.

As final evaluation on this topic, an in-depth analysis on the two best MEAs (H2O:IPA and H2O:IPA:EtOH) has been carried out. In order to be sure on the repeteability of the good outcomes of these two samples, more fibers have been prepared and tested.

In addition to the test performed until then, new analysis have been carried out:

- Performance at 40% $RH$;
- Carbon Corrosion procedure;
- Mass Activity;
- Evaluation of performance losses after the carbon corrosion (End Of Life);

To perform the test at 40% of relative humidity and mantaining the Fuel Cell temperature at 80 °C, both the gas feed temperature must be decreased from 80 °C to 59 °C (Because of the dew point). The end of life (EOL) evaluation has been carried out for each type of test. For both the solvents solution a beginning of life (BOL) and end of life test (EOL) has been done. A third table reports the variation, in percentage, between the BOL and the EOL.

## Water-IPA 50-50

| Beginning Of Life | |
|---|---|
| High Freq. Resis. (Ohms) | 0.008 |
| Hydrogen Crossover (A) | 0.023 |
| Mass Act (Amps/mg Pt) | 0.081 |
| ECSA ($m^2_{Pt}/g_{Pt}$) | 78 |
| Power @0.65V 100% RH 0 Bar (mV/cm2^2) | 578 |
| Power @0.65V 100% RH 1 Bar (mV/cm2^2) | 850 |
| Power 40% @0.65V RH 0 Bar (mV/cm2^2) | 180 |
| Power 40% @0.65V RH 1 Bar (mV/cm2^2) | 413 |
| Max Power 100% RH 0 Bar (mV/cm2^2) | 696 |
| Max Power 100% RH 1 Bar (mV/cm2^2) | 963 |
| Max Power 40% RH 0 Bar (mV/cm2^2) | 353 |
| Max Power 40% RH 1 Bar (mV/cm2^2) | 719 |

Table 4.4: Analysis of water-IPA 50-50 solvent solution at BOL

| End Of Life (1000 cycles) | |
|---|---|
| High Freq. Resis. (Ohms) | 0.008 |
| Hydrogen Crossover (A) | 0.025 |
| Mass Act (Amps/mg Pt) | 0.090 |
| ECSA ($m^2_{Pt}/g_{Pt}$) | 71 |
| Power @0.65V 100% RH 0 Bar (mV/cm2^2) | 440 |
| Power @0.65V 100% RH 1 Bar (mV/cm2^2) | 581 |
| Power 40% @0.65V RH 0 Bar (mV/cm2^2) | 206 |
| Power 40% @0.65V RH 1 Bar (mV/cm2^2) | 422 |
| Max Power 100% RH 0 Bar (mV/cm2^2) | 596 |
| Max Power 100% RH 1 Bar (mV/cm2^2) | 818 |
| Max Power 40% RH 0 Bar (mV/cm2^2) | 346 |
| Max Power 40% RH 1 Bar (mV/cm2^2) | 673 |

Table 4.5: Analysis of water-IPA 50-50 solvent solution at EOL

| % Variation Beginning Of Life-End Of Life | |
|---|---|
| High Freq. Resis. (Ohms) | 0% |
| Hydrogen Crossover (A) | 11% |
| Mass Act (Amps/mg Pt) | 11% |
| ECSA ($m^2_{Pt}/g_{Pt}$) | -9% |
| Power @0.65V 100% RH 0 Bar (mV/cm2^2) | -24% |
| Power @0.65V 100% RH 1 Bar (mV/cm2^2) | -32% |
| Power 40% @0.65V RH 0 Bar (mV/cm2^2) | 15% |
| Power 40% @0.65V RH 1 Bar (mV/cm2^2) | 2% |
| Max Power 100% RH 0 Bar (mV/cm2^2) | -14% |
| Max Power 100% RH 1 Bar (mV/cm2^2) | -15% |
| Max Power 40% RH 0 Bar (mV/cm2^2) | -2% |
| Max Power 40% RH 1 Bar (mV/cm2^2) | -6% |

Table 4.6: Performance variation between BOL and EOL for water-IPA 50-50 solvents solution

This solution composition behaved, as in the previuos case, very well. The maximum power at 100% $RH$ and 0 backpressure was slighlty below 700 $mW/cm^2$. Also the power at 0.65 $V$ was very high. The electrochemical surface area was larger than the average. An interesting fact is the behaviour of the MEA at 40% $RH$, in fact comparing the data with Vanderbilt's previous studies, it can be seen that there is a huge improvement between my polarization data and older polarization data. Moreover, again with regard to test at 40% $RH$, after 1000 start and stop cycles there was an increase in power of the MEA. This behaviour has already been pointed out and it can be explained with the formation of $C-O$ *group* on the electrodes surface during the carbon corrosion test. These groups have tendencies to absorb water, which is fine for PEM fuel cells, so even if the humidity is lower, after the CC process the MEA becomes more hydrophilic and keeps the proton exchange membrane more hydrated.

On the other hand, generally the loss in performance is very limited, in fact at 100% $RH$ there is only a $-14.4\%$ variation at maximum power and $-24\%$ at 0.65 $V$.

The least expected data has been the Mass Activity value. In fact previous studies have shown an avereage value around 0.11 $Amps/mg_{Pt}$ for what concern the Platinum catalyst. In this case the Mass Activity was below that average, and it should be expected that at this performance, mass activity would be very high.

## Water-IPA-EtOH 50-30-20

| Beginning Of Life | |
|---|---|
| High Freq. Resis. (Ohms) | 0.0088 |
| Hydrogen Crossover (A) | 0.0177 |
| Mass Act (Amps/mg Pt) | 0.1490 |
| ECSA ($m^2_{Pt}/g_{Pt}$) | 42 |
| Power @0.65V 100% RH 0 Bar (mV/cm2^2) | 525 |
| Power @0.65V 100% RH 1 Bar (mV/cm2^2) | 770 |
| Power 40% @0.65V RH 0 Bar (mV/cm2^2) | 200 |
| Power 40% @0.65V RH 1 Bar (mV/cm2^2) | 367 |
| Max Power 100% RH 0 Bar (mV/cm2^2) | 621 |
| Max Power 100% RH 1 Bar (mV/cm2^2) | 869 |
| Max Power 40% RH 0 Bar (mV/cm2^2) | 353 |
| Max Power 40% RH 1 Bar (mV/cm2^2) | 719 |

Table 4.7: Analysis of water-IPA-EtOH 50-30-20 solvent solution at BOL

| End Of Life (1000 cycles) | |
|---|---|
| High Freq. Resis. (Ohms) | 0.0088 |
| Hydrogen Crossover (A) | 0.0179 |
| Mass Act (Amps/mg Pt) | 0.1289 |
| ECSA ($m^2_{Pt}/g_{Pt}$) | 40 |
| Power @0.65V 100% RH 0 Bar (mV/cm2^2) | 192 |
| Power @0.65V 100% RH 1 Bar (mV/cm2^2) | 396 |
| Power 40% @0.65V RH 0 Bar (mV/cm2^2) | 155 |
| Power 40% @0.65V RH 1 Bar (mV/cm2^2) | 292 |
| Max Power 100% RH 0 Bar (mV/cm2^2) | 334 |
| Max Power 100% RH 1 Bar (mV/cm2^2) | 671 |
| Max Power 40% RH 0 Bar (mV/cm2^2) | 325 |
| Max Power 40% RH 1 Bar (mV/cm2^2) | 611 |

Table 4.8: Analysis of water-IPA-EtOH 50-30-20 solvent solution at EOL

| % Variation Beginning Of Life-End Of Life | |
|---|---|
| High Freq. Resis. (Ohms) | 0% |
| Hydrogen Crossover (A) | 1% |
| Mass Act (Amps/mg Pt) | -13% |
| ECSA ($m^2_{Pt}/g_{Pt}$) | -5% |
| Power @0.65V 100% RH 0 Bar (mV/cm2^2) | -63% |
| Power @0.65V 100% RH 1 Bar (mV/cm2^2) | -49% |
| Power 40% @0.65V RH 0 Bar (mV/cm2^2) | -22% |
| Power 40% @0.65V RH 1 Bar (mV/cm2^2) | -20% |
| Max Power 100% RH 0 Bar (mV/cm2^2) | -46% |
| Max Power 100% RH 1 Bar (mV/cm2^2) | -23% |
| Max Power 40% RH 0 Bar (mV/cm2^2) | -8% |
| Max Power 40% RH 1 Bar (mV/cm2^2) | -15% |

Table 4.9: Performance variation between BOL and EOL for water-IPA-EtOH 50-30-20 solvents solution

Here the behaviour has been different. The performance at the beginning of life are very good as in the previous case study with the same solvents composition, but after the 1000 start and stop cycles the MEA lowered a lot its performance. The value that is in contrast with the water-IPA 50-50 solution is the mass activity, in fact in this case Mass activity is above the average Platinum catalyst value.

Once again, the water-IPA 50-50 solution has proved to be the best case studied during the research experience.

To compare the data collected with data collected during the previous research ("Fabrication, In-Situ Performance, and Durability of Nanofiber Fuel Cell Electrodes" Matthew Brodt, Taehee Han, Nilesh Dale, Ellazar Niangar, Ryszard Wycisk, and Peter Pintauro on the Journal of Electrochemical Society)it has been decided to study their procedure differences with the standard used in the present study:

- Once the carrier (PAA) is added in the ink do not sonicate the dispersion (In literature is possible to find some papers in which PAA is considered to be very susceptible to sonication[68] );
- Use pre-dissolved carrier and ionomer in order to have a better mixing during stirring and sonication step;
- Fabricate the MEA with the Catalyst Coated Membrane (CCM) procedure;

For each of these difference, a comparative test has been carried out. These types of tests are important to find out if the procedure differences were the causes of the different results obtained.

### Third sonication step influence

To test the influence of the sonication on the ink containing the PolyAcrylic Acid, I chose to prepare two inks for Slurry GDEs (Painted) with the water-IPA 50-50 solution, in order to eliminate all the electrospinning process parameters, which may vary the accuracy of the final result, since the electrospinning is a very complex and sensitive process.

The procedure to prepare the ink with third sonication step is the same of the one used to test methanol painted GDE. The PAA is added in the last step, the ink is sonicated in a bath for 30 minutes and then stirred overnight.

For what concern the second ink, once the PAA powder is added, it is directly put on the stirring machine, avoiding the third sonication step.

The two inks were painted on the Sigracet 29 BC GDL until 0.1 $mg_{Pt}/cm^2$ Pt loading was reached.

The MEA was then fabricated with $Nafion$ 211 membrane, pressed at 4 $MPa$ at a temperature of 140 °C for 10 minutes. (There was no variation between my MEA fabrication method and Vanderbilt MEA fabrication method).

Once the MEA was ready, it was tested in the Fuel Cell station after a break in procedure. Only polarization test were carried out (Figure 4.30)

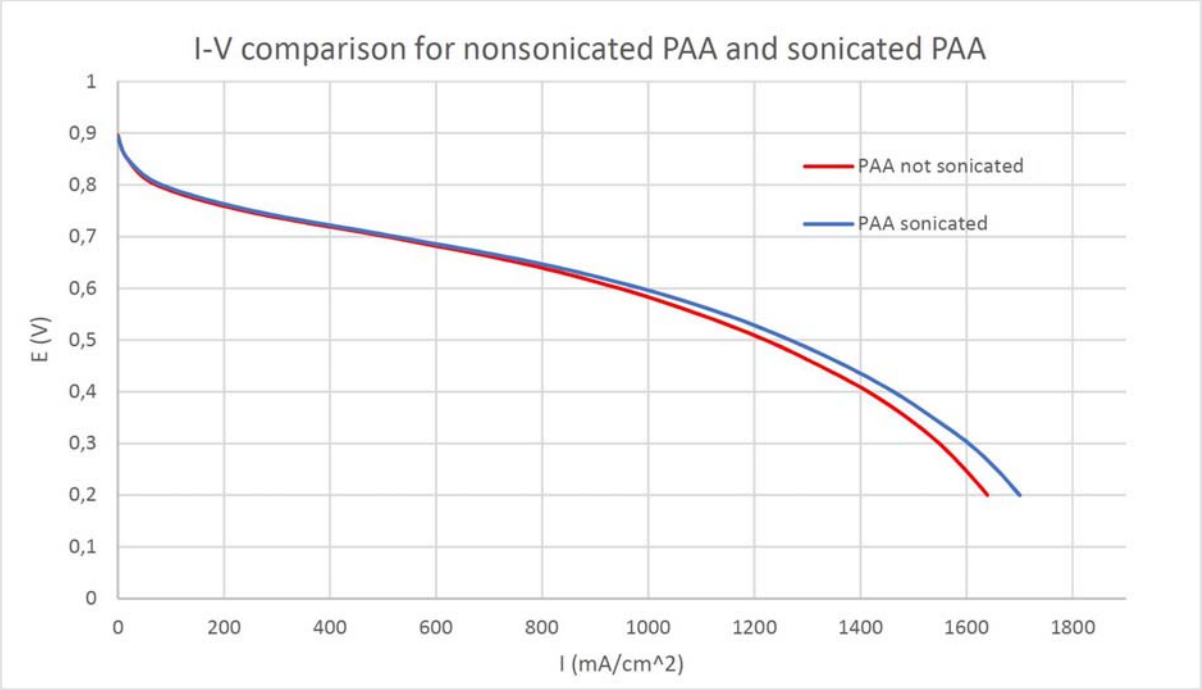


Figure 4.30: I-V comparison for nonsonicated PAA and sonicated PAA

The results were in contrast with what excpected from Vanderbilt researcher, in fact the ink with sonicated PAA behaves slightly better than the other, which was not sonicated. In the literature, and more specifically in the "Efficiently amplified ultrasonic degradation of spherical polyelectrolyte brushes by a magnetic field" which authors were Rui Zhang, Xiaoyan Hou, Yu Cang, Zhenchuan Yu, Zheqi Shen, Zhiming Zhou, Xuhong Guo, Junwei Wangb and Xuedong Zhu on the on the Royal Society of Chemistry journal, it has been observed that the sonication acts on the PAA chains by decreasing their thickness.

Since PAA is used only to allow the electrospinnability of Nafion, and it is know for its lowering performance characteristic, maybe a small PAA degradation leads to a system where the carrier still allows the spinnability of Nafion but its negative effects on the MEA performance are reduced. However the difference in the comparison is negligible, so the third sonication step does not influence the final result.

## Use of pre-dissolved polymers or pure polymers

To carry out this test, I chose to use painted GDEs for the same reason explained before. In this case, both the inks were sonicated at the third step.

One ink was prepared with Nafion and PAA powder. To prepare the other ink, PAA and Nafion were dissolved in a solution of water-IPA 50-50 to mantain the same composition of the ink. The procedure to obtain pre-dissolved polymers was very easy:

1. Weigh out the solid polymers;
2. Add the right amount of water-IPA 50-50 to reach a $20\% w_{polymer}/w_{tot}$;
3. Let the dispersion to mix on the the *Thermo Scientific tube roller* (Figure 4.31) for 48 hours at 10 rpm;
4. The pre-dissolved polymers are ready;


Figure 4.31: Thermo Scientific bottle roller

Once the inks are ready, the MEAs are fabricated and tested with the same procedure made before.

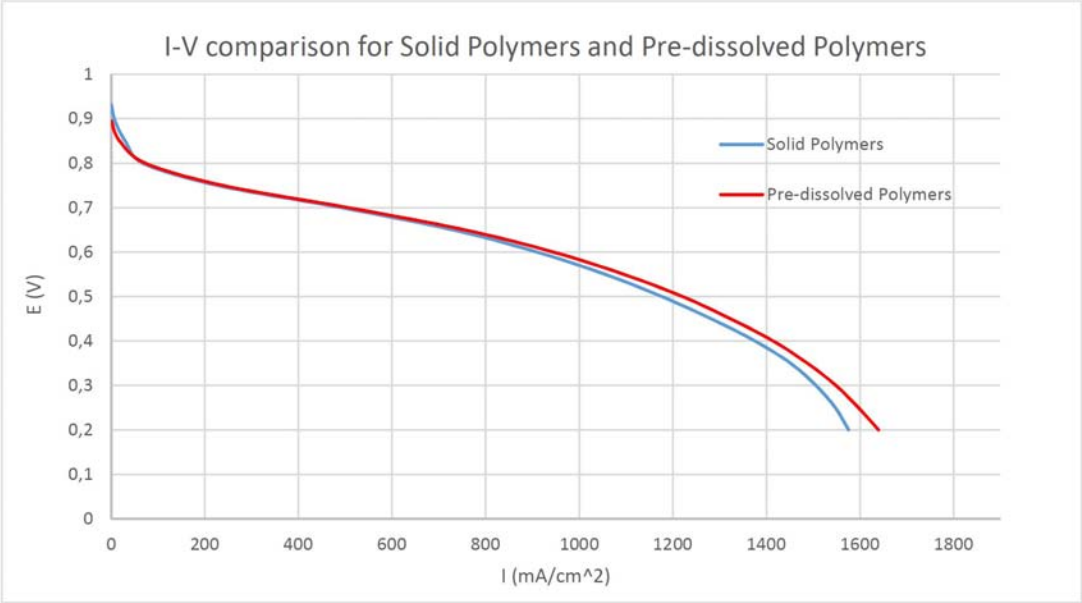


Figure 4.32: I-V comparison for Solid Polymers and Pre-dissolved Polymers

Also in this case the difference are negligible, so my procedure method can be considered as good as the Vanderbilt standard one.

## CCM method vs. Fibers pressed on GDLs method

The catalyst coated method requires to press first the fibers directly on the membrane (Figure 4.33) and only as last fabrication step, to put GDLs on the MEA and close the Fuel Cell without a secondary hot pressing procedure.

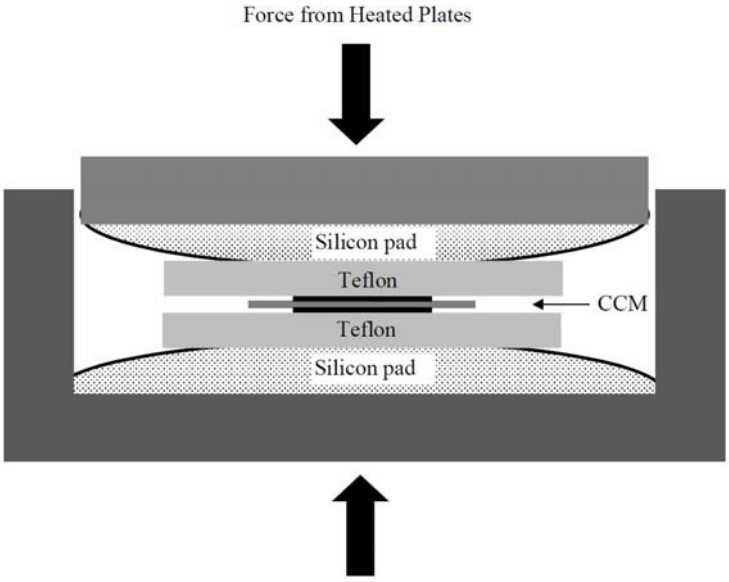


Figure 4.33: Schematic of hot-pressing set-up. Gas diffusion layers are physically pressed onto the hot-pressed CCM later when the CCM is loaded into the fuel cell test fixture.

To carry out this test, fibers were used instead of painted GDLs. I chose fibers prepared with water-Ipa 50-50 with non pre-dissolved polymers and third sonication step. The MEA fabrication procedure was the same for both the MEAs. I've always avoided the CCM method because to me the damage risks were higher respect than the one used by me. In fact with CCM method the membrane is directly in contact with the Teflon foils during the hot pressuring and it is not protected by gaskets, which are not present during the hot pressing in the CCM procedure (Nafion membrane is very fragile).

When the MEAs were ready, after the break in, a polarization test at 100% $RH$ and 0 atmosphere backpressure was carried out (Figure 4.34).

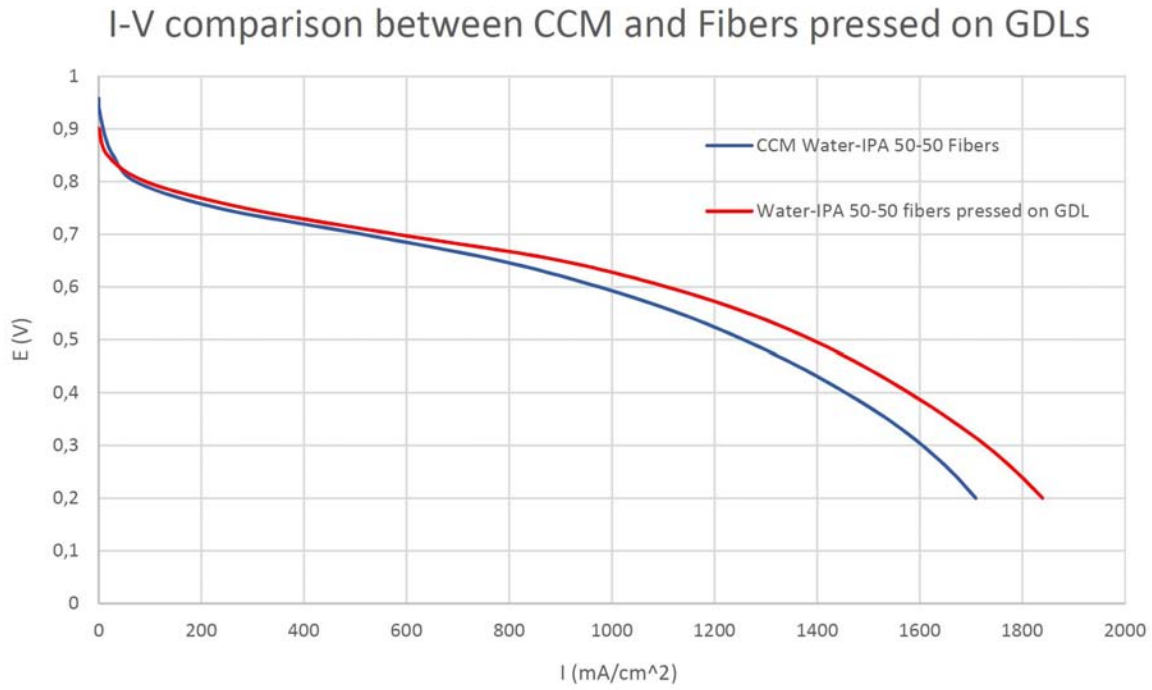


Figure 4.34: I-V comparison between CCM and Fibers pressed on GDLs

The plot shows that also in this case the procedure adopted during my research gave better result than the Vanderbilt standart one. But in order to compare the data collected during the experience, also this difference was considered negligible.

# Chapter 5

# Conclusion

Experimental results have been presented which show that solvents choice for fibers fabrication has an important role on the electrode performance. Several solvent compositions have been investigated, leading to a series of different behaviours.

First of all, experiments with methanol and other solvents were done, with whom it has been demonstrated that if methanol is present in the solution/dispersion, products with very good performance can be prepared. In contrast with the hypothesis, fibers behaved worse than painted GDEs.

After the last experiment with methanol, it has been chosen to investigate the effects of different solvents on the electrodes. Starting from solvent mixtures of only 2 components (water and one alcohol), qualitative and quantitative tests have been carried out. The goal was to find out which of the physical properties was influencing more the electrode performance. methanol and water mix, without the presence of other alcohols, was impossible to electrospin, and it has been hypothesized that it was due especially for the very low solution viscosity. When viscosity was above 1 $cP$ and below a certain value ($\approx$ 4 $cP$), electrospinning of fibers became more manageable (ethanol, n-propanol and iso-propanol with water produced fibers). By an in-depth analysis of these 3 solvents solution, knowing that Iso-propanol performed extremely well and, on the other hand, that n-propanol has yielded very poorly, it has been identified that:

- Mix with water and ethanol or iso-propanol at 50-50 composition have similar boiling point but the latter as an higher viscosity which allows a better fibers production;

- Mix with water and iso-propanol or n-propanol at 50-50 composition have equal viscosity but the latter has higher boiling point, which avoid the formation of pores on the polymer fiber[66], decreasing its specific area and the electrochemical surface area as well;

- No huge differences between the others properties were present so it was difficult to find out a relationship with the product;

In order to confirm these points, new solvent mixtures were prepared, by adding a third alcohol to the ink. water-IPA-methanol produced apparentely (by SEM images) very good fibers, but performed very badly. It has been hypotesized that another important parameter is the fibers density on the GDL (better to reach the right Pt loading with less layers possible), moreover the viscosity was slightly above 1 $cP$ which can be another point against good performance.

The solution with ethylene glycol produced very few fibers, and a lot of catalyst deposited on big random filaments with an undefined shape and huge diameters.

The solvents solution containing ethanol, worked very well, but it was less performant than water-IPA only. All its physical properties were comparable with water-IPA 50-50 except for the viscosity which was lower instead.

As final step a detailed analysis on these last two MEAs has been carried out. Beginning of life and end of life performance data, after 1000 Cycles of Carbon Corrosion procedure, have been collected. Moreover polarization tests have been carried out also at lower humidity.

Since the preparation techniques used during the experience were different from that used in the previous study, more experiments were done in order to make sure that a comparison between the data collected and the last paper published was possible. It came out that:

- The third sonication step didn't damage the ink;
- The use of pre-dissolved polymers didn't change a lot the final result;
- CCM fabrication method gave similar results to GDLs hot-pressed with fibers and membrane;

Generally the comparison was then possible. In the "*Fabrication, In-Situ Performance, and Durability of Nanofiber Fuel Cell Electrodes*" two differents preparation methods are investigated. Nanofiber electrode MEAs ($0.10 mg/cm^2$ Pt loading for the anode and cathode) were clearly superior to sprayed MEAs; they produced more power at beginning of life and maintained a higher percentage of their power after the carbon corrosion durability protocol, resulting in much higher end of life fuel cell performance. The present study shows a similar trend, in which painted GDLs (see *Third sonication step influence* and *Use of pre-dissolved polymers or pure polymers* sections in the previous chapter) performed less well than fibers electrode (see the Figure 5.1 in the next page). At 0.65 $V$ painted GDE power was 491 $mW/cm^2$ whereas fibers power was $575 mW/cm^2$ ($\geq$ 17% performance increase)

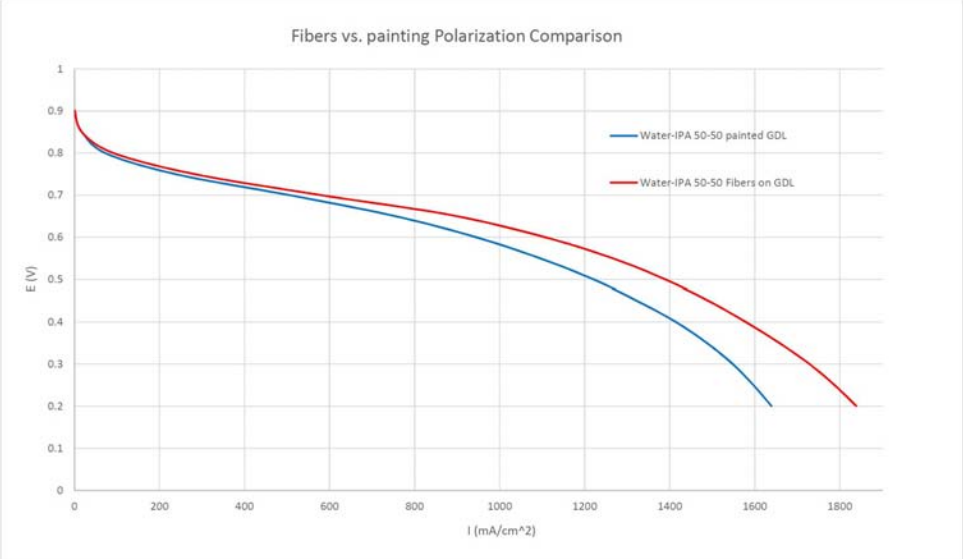


Figure 5.1: Fibers vs. painting Polarization Comparison

At beginning of life and ambient fully humidified at 0 atm backpressure, fibers prepared in the present study performed much better than that prepared and showed in the last published paper (see Figure 5.2 ).

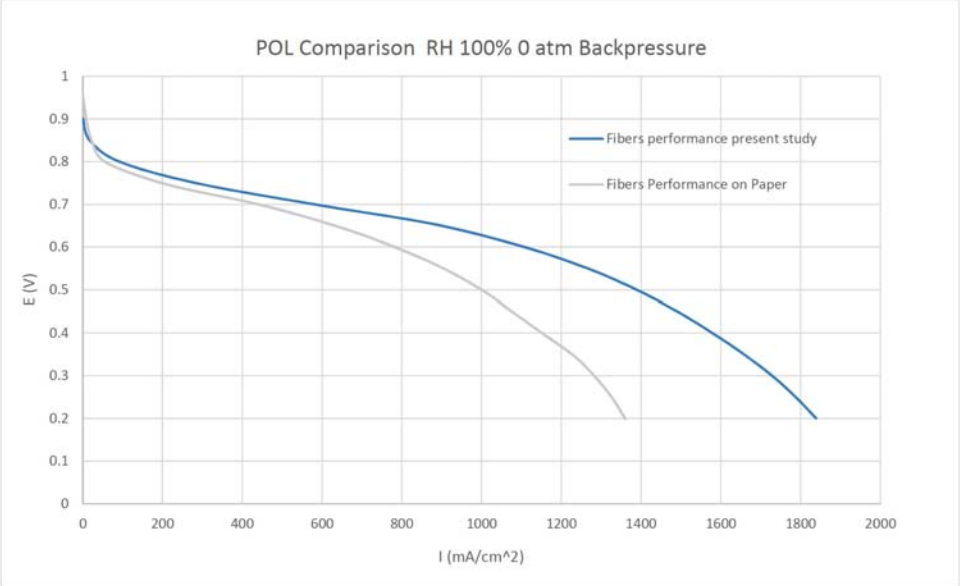


Figure 5.2: POL Comparison RH 100% 0 atm Backpressure

There is a clear difference between the two MEAs performance which have been made with same components and same Pt loading. The power generated at 0.65 $Volts$ was:

- 575 $mW/cm^2$ for H2O-IPA 50-50 fibers;
- 420 $mW/cm^2$ for fibers prepared in the previous study;

After the carbon corrosion procedure, water-IPA 50-50 fibers presented a lower loss in performance than other fibers. In fact, while the EOL/BOL of previous fibers was 0.53 at 0.65 $V$ and 0.85 at max power, fibers loss in the present study was 0.76 at 0.65 $V$ and 85.6 at max power. Since for the automotive standard, power generated at 0.65 $V$ is much more important than max power, and knowing that at beginning of life H2O-IPA 50-50 showed a 36% better performance at 0.65 $V$ than fibers of the previous study, it is possible to state that there has been an huge improvement for what concern the fibers performance.

Moreover, while in the previous at a low RH feed gas condition (40% RH), the electrospun MEA showed significantly higher HFR and poor i-V performance, due to fiber dehydration, in the present study fibers seemed to have better water management, leading to a lower High Frequency Resistance and much better i-V performance (see Figure 5.3)


Figure 5.3: POL Comparison at 40% Rh and 1 atm Backpressure

In both the studies fibers at 40% $RH$ behaved in a similar way, where the EOL performance improved and was significantly better than the BOL performance after the harsh start-stop potential cycling test. This results is associated with a more optimal water content/hydration in the nanofiber electrode mat due to the increased hydrophilicity/water retention of the carbon support after start-stop potential cycling.

## 5.1 Future Work

As written in the *Introduction* not all variables have been taken in consideration. Physical properties have a strong influence on the electrodes fabrication and performance, but it is important to take in account that isopropyl Alcohol is a common solvent used in several case studies. The high performance reached are also due to a specific preparation procedure. The variables involved in electrodes preparation are many. An in-depth analysis on the influence of solubility parameters is strongly suggested. A predictive model for the electrospinning process is necessary. It is also recommended to try the use of Poly Acrylic Acid with lower molecular weight in order to see if smallar polymers chains can still produce fibers while decreasing the MEAs performance loss.

Moreover, for what concern the laboratory in Vanderbilt, a perfect environmental control must be implemented, because it has been seen that the same ink behaved in different ways depending on the outside weather.

# Chapter 6

# Bibliography


[1] Litster, S. and G. McLean (2004) *Journal of Power Sources*, 130, 61-76.

[2] Long, N. V., Y. Yang, C. Minh Thi, N. V. Minh, Y. Cao, and M. Nogami (2013) *Nano Energy*, 2, 636-676.

[3] Ma, Y., H. Zhang, H. Zhong, T. Xu, H. Jin, and X. Geng (2010) *Catalysis Communications*, 11, 434-437.

[4] Serov, A., M. H. Robson, M. Smolnik, and P. Atanassov (2013) *Electrochimica Acta* , 109, 433-439.

[5] Othman, R., A. L. Dicks, and Z. Zhu (2012) *International Journal of Hydrogen Energy* , 37, 357-372.

[6] Kocha, S. S., *Chapter 3 - Electrochemical Degradation: Electrocatalyst and Support Durability, in Polymer Electrolyte Fuel Cell Degradation, M.M. Mench, E.C. Kumbur, and T.N. Veziroglu, Editors. 2012*, Academic Press: Boston. p. 89- 214

[7] Parrondo, J., T. Han, E. Niangar, C. Wang, N. Dale, K. Adjemian, and V. Ramani (2014) *Proceedings of the National Academy of Sciences*, 111, 45-50.

[8] Stassi, A., I. Gatto, V. Baglio, E. Passalacqua, and A. S. Aricò (2013) *Applied Catalysis B: Environmental* , 142–143, 15-24.

[9] Kumar, A. and V. K. Ramani (2013) *Applied Catalysis B:Environmental*, 138– 139, 43-50.

[10] Hara, M., M. Lee, C.-H. Liu, B.-H. Chen, Y. Yamashita, M. Uchida, H. Uchida, and M. Watanabe (2012) *Electrochimica Acta*, 70, 171-181.

[11] Hwang, K., B. Kwon, and H. Byun (2011) *Journal of Membrane Science*, 378, 111-116.

[12] Zhang, Y., C. Lim, S. Ramakrishna, and Z.-M. Huang (2005) *Journal of Materials Science: Materials in Medicine*, 16, 933-946.

[13] Lannutti, J., D. Reneker, T. Ma, D. Tomasko, and D. Farson (2007) *Materials Science and Engineering: C* , 27, 504-509.

[14] Lee, S. and S. Kay Obendorf (2006) *Journal of Applied Polymer Science*, 102,3430-3437.

[15] Sawicka, K., P. Gouma, and S. Simon (2005) *Sensors and Actuators B: Chemical*, 108, 585-588.

[16] Luoh, R. and H. T. Hahn (2006) *Composites Science and Technology*, 66, 2436-2441.

[17] Ballengee, J. B. and P. N. Pintauro (2011) *J. Electrochem. Soc.*, 158, B568-B572.

[18] Park, A. M. and P. N. Pintauro (2012) *Electrochem Solid St*, 15, B27-B30.

[19] Zhang, W. and P. N. Pintauro (2011) *ChemSusChem*, 4, 1753-1757.

[20] Frano barbir (2005) *PEM Fuel cell: Theory and Practice*, 1.

[21] MacLean, H. L. and L. B. Lave (2003) *Progress in Energy and Combustion Science*, 29, 1-69.

[22] Curtin, D. E., R. D. Lousenberg, T. J. Henry, P. C. Tangeman, and M. E. Tisack (2004) *Journal of Power Sources*, 131, 41-48.

[23] Joo, J. B., P. Kim, W. Kim, and J. Yi (2006) *Journal of Electroceramics*, 17, 713-718.

[24] Neyerlin, K. C., W. B. Gu, J. Jorne, and H. A. Gasteiger (2007) *Journal of the Electrochemical Society*, 154, B631-B635.

[25] Mench, M. M., E. C. Kumbur, and T. N. Veziroglu,*Polymer Electrolyte Fuel Cell Degradation. 2011: Elsevier Science* .

[26] Ralph, T. R. and M. P. Hogarth (2002) *Platinum Metals Review*, 46, 3-14.

[27] Sasikumar, G., J. W. Ihm, and H. Ryu (2004) *Journal of Power Sources*, 132, 11-17.

[28] Gasteiger, H. A., S. S. Kocha, B. Sompalli, and F. T. Wagner (2005) *Applied Catalysis B: Environmental* , 56, 9-35.

[29] Antoine, O., Y. Bultel, and R. Durand (2001) *Journal of Electroanalytical Chemistry*, 499, 85-94.

[30] Wilson, M. S., J. A. Valerio, and S. Gottesfeld (1995) *Electrochimica Acta* , 40, 355-363.

[31] Warshay, M. and P. R. Prokopius (1990) *Journal of Power Sources*, 29, 193-200.

[32] Srinivasan, S., E. A. Ticianelli, C. R. Derouin, and A. Redondo (1988) *Journal of Power Sources*, 22, 359-375.

[33] Murphy, O. J., G. D. Hitchens, and D. J. Manko (1994) *Journal of Power Sources*, 47, 353-368.

[34] Chun, Y. G., C. S. Kim, D. H. Peck, and D. R. Shin (1998) *Journal of Power Sources*, 71, 174-178.

[35] Uchida, M., Y. Aoyama, N. Eda, and A. Ohta (1995) *Journal Electrochem Society*, 142, 4143-4149.

[36] Tintula, K. K., A. Jalajakshi, A. K. Sahu, S. Pitchumani, P. Sridhar, and A. K.Shukla (2013) *Fuel Cells* , 13, 158-166.

[37] Kim, H. J., Y. S. Kim, M. H. Seo, S. M. Choi, and W. B. Kim (2009) *Electrochemistry Communications*, 11, 446-449.

[38] Pourbaix, M. (1966) *Atlas of electrochemical equilibria in aqueous solutions*, Pergamon Press.

[39] de Bruijn, F. A., V. A. T. Dam, and G. J. M. Janssen (2008) *Fuel Cells*, 8, 3-22.

[40] Meyers, J. P. and R. M. Darling (2006) *Journal of the Electrochemical Society*,153, A1432-A1442.

[41] Kulikovsky, A. A. (2011) *Journal of the Electrochemical Society*, 158, B957-B962.

[42] Tintula, K. K., A. Jalajakshi, A. K. Sahu, S. Pitchumani, P. Sridhar, and A. K.Shukla (2013) *Fuel Cells*, 13, 158-166.

[43] Kocha, S. S. M.M. Mench, E.C. Kumbur, and T.N. Vezirogl (2012), *Chapter 3 - Electrochemical Degradation: Electrocatalyst and Support Durability, in Polymer Electrolyte Fuel Cell Degradation*,p. 89-214.

[44] http://www.fuelcellstore.com/fuel-cell-components/membranes.

[45] Paul William Majsztrik (2008) *Mechanical and transport properties of Nafion for PEM fuel cells; Temperature and Hydration effects.*

[46] http://www.fuelcellsetc.com/store/Layers.

[47] http://www.fuelcellstore.com/fuel-cell-components/gaskets.

[48] http://fuelcell.com/gaskets.

[49] Bernard Bladergroen, Huaneng Su, Sivakumar Pasupathi and Vladimir Linkov (2012) *Overview of Membrane Electrode Assembly Preparation Methods for Solid Polymer Electrolyte Electrolyzer.*

[50] Luke Michael Haverhals (2008) *Fuel Cells as Power Sources and Sensors.*

[51] N. P. Kulkarni, T. E. Sparks, G. Tandra, F. W. Liou (2010) *MEA manufacturing using an additive manufacturing process to deposit a catalyst pattern in an MEA and its impact on cost reduction.*

[52] Áron Varga, Nicholas A. Brunelli, Mary W. Louie, Konstantinos P. Giapisb and Sossina M. Hailea *Composite Nanostructured Solid-Acid Fuel-Cell Electrodes via Electrospray Deposition*

[53] Figure 2.11 http://rdgroups.ciemat.es/documents/50365/84935/PEMFC2-1.png/e7b7f4cd-d168-48ee-9020-80216dda211f

[54] Travis J. Sill, Horst A. von Recum (2008) *ReviewElectrospinning: Applications in drug delivery and tissue engineering*

[55] (2008) *Fuel Cell Characterization M.Olivier Facultè polytechnique de Mons*

[56] http://www.scribner.com/files/tech-papers/Scribner-on-Crossover-Fuel-Cell-Magazine-2008.pdf

[57] Jay B. Benziger , M. Barclay Satterfield, Warren H.J. Hogarth, James P. Nehlsen, Ioannis G. Kevrekidis (2005) *The power performance curve for engineering analysis of fuel cells.*

[58] Heikki Kumpulainen, Terttu Peltonen, Ulla Koponen, Mikael Bergelin, Matti Valkiainen and Mikael Wasberg (2002) *In situ voltammetric characterization of PEM fuel cell catalyst layers*

[59] Dr. Kevin R. Cooper *In situ PEM Fuel Cell electrochemical surface area and catalyst utilization measurement* Scribner Associates Incorporated

[60] (2005) *Advanced Fuel Cell Diagnostic Techniques for Measuring MEA Resistance Scribner Associates* Inc. Fuel Cell Magazine

[61] Chi-Yuan Lee , Yu-Ming Lee and Shuo-Jen Lee (2012) *Local Area water Removal Analysis of a Proton Exchange Membrane Fuel Cell under Gas Purge Conditions*

[62] C. Tötzkea,b, G. Gaiselmannc , M. Osenberga, T. Arlta, H. Markötterа, A. Hilgera,d, A. Kupsche, B.R.Müller, V. Schmidtc, W. Lehnertf,g, I. Mankea (2016 ) *Influence of hydrophobic treatment on the structure of compressed gas diffusion layers*

[63] Li, Zhenyu, Wang (2003) *One-Dimensional nanostructures Electrospinning Technique and Unique Nanofibers*

[64] Steven Romel Givens (2008) *The effect of solvent properties on electrospun polymer fibers and application in biomaterials*

[65] Effects of Working Parameters on Electrospinning Springer

[66] C.J. Luo, M. Nangrejo, M. Edirisinghe (2010) *A novel method of selecting solvents for polymer electrospinning*

[67] Surawut Chuangchote, Takashi Sagawa, Susumu Yoshikawa (2009) *Electrospinning of Poly(vinyl pyrrolidone): Effects of Solvents on Electrospinnability for the Fabrication of Poly(p-phenylene vinylene) and TiO2 Nanofibers*

[68] Rui Zhang, Xiaoyan Hou, Yu Cang, Zhenchuan Yu, Zheqi Shen, Zhiming Zhou, Xuhong Guo, Junwei Wangb and Xuedong Zhu (2016) *Efficiently amplified ultrasonic degradation of spherical polyelectrolyte brushes by a magnetic field* Royal Society of Chemistry journal

# Chapter 7

# Aknowledgment

My deep gratitute goes first to Professor Peter N. Pintauro who gave me the opportunity to live an amazing and unforgettable experience in Vanderbilt University. The door to Prof. Pintauro office was always open whenever I ran into a trouble spot or had a question about my research or writing. He consistently allowed this thesis to be my own work, but steered me in the right direction whenever he thought I needed it.

My appreciation also extend to Professor Michele Modesti and Dr. Martina Roso at University of Padova. Thanks to their professionalism and availability it has been possible to write this thesis.

My gratitude goes also to Gianluca Aldrighetti, with whom I spent almost all my life in the good and bad period. He is the friend that anyone needs.

Finally, I must express my very profound gratitude to my family and to my partner Francesca Meneghelli for providing me with unfailing support and continuous encouragement throughout my years of study and through the process of researching and writing this thesis. Thank you also to all my friends with whom it has been possible to state that life is a present. This accomplishment would not have been possible without them. Thank you.

# Ringraziamenti

La mia profonda gratitudine va prima di tutto al Professor Peter N. Pintauro, il quale mi ha dato la possibilità di vivere una fantastica ed indimenticabile esperienza in Vanderbilt University. La porta dell'ufficio del Professor Pintauro era sempre aperta qualsiasi volta avessi problemi di ogni tipo riguardo al progetto e alla tesi.

I miei più sinceri apprezzamenti vanno anche al Professor Michele Modesti e Dottoressa Martina Roso dell'Università di Padova per essere sempre stati professionali e molto disponibili nella risoluzione di vari problemi e nella stesura della tesi.

La mia gratitudine inoltre va a Gianluca Aldrighetti, con il quale ho speso quasi tutta la mia vita nella buona e nella cattiva sorte. Lui è l'amico di cui tutti hanno bisogno.

Infine, devo esprimere la mia più profonda gratitudine alla mia famiglia e alla mia compagna Francesca Meneghelli per avermi sempre supportato e continuamente incoraggiato in tutti questi anni di vita e di studio. Grazie anche a tutti i miei amici con i quali è stato possibile stabilire che la vita è un dono. Questo traguardo non sarebbe stato possibile senza di loro. Grazie.

# List of Figures

# List of Tables